AN ABSTRACT OF THE THESIS OF

FRANK ALLEN HENNING (Name) for the DOCTOR OF PHILOSOPHY (Degree)

in CHEMICAL ENGINEERING (Major) presented on Dec 18, 1971 (Date)

Title: A MATHEMATICAL MODEL OF n-HEXADECANE TRANSFORMATION BY AN ARTHROBACTER SPECIES

Abstract approved: Redacted for privacy
Charles E. Wicks

The subterminal oxidation of n-hexadecane by non-growing cells was studied by following the product concentrations of the transformation process in a 14-liter batch fermentor. A mixture of the 2-, 3- and 4- isomeric alcohols and the corresponding ketones were isolated as products of the oxidation. It was demonstrated that isomer interconversion did not take place, and the following pathway was shown to apply independently to the production of each of the positional isomers:

hexadecane $\longrightarrow$ hexadecanol $\longrightarrow$ hexadecanone $\longrightarrow$ further products

A mathematical model for the production of 2-hexadecanol and 2-hexadecanone was proposed. The constants of the model have direct physical significance, and they are easily evaluated from the measured product concentrations by the application of simple graphical procedures. The qualitative and quantitative characteristics of the hydrocarbon transformation were described by the following expressions:

$$\frac{dS_A}{dt} = \frac{R}{\phi_A} - k_A S_A \qquad \text{for } t < t^*$$

$$\frac{dS_A}{dt} = \frac{R}{\phi_A} e^{-k_D(t - t^*)} - k_A S_A \qquad \text{for } t \geq t^*$$

$$\frac{dS_K}{dt} = \left(k_A \frac{\phi_A}{\phi_K}\right) S_A - k_K S_K \qquad \text{for } t > 0$$

where

S_A = measured weight fraction of 2-hexadecanol

S_K = measured weight fraction of 2-hexadecanone

t = time, hour.

The physical significance of the model constants is summarized below:

Constant	Physical Significance
R: $\left(\frac{\text{weight}}{\text{fraction}}\right)$ hour^{-1}	Constant rate of reaction: H⟶A
k_A: hour^{-1}	Reaction rate constant: A⟶K
k_K: hour^{-1}	Reaction rate constant: K⟶?
k_D: hour^{-1}	Decay constant denoting the speed of enzyme deactivation for the reaction: H⟶A
t*: hour	Time at which enzyme decay was initiated.
$\frac{\phi_A}{\phi_K}$: dimensionless	Measure of the extent of reaction products localized in the region of the transformation enzymes.

The model expressions contained a term to account for the decay of the enzyme system with time. The results indicated that the measured product concentrations did not reflect the "local" concentrations in the region of the enzymes, and a ϕ factor was introduced to account for this effect.

A Mathematical Model of n-Hexadecane Transformation by an Arthrobacter Species

by

Frank Allen Henning

A THESIS

submitted to

Oregon State University

in partial fulfillment of
the requirements for the
degree of

Doctor of Philosophy

June 1971

APPROVED:

Redacted for privacy

Professor and Head of Department of Chemical Engineering
in charge of major

Redacted for privacy

Dean of Graduate School

Date thesis is presented Dec. 18, 1971

Typed by Donna L. Olson for Frank Allen Henning

ACKNOWLEDGEMENT

The author expresses special thanks to the following institutions and individuals:

The Department of Chemical Engineering, Oregon State University for financial assistance.

The Department of Microbiology, for extension of their facilities.

Dr. Donald Klein and Dr. Charles Wicks, for guidance and friendship.

My wife, Elli, for unfailing support.

TABLE OF CONTENTS

LIST OF TABLES

LIST OF FIGURES

NOMENCLATURE

Symbol	Significance
A	Alcohol; 2-hexadecanol unless otherwise specified.
C_i	Concentration of component i in hexadecane: moles/ml.
H	n-Hexadecane.
K	Ketone; 2-hexadecanone unless otherwise specified.
k_A	Rate constant for conversion of A to K: $hour^{-1}$.
k_D	Decay constant: $hour^{-1}$.
k_i'	Specific rate constant for component i: (ml H) (ml aqueous)/(hour) (mg cells).
k_K	Rate constant for conversion of K to unknown product: $hour^{-1}$.
M_H	Total mass of hydrocarbon: grams.
MW_i	Molecular weight of component i: gram/mole.
nC_{16}	n-Hexadecane.
N_i	Moles of component i.
r_i'''	Specific rate of formation of component i by reaction: (moles i) (ml aqueous)/(hour) (mg cells).
R	Constant total rate of conversion of H to A: weight fraction/hour.
R'	Constant specific rate of conversion of H to A: (moles) (ml aqueous)/(hour) (mg cells)
s_i	Local concentration of component i near the enzyme surface: weight fraction.
$\bar{S}$	Ratio of S_A to S_K at a given time: dimensionless.

Symbol	Significance
S_A	Measured weight fraction of 2-hexadecanol (unless otherwise specified) in n-hexadecane.
S_{AO}	Initial value of S_A.
S_A^*	Maximum value of S_A attained during a run.
S_K	Measured weight fraction of 2-hexadecanone (unless otherwise indicated) in n-hexadecane.
S_{KO}	Initial value of S_K.
t	Time: hours.
t*	Time at which decay of the first-step enzyme was initiated: hours.
W	Dry weight of cells relative to the aqueous phase: mg/ml.
H	Density of hydrocarbon: gram/ml.
ϕ_i	Constant factor relating measurement and local concentrations of component i.

A MATHEMATICAL MODEL OF n-HEXADECANE TRANSFORMATION BY AN ARTHROBACTER SPECIES

INTRODUCTION

The development of a mathematical model normally entails the proposal of a set of equations based on the available theoretical knowledge about the physical situation in question. In setting about the task of mathematically describing a fermentation process, it soon becomes evident that the accepted theory is grounded on surprisingly little physical data. This is a reflection of the complex nature of the physical processes involved in the growth of bacterial cells, and subsequent formation of fermentation products.

The quantitative treatment of cellular growth at the simplest level is usually in terms of the familiar exponential growth rate expression found in elementary microbiology texts. Unfortunately, this expression does not account for the dependence of the growth process on the concentration of nutrients available. For this more complex situation, the quantitative treatment is usually based on the empirical Monod expression developed nearly 30 years ago. While this expression is unable to describe the complete course of the microbial growth process, it is commonly used, and is the best general expression offered to date.

The next level in the quantitative treatment of fermentation processes is the description of product formation. This situation is more complex than the description of cellular growth, since a wide range of qualitative patterns have been observed. The accepted theory is even less well developed than the growth theory, and reliable data is almost non-existant.

It was the intent of the present study to describe the formation of products for the bacterial transformation of hydrocarbons. An additional level of complexity was added, since a two-phase fermentation was involved. In order to eliminate the effect of a changing catalyst mass, a non-growth system was studied. By using this technique, it was intended that the product formation could be described without the usual masking effect of the growth process. The simplest possible mathematical expression consistent with the observed characteristics of the system was sought, with the hope that the resulting model would not only describe the process, but would possess constants having direct physical significance.

LITERATURE REVIEW

This literature review is divided into two main parts. The first section is intended to summarize the major aspects of straight-chain alkane degradation by microorganisms. Emphasis is placed on the qualitative nature of the phenomenon. Special attention is given to subterminal oxidation, since the experimental portion of the present study falls in this category. The second section is concerned with summarizing the current state of the art for the quantitative description of fermentations. This section concludes with a summary of the work aimed at describing the quantitative nature of hydrocarbon utilization. It is the intent of the author that this review place the present study in perspective.

Degradation of n-Alkanes by Microorganisms

Point of Initial Attack

A primary concern in the study of hydrocarbon degradation by microorganisms has been with the mode of the initial attack on the hydrocarbon molecule by the enzymatic system. Fuhs (17) pointed out that the uniqueness of the hydrocarbon degradative process is attributed to this step. After the first chemical attack on the carbon skeleton, the path leading to the point of entry to the conventional degradative pathways of the cell is considered to be relatively short.

Reference here is to microorganisms which are capable of utilizing hydrocarbons as sole sources of carbon for energy and growth, and exceptions to this case will be considered in later discussion.

The overwhelming bulk of accumulated evidence points to an oxidative mechanism for the initial attack on the hydrocarbon molecule. Hansen and Kallio (20) showed, by indirect means, that molecular oxygen was directly involved in the first stages of dodecane oxidation and did not simply act as a terminal electron acceptor. Subsequent research by many workers with oxygen-18 provided unequivocal support that O_2 incorporation occurs in the earliest steps of the oxidation sequence. Furthermore, several workers agree that the first stable product of gaseous alkane oxidation is the primary alcohol (24, 40, 50). Stewart et al. (55) offered evidence that this was also the case for n-hexadecane oxidation by an aerobic gram-negative coccus. Confirmation of these findings was provided by Coon and coworkers (5, 18) who demonstrated that octanol was the first detectable product of octane oxidation by a cell-free system. Details of the various proposed mechanisms leading to alcohol formation can be found in reviews such as those authored by McKenna and Kallio (44) and Foster (13, 15). Since support for each of the various oxidative mechanisms was usually based on evidence for a specific system, a general scheme is not agreed upon, and may not exist. However, there is general agreement that molecular oxygen is incorporated in the initial steps of

oxidation of n-alkanes to form the primary alcohol as the first stable intermediate.

Paths of Further Degradation

Monoterminal Oxidation

The oxidation of alkanes can be subdivided according to the site of attack by oxygen. Generally, oxygenation appears to occur at one end of the alkane molecule, a scheme termed monoterminal oxidation. Zajic (63) postulated that alcohol formation procedes by the formation of a free radical as the precursor. The alcohol is then thought to be oxidized to the corresponding aldehyde or aliphatic acid. The simplest form of this general type of pathway is summarized by Foster (15):

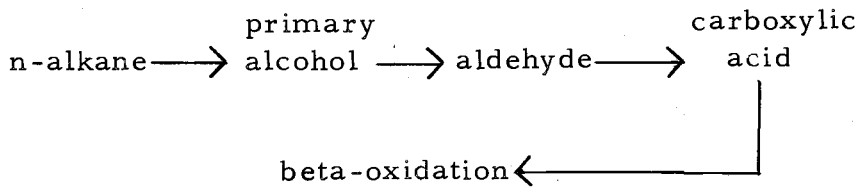

This mechanism has been supported by a number of workers including Famer, Webley and Duff (61), Heringa (23), Proctor (50), and Heydeman (24). For example, Heringa used multiple adaption techniques in demonstrating that a Pseudomonas strain oxidized short chain alkanes (C_2 through C_6) in the order of n-alkane, primary alcohol, aldehyde, and CoA-derivative of the corresponding fatty acid.

Subterminal Oxidation

Growth Systems. The above scheme involves an oxygenative attack at the terminal carbon of the hydrocarbon molecule. There are several examples in the early literature which indicate the detection of methyl ketones, suggesting the possibility of internal oxidation of the carbon skeleton. Chibnall (26), in 1932, found that the fungus Aspergillus versicolor grew vigorously on ketones, although no oxidation products except CO_2 and mycelium were detected when growth took place on n-alkanes. In 1941 Goepfert (19) detected methyl ketones in the fungal degradation of the higher primary and secondary alcohols, and found fermentation products suggesting further utilization of these ketones. Foster (14) later summarized the involvement of methyl ketones in the fungal dissimilation of long chain fatty acids and indicated disagreement in the literature concerning the role of the secondary alcohols as precursers for the ketones. Ladd (38) indicated a vigorous bacterial oxidation of methyl ketones by a Corynebacterium, but suggested that such compounds probably occurred in some activated form in n-alkane degradation, rather than as the free ketones.

In the early years of the 1960's, a study of gaseous alkane utilization by bacteria provided the first significant work on the mechanism of this alternative mode of attack. Leadbetter and Foster (40) studied a Pseudomonas methanica strain which yielded products oxygenated at

the 2- or alpha-position (methyl ketones) as well as products oxidized at the terminal carbon. In both cases, no disruption of the carbon chain occurred. These workers postulated that both of these products arose from a single free radical mechanism for oxidation, as opposed to two simultaneous, independent paths. The following pathway was suggested:

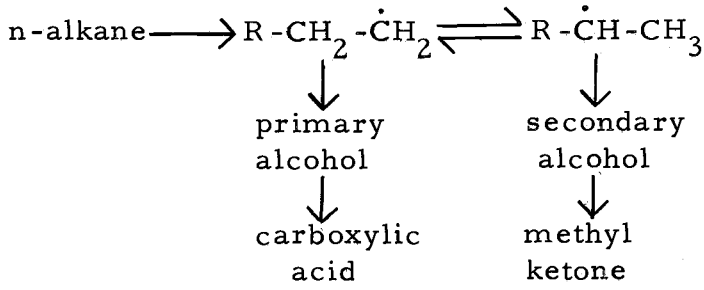

This work was soon extended by Lukins and Foster (43), who conclusively demonstrated the formation of methyl ketones during the oxidation of gaseous hydrocarbons (n-propane through n-hexane). Lukins addressed his work to the problem of whether the methyl ketones were direct intermediates in the reactions of alkane metabolism or simply the side products of the oxidation step. The basic tool of Lukins' work was the technique of simultaneous adaption, developed by Stanier (53). Simply stated in application to this problem, if methyl ketones are intermediates in the metabolism of an alkane, then cells capable of (adapted to) the oxidation of the alkane would also be capable of oxidizing the corresponding methyl ketone. Cells which are not adapted to oxidize the alkanes should thus be unable to utilize methyl ketones.

The work of Lukin conforms to this hypothesis, and this was interpreted as supportive evidence for the contention that methyl ketones are direct intermediates involved in the oxidation of n-alkanes. Although there appeared to be no direct correlation between the capacities to grow on a given alkane and its ketone (subject to the possibility that the ketones may have been toxic at the levels tested), it was found that microorganisms isolated for their ability to grow on the ketones likewise possessed the ability to attack the corresponding hydrocarbon.

There has been no indication of the balance between the terminal and ketone pathways for a given system, but studies of a number of soil bacteria, fungi and actinomycetes carried out by Lukins (43) have shown that methyl ketone production occurs rather commonly. While these results applied strictly the the gaseous alkanes, Foster (15) postulated that similar pathways existed for the degradation of long chain alkanes, and this was later confirmed.

With the exception of the work of Foster and his coworkers which was cited above, the research concerned with production and metabolism of methyl ketones has all been published since 1967. Fredricks (16) studied the production of methyl ketones by a Pseudomonas strain which utilized n-decane as the sole source of growth carbon. The resulting oxidation products included 1-, 2-, 3-, 4- and/or 5-decanol and the corresponding ketones. The quantities

of alcoholic isomers were equally distributed, indicating that the attack on the hydrocarbon molecule was apparently non-specific with respect to the position of oxygen incorporation. As pointed out by Fredricks, the analytical techniques employed by the coworkers of Foster may not have been capable of separating any non-primary isomers present in their experiments; thus, failure to detect such isomers previously might have been an analytical problem. Fredricks considered his results to be compatable with the suggestion of Foster that a free radical mechanism determined the distribution of oxidation products. Additional products of the fermentation (decanoic, nonanoic, octanoic and heptanoic acid) indicated that scission at the keto group followed the production of the ketone.

Markovetz and coworkers concentrated on the elucidation of the means by which methyl ketones are further metabolized. The organism used in the studies of Forney, Markovetz and Kallio (12) was a pseudomonad isolated for its ability to grow on a methyl ketone. The employment of enrichment culture techniques suggested that soil microorganisms capable of methyl ketone utilization are widespread. Interestingly, the isolated microorganisms generally utilized ketones and alcohols more readily than the corresponding alkanes. The fermentation products resulting from growth on 2-tetradecanone were isolated and identified, and a tentative pathway was outlined. It was proposed that the primary attack on the methyl ketone was a

subterminal oxidation. Forney and Markovetz (10) further characterized this system by isolating and identifying undecyl acetate as an intermediate in the degradation of 2-tridecanone. The following pathway was proposed:

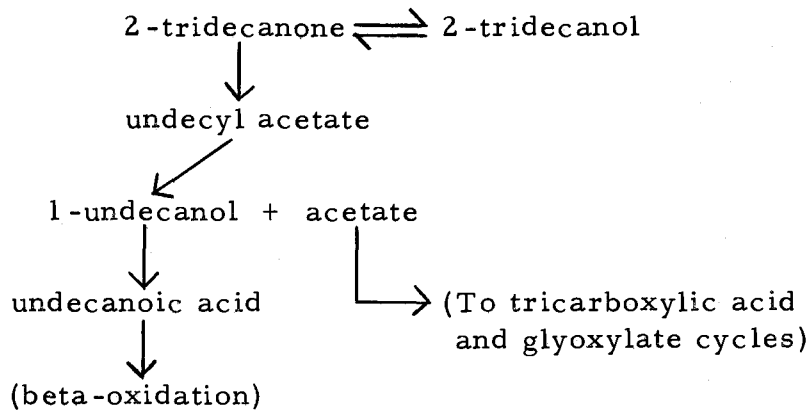

An interesting feature of this system was the apparent interconversion of 2-tridecanone and 2-tridecanol. Growth on either substrate produced the other, in addition to the other indicated products of oxidation. Forney and Markovetz (11) subsequently considered growth of this pseudomonad on n-tridecane and found that the same pathway was operative.

Allen and Markovetz (2) investigated the oxidation of n-tridecane by fungi. Growth of a Penicillium species on this alkane indicated that degradation occurred by a subterminal mechanism analogous to the pathway postulated by Forney and Markovetz.

Non-Growth Systems. All previously-cited work concerning the involvement of methyl ketones and secondary alcohols in alkane

oxidation has referred to bacterial systems capable of utilizing the hydrocarbon as a growth substrate. Methyl ketones have also been observed under circumstances in which the hydrocarbon could not be utilized as a growth carbon source by the microorganism. Klein, Davis and Casida (32) studied the oxidation of alkanes by an Arthrobacter species which required the presence of an additional carbon source for growth. When cells were grown in the presence of yeast extract and n-hexadecane or pentadecane, the corresponding 2-, 3- and 4-ketones were accumulated. The distribution of isomers was found to vary slightly with the length of fermentation and hydrocarbon source. However, for a given time, the ratio of ketonic products was observed to be independent of the supplemental carbon source used. For oxidation of n-hexadecane, the approximate ratio of 2-, 3- and 4-hexadecanone was reported to be 72%, 24% and 4%, respectively. The presence of small quantities of two additional fermentation products was noted, but these were not identified; whether these were products of alkane degradation, or arose from the utilization of the supplemental carbon source was not determined.

Klein and Henning (33) extended this work using an Arthrobacter species isolated from a different source, but possessing characteristics similar to those described above. The microorganism was incapable of utilizing n-hexadecane as a growth carbon source, but transformed the alkane to isomeric ketones as described above. In

addition, the presence of the internal 2- and 3-hexadecanols was confirmed. Experiments indicated that the hexadecanols were intermediates in the formation of hexadecanones, and that after independent formation of the isomeric alcohols, oxidation to the corresponding ketones took place. In contrast to the finding of previous workers, the complete absence of primary alcohols was noted.

Diterminal Oxidation

Until 1962, all alkane oxidations described were terminal or alpha-carbon mono-oxidations yielding the primary alcohol or methyl ketone, respectively. There was no evidence that a distinction was made between the two similar terminal methyl groups of a n-alkane. Once a terminal oxygenative attack is made, however, the terminal methyls become distinguishable; it was found that the enzyme systems involved are sensitive to this difference. Thijsse and Van der Linden (57) found that oxidation by a Pseudomonas on 2-methylhexane formed a mixture of 2-methylhexanoic and 5-methylhexanoic acids. They concluded that the microorganism did not initially distinguish between the ends of the molecule; however, once oxygen had been incorporated, the unoxidized terminal methyl groups became recognizable and remained unattacked. Thijsse (58) and Heringa (23) both found support of the monoterminal mechanism, but rejected the possibility of a diterminal scheme.

In 1962, Kester and Foster (31) substantiated the first instance of a microorganism (genus Corynebacterium) which lacked the ability to discriminate between the ends of long-chain hydrocarbon molecules. It was observed that both terminal groups were oxidized via diterminal oxidation (often called omega-oxidation) without change in the carbon skeleton. The mechanism consisted essentially of monoterminal oxidation of an alkane to its fatty acid followed by omega-oxidation of this fatty acid to yield a dioic acid. In effect, this consisted of two successive monoterminal oxidations. It was not decided if the fatty acid was required for the omega-oxidation, or whether the primary alcohol sufficed. However, it was postulated that the oxidized nature of the remote end of the molecule probably had little effect on an omega-methyl oxidation of the other end. The fact that the dioic acids have not been produced from alkanes with fewer than ten carbon atoms might be construed to mean that the "remoteness" of the oxidized end is necessary for the enzyme system to accept the omega methyl. Another possibility is that dioic acid is produced from the shorter chains, but simply does not accumulate in detectable amounts.

Kester and Foster found that long-chain dioic acids could serve as the sole carbon and energy sources for the growth of Corynebacterium, and investigated whether the diterminal acid was a necessary intermediate in alkane utilization, or was simply involved in a minor,

secondary pathway. In general, they concluded that evidence indicated that this was probably a minor pathway related to the monoterminal acid as shown:

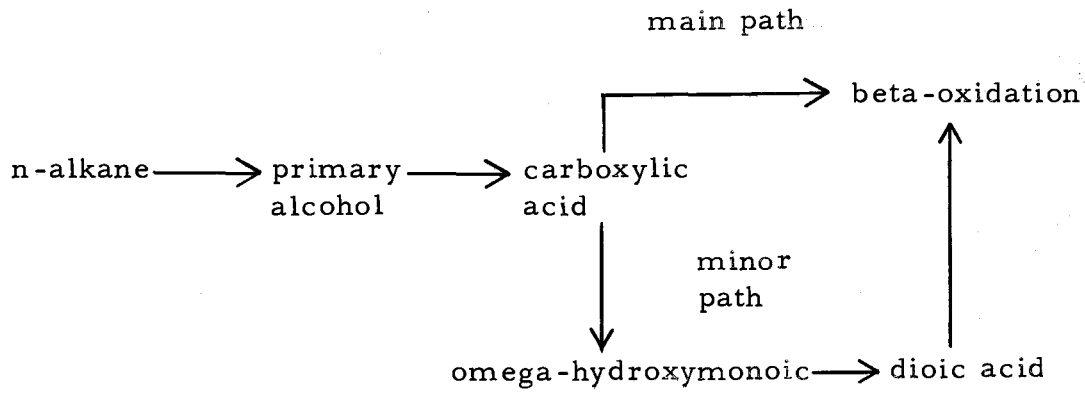

The diterminal pathway proposed above has been confirmed by Kahn (29) with a Pseudomonas which produced n-octane-dioic acid from n-octane. A more recent confirmation was made by Iida (28). Working with a Candida strain and decane as the sole carbon source, dioic acid was formed by a path identical to that shown above.

Ester Formation

Stewart and Kallio (55) have worked with a gram-negative coccus which utilized long-chain alkanes as a sole carbon source, producing appreciable quantities of long-chain esters. The acid portion of these waxes was palmitic acid, with the alcohol moiety possessing the same carbon skeleton as the substrate paraffin. For example, experiments with oxygen-18 showed that the oxidation of hexadecane occurred as

follows:

$$2\ CH_3(CH_2)_{14}CH_3 + 2\ O_2^{18} \longrightarrow CH_3(CH_2)_{14}\overset{\overset{O}{\|}}{C}\text{——}O^{18}\text{——}(CH_2)_{15}CH_3$$

(18, 16)

Finnerty and Kallio (54) later made a study of the origin of palmitic acid carbon in the esters formed from hexadecane and tetradecane when acted upon by the microorganism Micrococcus cerificans. It was demonstrated that hexadecane was oxidized at the C-1 position, the cetyl alcohol and palmitic acid thus formed being directly esterified. This was in line with the earlier findings discussed above.

Summary of n-Alkane Degradation

The significant points of straight-chain, saturated hydrocarbon metabolism are summarized below. For the sake of clarity, only the carbon skeleton is indicated:

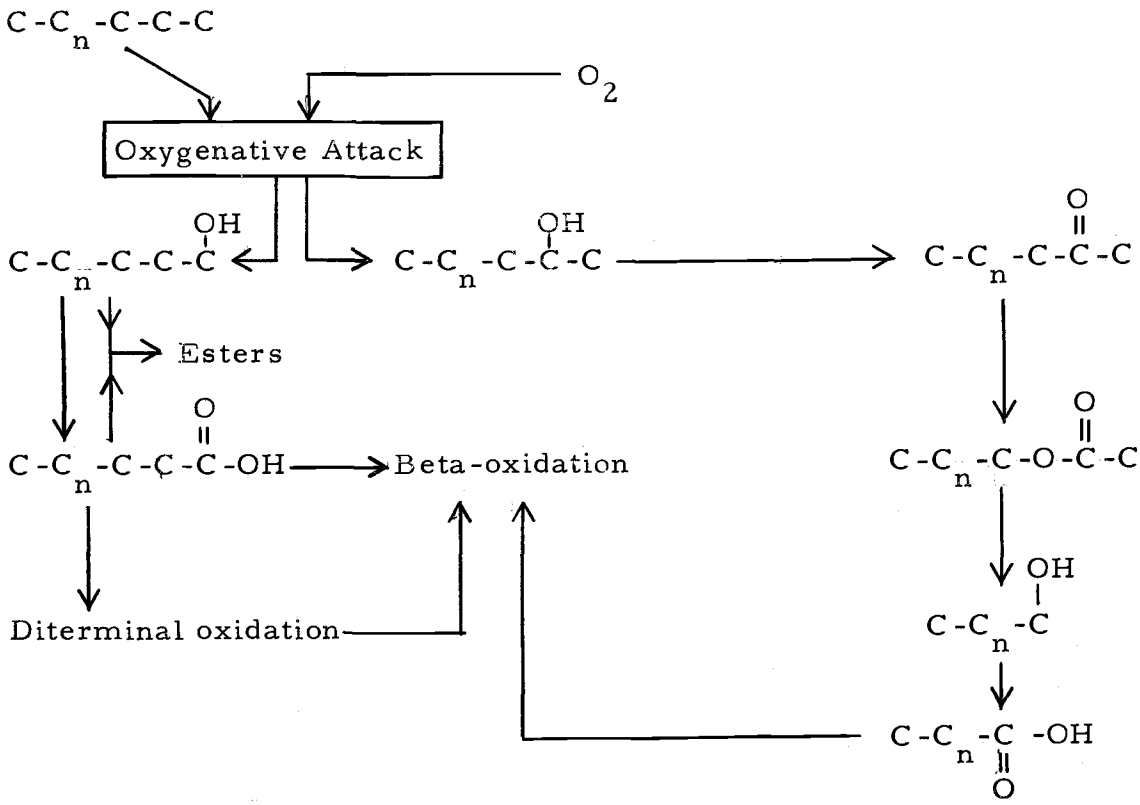

It is emphasized that this diagram is a summary of the major aspects of alkane degradation which have been reviewed. It represents the findings of many workers in studying a variety of systems, and it should not be construed to mean that the indicated pathways act simultaneously in any particular instance.

Fermentation Kinetics

Pure-Enzyme Kinetics

It is helpful to briefly trace the development of the expression commonly used to describe the action of a pure, isolated enzyme on a single substrate. A reaction product, P, is assumed to be the

result of conversion of the reactant "substrate", S, by reaction on the surface of the enzyme, E. The conversion procedes via the formation of an enzyme-substrate complex, ES. Michaelis and Menten suggested a general theory for the enzyme kinetics of this reaction which will be outlined here. Detailed discussion and extension of these results is readily available in various texts on the subject (48, 62). The basic scheme assumed by Michaelis and Menten in their development was:

$$E + S \underset{k_2}{\overset{k_1}{\rightleftharpoons}} ES \underset{k_4}{\overset{k_3}{\rightleftharpoons}} P + E$$

where k_1, k_2, k_3, and k_4 are the rate constants for the indicated reaction steps. The reactant substrate is assumed to be in excess with respect to enzyme in this development. Utilizing the "steady state" assumption, which postulates that the rate of change of the concentration of ES with respect to time is zero, leads to the following expression:

$$v_o = \frac{v_{max}[S]}{K + [S]}$$

where

v_o = the initial rate of production of P

v_{max} = maximum possible initial rate of production of P

[S] = concentration of substate, S

$K = \frac{k_2 + k_3}{k_1}$ = Michaelis constant

Many of the assumptions implicit in the derivation of the Michaelis-Menten equation are open to question, as pointed out by Walter (59). In addition, it is emphasized that the expression only gives an indication of the initial rate of product formation. However, the quantitative behavior of enzyme systems often conforms experimentally to this form, and it is widely used as the basis for modeling enzymatic reactions.

Cellular Kinetics

Since the physical situation obtained during the production of metabolites by a cell is obviously considerably more complex than the interaction of a pure enzyme and substrate, it is not surprising that the study of cellular kinetics is chiefly empirical and poorly developed. The qualitative nature of the problem has been adequately treated in the review of Luedeking (41), who has summarized the various qualitative classification schemes for fermentations. Relative to the study of chemical kinetics, the quantitative aspects of the kinetics of fermentation processes are largely unexplored.

Production of Cells

Most study of fermentation kinetics has been concerned with processes for which the primary product is cellular tissue, and this is often the simplest case to treat mathematically. The basis of the mathematical treatment is an expression set forth by Monod (46) in 1942. Monod's expression takes the following form:

$$\frac{1}{[C]}\frac{d[C]}{dt} = \mu = \mu_m \frac{[S]}{K + [S]}$$

where

μ = specific growth rate

$[C]$ = cell concentration

t = time

μ_m = maximum growth rate for large S

$[S]$ = concentration of the limiting growth nutrient

K = a constant

Monod further postulated a simple relationship between cell growth and utilization of the substrate. For the case of a growth medium containing a single organic substrate (e.g., glucose and salts), Monod stated that the growth rate is a constant fraction, Y of the substrate utilization rate:

$$\frac{d[C]}{dt} = -Y \frac{d[S]}{dt}$$

where Y is called the yield constant. For a finite period of time,

$$\frac{\text{weight of cells produced}}{\text{weight of substrate utilized}} = Y$$

Based on the theory of Monod, the determination of μ_M, K and Y provides all of the information needed for the quantitative description of bacterial growth and substrate utilization.

While the expression of Monod takes the form of the Michaelis-Menten expression, it is emphasized that the Monod equation is empirical in nature; the form was assumed because it exhibits mathematical characteristics compatable with the observed growth pattern of many bacterial growth systems.

Many examples of the application of the Monod-type equations can be found in the literature and only typical examples are indicated here.

Knowles (34) applied this theory to the growth of nitrite- and ammonia-oxidizing bacteria in batch culture. The resulting model closely followed the experimental data, and the author was able to determine the effect of temperature and dissolved oxygen level on the kinetic constants. Knowles pointed out that the ammonia-oxidizing system of the Nitrosomonas species studied was thought to be effectively situated in the external medium. Consequently, a pure enzyme-substrate reaction was approximated and the system was expected to

conform well to the model expression patterned after the Michaelis form.

Aiba and coworkers (1) applied the theory of Monod to the growth of Azotobacter vinelandii on glucose in continuous culture. The model constants were evaluated from batch culture experiments and were then used to predict the results of continuous culture. In addition to successfully simulating the cellular growth and concentration, analysis of the yield constant and the specific growth rate allowed determination of the fractions of substrate used for growth and cellular maintenance.

Andrews (3) proposed a more general form of the Monod expression for the case of microorganisms utilizing substrates inhibitory at high concentrations. The functional form suggested was:

$$\frac{\mu}{\mu_m} = \frac{1}{1 + K/[S] + [S]/K_i}$$

where K_i is the parameter accounting for inhibition. This model has not been applied to experimental data. However, a qualitative evaluation indicates that the function is capable of describing the lag observed with growth of bacteria on substrates at concentrations which are inhibitory. The form of the expression is similar to equations used to describe competitive inhibition of pure enzyme-substrate reactions.

Kono (36) took exception to the Monod theory, emphasizing that the yield "constant" often varies throughout the course of an experimental fermentation. In addition, he pointed out that the Monod theory is incapable of describing the characteristics of the lag, induction and transient periods of cellular growth. Kono approached the problem from the standpoint of chemical kinetics. He wrote a general expression for the growth of microorganisms in terms of n^{th} order expressions for the cell concentration, the limiting substrate concentration and a "substance" which represented the overall activity of enzymes produced during cellular growth. Through a series of assumptions and manipulations, the general expression was reduced to four relatively simple equations representing the various growth regions. A basic assumption in the development was that the effect of the growth substrate concentration is expressed only in the declining phase. Consequently, the author's expression for the logarithmic growth region reduced simply to an expression of constant specific growth rate. No experimental verification on the part of the author was attempted, but the model equations were applied, via simple graphical procedures, to a number of experimental studies in the literature. The equations were flexible, simple to apply and capable of fitting the illustrated experimental studies with good results.

Powell (49) has commented on other empirical expressions, such as those put forward by Tissier (56) and Moser (47). These

expressions were of the form:

$$\frac{\mu}{\mu_m} = 1 - e^{-k[S]} \qquad \text{(Teissier)}$$

and

$$\frac{\mu}{\mu_m} = \frac{[S]^r}{K + [S]^r} \qquad \text{(Moser)}$$

where k and r are constants. Powell pointed out that the Teissier form is difficult to handle mathematically and that the expression of Moser is physically unrealistic as S approaches zero. Powell suggested that the form proposed by Monod is more likely applicable to the concentrations of substrate inside the organism and suggested that the external concentration is given by:

$$[S] = \frac{K\mu}{\mu_m - \mu} + \phi \frac{\mu}{\mu_m}$$

This is simply obtained by solving the original expression of Monod for [S] and adding the term $\phi \frac{\mu}{\mu_m}$. The factor ϕ was added to account for permeability and diffusional resistances encountered by the substrate molecules in reaching the interior of the cell. No experimental verification was offered by Powell.

For completeness, the modeling technique proposed by Edwards and Wilke (7) is considered. These workers also realized the limitations of the Monod expression in describing the various regions of

cellular growth, and sought a more flexible function for the description of batch culture data. A generalized "logistic" equation was proposed. The form of this expression was as follows:

$$y = \frac{K}{1 + \exp F(t)}$$

where

K = constant

F(t) = a polynomial n^{th} order in t

t = time

This expression was applied to a wide variety of experimental data from the literature, and the flexibility of the logistic equation was readily apparent. The authors pointed out the advantages in using the expression to differentiate and manipulate data, as well as its utility as a means of data storage. The principle disadvantage of the method is the necessity of using a non-linear regression technique to evaluate the constants of the model. In addition, the model constants have limited physical significance.

Formation of Products

Luedeking and Piret (42) developed a model for product formation in their kinetic study of the batch lactic acid fermentation. These authors pointed out the dearth of reliable kinetic rate data in the field of fermentation. The later use of their data in several theoretical

studies by other workers is a tribute to their experimentation. The experimental system was wisely chosen for its characteristically simple conversion of a single reactant to a single product with negligible intermediate accumulation or side reaction. As a result, reliable data were obtained for the rate of nutrient (glucose) disappearance, product (lactic acid) formation and cellular production.

In the treatment of the data, the authors pointed out that one of two assumptions is usually made in relating product formation to cellular growth. The first assumption is that the rate of product formation is proportional to the number of bacteria present. Mathematically, this requires that $\frac{1}{[C]} \frac{d[P]}{dt}$ is constant, where $[P]$ represents the product concentration and $[C]$ was previously defined as the cell concentration. The specific rate of product formation, $\frac{1}{[C]} \frac{d[P]}{dt}$, is analagous to the specific growth rate. The physical interpretation of this requirement is that the bacteria maintain the same level of metabolic activity throughout the fermentation. The second possible assumption is that the rate of product synthesis is proportional to the rate of cellular production. This requires the value of $\frac{d[P]}{d[C]}$ to be a constant, and is analagous to the definition of the cell yield coefficient, Y, which related the substrate level to the cell yield. The authors found that neither of these assumed relationships were compatible with their experimental data, but that a combination of the two relationships was satisfactory. Luedeking and Piret

assumed the form

$$\frac{d[P]}{dt} = a\frac{d[C]}{dt} + b[C]$$

as a model for the data, where a and b are constants of proportionality. If both sides of this expression are divided by C, the model equation is seen to be an expression of linearity between the specific growth rate and the specific rate of product formation. The data were observed to follow this relationship quite closely.

Koga and Humphrey (35) have successfully simulated a batch gluconic acid fermentation. The growth of Pseudomonas ovalis on glucose results in the production of cells and gluconic acid. The gluconic acid is produced by non-enzymatic hydrolysis of the enzymatically formed intermediate, gluconolactone. The production of cells in this fermentation was described by an expression of the form of Monod, using a non-constant value for μ_m; for purposes of the simulation, experimental values of μ_m as functions of time were used. The non-enzymatic hydrolysis was demonstrated to be a first order process, but a Monod-type expression was used to describe the enzymatic production of lactone. Lactone production was modeled as follows:

$$\frac{d[L]}{dt} = k_m \frac{[S]}{K_L + [S]} [C] - k_3[L]$$

where

$[L]$ = concentration of lactone

t = time

$[S]$ = concentration of glucose (growth substance)

$[C]$ = cell concentration

$k_3[L]$ = rate of non-enzymatic hydrolysis of lactone

The value of K_L was determined to be constant. Similarly, the value of k_m was constant for the first eight hours of the 12-hour fermentation, but deviation from this value occurred in the final hours of the experimental runs. This deviation was attributed to inhibition. For purposes of simulation, no attempt was made to obtain a quantitative equation describing the time variation of k_m. Rather, the data was smoothed, and the coordinates of the resulting curve were used in the digital simulation. The solution to the set of differential equations comprising the process model was found using a standard "canned" program on a digital computer. The authors interpreted the good match of the model and the experimental data as justification for confidence in the kinetic model. However, while the accomplishment of fitting a model to such data should not be minimized, it is emphasized that the Monod form was forced to fit the data by allowing variation of μ_m and k_m to that end. Thus, physical interpretation of the model is subject to question.

Kono and Asai (37) extended the previously cited work of Kono

to allow description of the product formation, as well as the cellular growth. The technique of Kono was used to model production of cells and the rate of formation of product was expressed by a general equation which considered $\frac{d[P]}{dt}$ to be proportional to the concentration of cells. Two terms were included to allow for product formation from either growing or non-growing cells. The model reduced to a set of equations which applied to the various growth regions, and allowed for a wide variety of qualitative relationships between cellular growth and product formation. The flexibility of the model was illustrated by application of the derived expressions to experimental studies from the literature.

Shu (52) developed a model of product formation based on the premise that the metabolic characteristics of an individual cell are a function of the age of that cell. He suggested a quantitative model for product formation by an individual cell, and then related this to the overall product accumulation by estimating the cell-age distribution of the total population in the vessel. Shu approximated the individual cellular rate of product formation by means of a sum of exponential terms and obtained the cell age distribution from the growth curve. He successfully applied his method to the data of Luedeking and to other fermentation data available in the literature.

Although the method of Monod is the most widely used expression for modeling fermentation growth processes, it should be apparent

from the above discussion that no single approach is accepted as suitable for the description of the complex nature of the microbial growth process. Furthermore, most of the treatments proposed to date are basically empirical, although the model constants are related to the physical characteristics of the gross culture in some cases. The treatment of product formation generally follows an approach analogous to the theory that Monod applied to cellular growth.

A considerable bulk of experimental knowledge about hydrocarbon fermentation is in the literature, but very little specific information concerning the quantitative description of such processes is available. The small amount of work that has been undertaken in this area has been concerned exclusively with cellular growth, and this author is aware of no attempt to quantitatively describe the formation of products of hydrocarbon degradation.

Dunn (6) has proposed an experimental technique for differentiating between growth in the aqueous phase and growth at the hydrocarbon-water interface. The basic assumption of Dunn is that regardless of where the cellular growth takes place, it can be described by a logarithmic rate expression. For the case of interfacial growth, the growth expression was written in terms of the interfacial cell concentration, which was then related to the concentration in the aqueous phase by means of a Langmuir isotherm-type expression. By considering the limiting cases, Dunn demonstrated that for high cell

concentrations, the interface is saturated with cells, and the growth rate is proportional to the interfacial area and independent of the total cell population. For very small cell concentrations, the growth rate becomes directly proportional to both the interfacial area and the cell concentration.

This interfacial model was contrasted with the homogeneous model, in which cells have access to the hydrocarbon only in the dissolved form. This situation is distinguishable from the interfacial case by virtue of the fact that the growth rate is independent of the interfacial area at low cellular concentrations. The author attempted no experimental verification of the postulated relationships. It should be mentioned that while the author accepted Monod's relationships for relating the specific growth rate to the substrate concentration, he suggested working under experimental conditions for which the specific growth rate, μ, is constant.

Humphrey and coworkers, in a series of theoretical studies, proposed growth models for batch cultures with two liquid phases. Erickson, Humphrey and Prokop (8) considered several cases for the general situation in which a growth-limiting substrate was dissolved in the dispersed phase and the interfacial area remained constant. The various cases involved different growth regions and can be summarized as follows:

(1) The case for which growth is entirely interfacial.

(2) The case for which growth occurs both interfacially and in the bulk of the aqueous phase, with equilibrium of the substrate between the two phases.

(3) The case for which there is both interfacial and homogeneous growth, with mass transfer of substrate limiting the growth in the continuous phase.

The defining conditions for the physical situations considered required several different significant assumptions, but the specific growth rate was assumed to follow the theory of Monod. Conventional mass transfer theory was used to describe interphase substrate transfer in terms of a concentration driving force.

Erickson and Humphrey (9) extended the study to the growth of cells on a pure substrate in the dispersed phase. In this situation, the concentration of substrate remained constant, but the interfacial area changed during the course of the fermentation. Using the approach outlined above, the model equations were developed for the same three cases considered in the first study. Various dispersed-phase drop number and size distributions were considered.

In both of these studies, the qualitative nature of the model equations was examined. Where possible, the authors compared the models with data available from the literature. These comparisons were generally favorable, although no experimental attempt was made on the part of the authors to verify the validity of the many assumptions involved in the model equations.

PROCEDURES

Experimental Run

Regular Run

The microorganism used throughout the study was an Arthrobacter species, ATCC 25581. The bacterium was isolated for its ability to chemically transform hydrocarbons which could not be utilized as sole sources of carbon for growth. Details concerning the isolation of the bacterium are found in reference (33).

A schematic outline of the procedure used for a typical resuspended cell run is shown in Figure 1. The summary sheet found in Appendix I notes specific deviations from the following procedure for all experimental runs. The inoculum source for each run was a streak plate of the microorganism grown on plate count agar. The source of this plate was the inoculum vessel for the previous run. A loop from a pure colony of Arthrobacter on the source plate was transferred to a standard 2-liter Pyrex aspirating bottle containing 1500 ml of sterile mineral-salts medium and 1% (weight/volume, w/v) yeast extract; the composition of the mineral-salts medium used in all cases is given in Table 1. The top of the inoculum vessel was cotton stoppered and a standard ground-glass joint was connected to the bottom outlet with rubber tubing which was sealed by a pinch clamp.

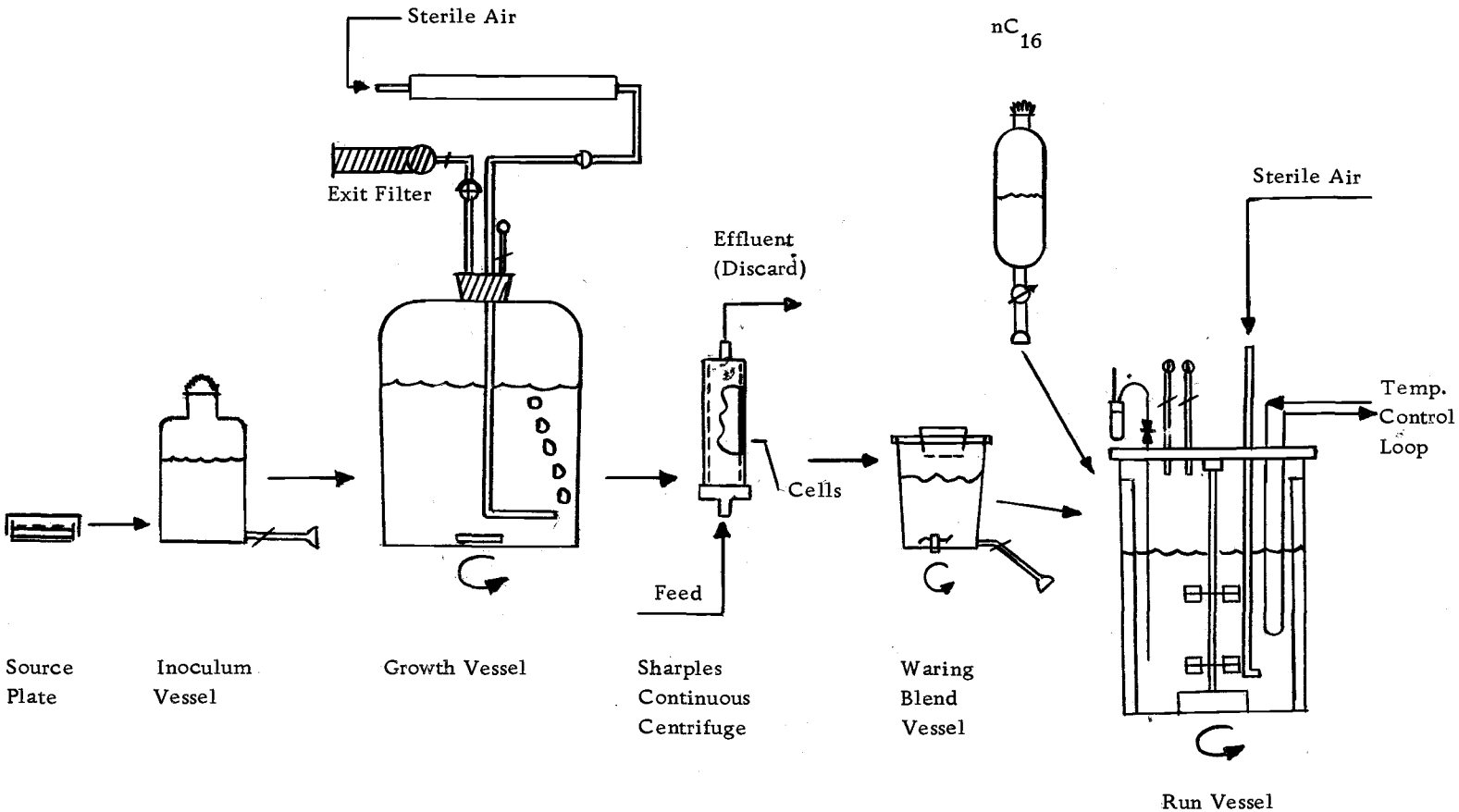

Figure 1. Schematic of resuspended cell run.

The ground-glass joint was cotton-covered and foil-wrapped to maintain sterility after autoclaving. Similar ground-glass joints were used throughout the procedure to facilitate the transfer of culture media between vessels. In order to maintain sterility during transfer, the foil and cotton were removed from the male and female joints, the glass flamed with a Bunsen burner, and the parts joined with a standard clamp. Aeseptic transfer between vessels was always made in this manner and details will not be repeated in the following description.

Table 1. Mineral-salts medium (for ten liters of distilled water).

Reagent grade salts	Grams
K_2HPO_4	7.600
KH_2PO_4	7.600
$MgSO_4 \cdot 7H_2O$	3.800
$CaCl_2$	0.065
$FeSO_4 \cdot 7H_2O$	0.065
$NaNO_3$	36.000

The inoculum vessel was placed on a standard New Brunswick rotary shaker set at a speed of 160 rpm. The period of incubation was 48 hours at room temperature, after which the culture contents were transferred through glass joints to the growth vessel.

The growth vessel was a 20-liter, Pyrex carboy. The top was fitted with a rubber stopper containing three 3/8 inch o.d. glass tubing ports, each connected to ground-glass joints. Two of these ports terminated just below the stopper on the vessel interior. The third length of tubing reached to the bottom of the vessel and extended six inches radially. This long tubing acted as a sparger for air during the incubation of the growth vessel. Prior to inoculation, this vessel was charged with 12.0 liters of mineral-salts medium and 0.75% (w/v) certified grade (Difco) yeast extract. A calcium chloride type drying tube was packed with cotton and attached to one of the short, jointed outlets to provide venting during sterilization and to act as an exhaust filter during the growth period. The sparge tube and remaining inlet were clamped and the vessel was autoclaved in toto and cooled to room temperature. A three inch, nylon-coated magnetic stirring bar was included in the vessel to provide agitation. Before transfer of the inoculum to the growth vessel, a pre-sterilized filter was placed between the air inlet of the growth vessel and a sterile air source. The filter consisted of a piece of stainless steel tubing one inch in diameter and 14 inches long which was packed with glass wool. Just before addition of the growth inoculum, sterile air was supplied to the vessel at 1.75 liters/minute and a magnetic stirring unit beneath the vessel was turned on at a speed of 240 rpm.

The air for the growth vessel was supplied by tapping the

air-supply system of a 30-liter New Brunswick Model CF-50 "Fermacell" fermentor. Air from a compressor was fed to an incinerator unit which heated the air to 900°C, and then cooled it to room temperature. This sterile air was then passed through a rotameter to the filter described above. Yeast extract normally tends to produce heavy foam under conditions of high aeration, however, natural cellular products depressed the foaming adequately, and antifoam agent was not required during the growth stage.

The inoculum was added through the free short port, which was then sealed for the duration of the vessel use. After addition of the inoculum, a purity check streak plate was made from the inoculum vessel. The growth vessel was allowed to incubate for 48 hours. At the end of this growth period, the entire vessel contents were fed to a continuous Sharples centrifuge. The effluent from the Sharples was discarded. The centrifugation process required about 25 minutes, after which the cells were removed aseptically from the bowl and transferred to a blend vessel. This transfer was accomplished by using a stainless steel scraper blade constructed from 3/16 inch stainless steel sheet. The blade was one inch wide, with a sharpened leading edge which fit flush against the wall of the bowl from bottom to top. The bowl top was removed, the blade was inserted and the bowl was rotated so that the cells were scraped from the bowl sides onto the blade. The blade was previously sterilized in an autoclavable plastic

bag of the type available from Cedanco (Framingham, Mass.). To avoid contamination, the mouth of the bag was placed over the open end of the bowl and the scraper was handled through the bag during this procedure. The bag mouth was then placed over the blend vessel opening and the cells were scraped from the blade with the aid of a small stainless steel spatula also contained in the bag.

The blend vessel was a slightly modified Pyrex one-quart Waring blender vessel. The conventional plastic stopper in the rubber top plate was replaced by an autoclavable rubber stopper, and a glass outlet tube was fused to the side at the vessel bottom to facilitate transfer of the contents to the run vessel. The assembly was filled with 500 ml of distilled water, autoclaved and cooled prior to transfer of cells from the Sharples bowl. After addition of the cells, the blend vessel was sealed and placed on the Waring Model DL 202 blender base. Operation at the low setting for 60 seconds completely homogenized the cell cake in the distilled water. A calibrated scale attached to the side of the blend vessel allowed an accurate measure of contents delivered to the run vessel.

The run units used in this work were Model MA14F1 benchtop, magnetically-driven fermentors manufactured by Fermentation Design (Allentown, Pennsylvania). The 14-liter capacity baffled vessels supplied with the units were manufactured by New Brunswick Scientific Co. (New Brunswick, N.J.), and are pictured in Figure 2. The two

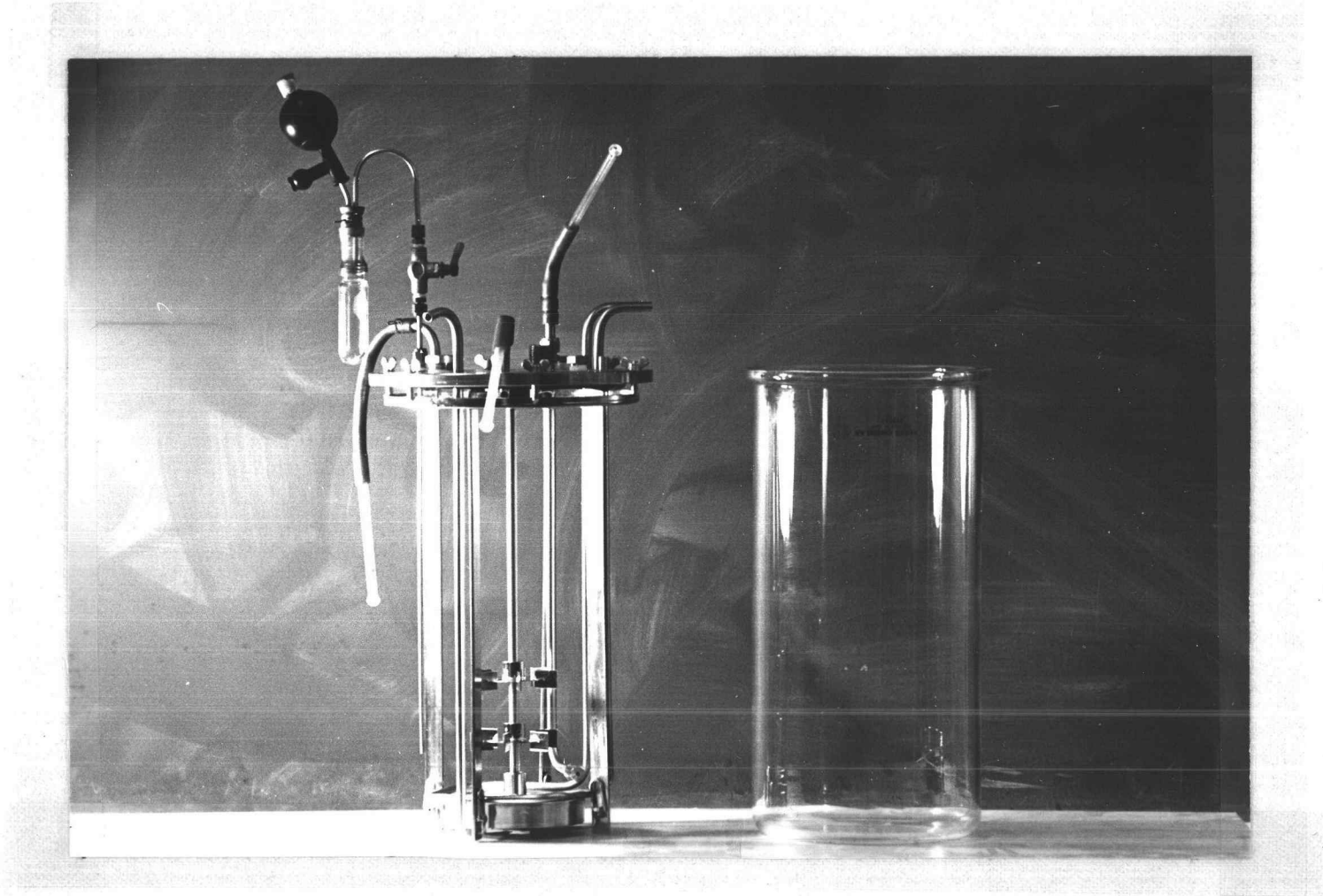

Figure 2. Run vessels used in the experimental study.

six-vaned impellors were set at 10 and 14 inches from the top plate in all runs; agitation was quite vigorous and mixing was visually judged to be excellent.

Before addition of blend contents to the run vessels, the two fermentors were each charged with seven liters of mineral-salts medium. The nitrogen-containing salt was excluded from this medium to minimize protein synthesis during the run. A one-inch port was plugged with cotton to act as a vent during the autoclaving and run periods. The sparge inlet and three 3/8-inch ports were fitted with rubber tubing and glass joints and prepared for sterilization as previously described. The entire vessel was autoclaved for 90 minutes at 15 psig and 110°C and then cooled. Before initiation of the run, the temperature control system was connected to the vessel and the temperature was brought to 30°C ± 0.5°C. Sterile air was supplied as it was to the growth vessel, with the exception that two stainless steel,packed tubes in series were used as finishing filters before entry to the run vessels. The air rate was 4.0 liters/minute with the magnetic drive unit at 400 rpm.

After completion of the blend, the cell concentrate was equally split between the two run vessels. Five minutes was allowed to provide a uniform cell suspension before a 50 ml sample was drawn from each vessel; this sample was refrigerated and later used to determine vessel pH and cell concentration. A 320 ml volume of n-hexadecane,

nC_{16}, was previously measured into a graduated separatory cylinder; the top opening was cotton-stoppered and the bottom was fitted with a glass joint. The hydrocarbon vessel was autoclaved for 15 minutes and cooled. The run was initiated with the addition of 160 ml of nC_{16} to each vessel. This was marked as time zero, and a sample for hydrocarbon analysis was immediately drawn. Separate hydrocarbon vessels were used for the two run vessels in the runs where an additive reaction product was contained in the nC_{16}.

Growth Run

The above-outlined procedure is valid for resuspended cell runs. In the case of growth runs, the growth vessel, centrifugation and blend steps were eliminated. A 50 ml seed flask containing 1% (w/v) yeast extract in mineral-salts medium was grown for 48 hours; a ten ml volume of this culture was pipetted aseptically into one liter of 1% (w/v) yeast extract in mineral-salts medium; this was incubated for 48 hours, and corresponded to the inoculum vessel step described in the above procedural outline. The entire contents of this vessel were then transferred to a single Fermentation Design unit containing five liters of 1% (w/v) yeast extract and 150 ml of nC_{16} which were added before cell addition. Time zero for the run was taken as the time of addition of the inoculum to the run vessel.

Sampling

Samples were drawn into Pyrex, heavy-walled centrifuge tubes by applying suction to a 1/8 inch stainless steel tube which extended into the vessel. Prior to drawing each nine ml sample for analysis, the stainless tube was flushed with a nine ml volume which was discarded. The centrifuge tubes were cooled in a freezer at -5°C prior to sampling, and returned immediately after the sample was drawn. The cell-containing hydrocarbon layer rapidly separated to the top of the sampling tube and solidified after about one minute. The aqueous portion of the sample was completely frozen in less than five minutes. Samples were stored in this form until the termination of the run, when they were prepared for analysis.

In the preparation of the samples for chromatographic analysis, the tubes were removed from the freezer and rapidly thawed in warm water. One milliliter of petroleum ether was added to each tube and the sample group was placed on a rotary shaker at 100 rpm for ten minutes to allow adequate contacting of the solvent. The method of extraction did not appear to influence the detected levels of reaction products. After extraction, the solvent layer containing the hydrocarbon was drawn off with a clean liquid dropper and placed in 1/4 x 1 inch sample tubes. These tubes were placed in a hood overnight to evaporate the petroleum ether solvent, and then stored in a refrigerator at +2°C until the chromatographic analysis. No cellular material

was visible in these extracts. The final hydrocarbon sample size was 0.1-0.2 ml.

Chromatographic Analysis

Specifications

The gas chromatograph used in all phases of this work was an Aerograph (Varian Aerograph, Walnut Creek, Cal.) Hy-Fi III Model 1200 single-column unit with a flame-ionization detector. The injector was fitted to allow on-column injection of samples. Nominal sensitivity of the unit was reported as 10^{-10} grams in the instruction manual specification list.

The recorder used with the Aerograph chromatograph was a Barber-Colman (Wheelco Instrument Division, Rockford, Illinois) Model 8000-2600-15 with a useable full-scale width of 11 inches and a chart speed of 0.845 inches/minute.

Hamilton (Hamilton, Whittier, Cal.) one microliter, series 7000 syringes were used for sample injection.

The materials used in connection with the chromatographic analysis are noted in Table 2.

The chromatographic columns used were five-foot x 1/8-inch stainless steel, containing 10% FFAP (by weight) stationary phase on 100/120 mesh Chromosorb "W" solid support. The packing was

prepared by coating 25.0 grams of the Chromosorb "W" support with 2.50 grams of FFAP. About 14 ml of packing per ten feet of column length were required. Before use, the column was conditioned at 200°C with an Argon carrier flow rate of 30 ml/minute for 24 hours.

Table 2. Chromatographic materials.

Item	Specifications
Column tubing	1/8 inch o.d., .020 inch wall, 321 stainless
Support material	Chromosorb "W" A/W 100/120 mesh #82-000044-00 Varian Aerograph, Walnut Creek, Cal.
Stationary phase	FFAP 82-001350-00 Varian Aerograph
Gases	H_2, Air NCG (Chemetron), Chicago Ar (carrier), 99.995% NCG
n-hexadecane	99% purity Humphrey Chemical Co. Lot No. 273 (9-8-68) New Haven, Connecticut 281 (3-17-70)
2-hexadecanol	High purity; Lot No. 7553 K & K Lab., Plainview, N.Y.
3-hexadecanone	High purity; Lot No. 6864 K & K Lab.

Column Characteristics and Sample Analysis

The optimal operating conditions for the chromatograph are summarized in Table 3.

Table 3. Summary of chromatograph operating conditions.

Column (oven) temperature	190°C (isothermal)
Injector temperature	230°C
Detector temperature	280°C
Carrier flow rate	27 ml/min
Range	10^{-12} amp/mv (range of maximum sensitivity)

The hydrocarbon samples analyzed consisted of nC_{16} containing the 2-, 3- and 4-positional isomers of hexadecanol and hexadecanone as reaction products. These reaction products were present in very low concentrations relative to the nC_{16}; hexadecanones reached the order of magnitude of 10^{-3} weight fraction while hexadecanol reached a maximum concentration on the order of magnitude of 10^{-4} weight fraction. A typical chromatographic trace is shown in Figure 3. The retention times indicated on the figure are relative to the first solvent peak, which was a remaining trace of the petroleum ether used in the extraction of the samples. The large second peak is n-hexadecane, the reaction substrate. The next three peaks, in order of elution, are

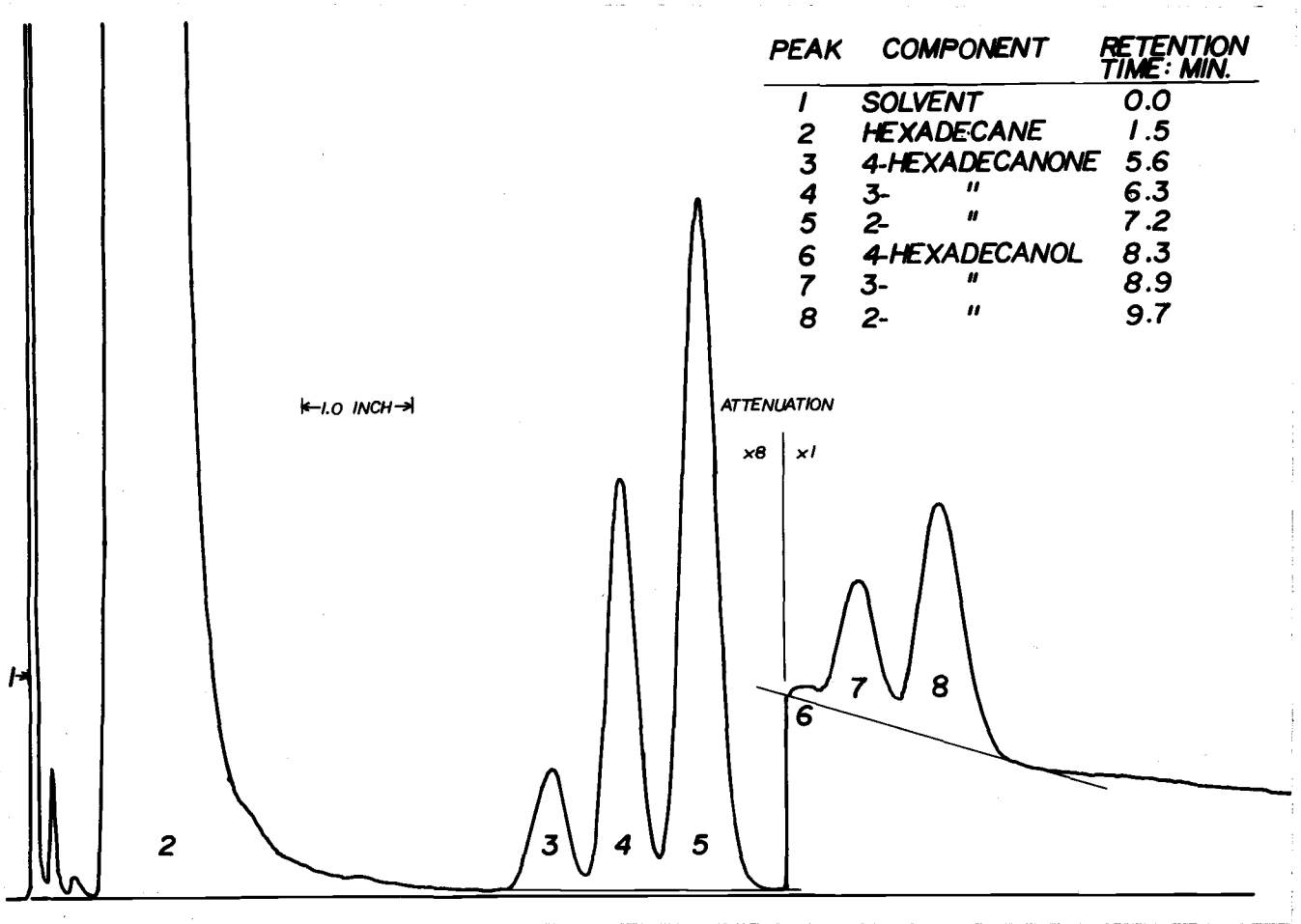

Figure 3. Typical chromatographic trace from run sample analysis.

the 4-, 3- and 2-hexadecanones; these are followed by the 4-, 3- and 2-positional hexadecanol isomers, with a total elution time of approximately ten minutes from injection.

A large number of samples resulted from each run, and hence an acceptable resolution of peaks with a minimum of on-column time was especially desirable. Although slight overlap of peaks resulted with the five-foot column which was used, complete resolution of the peaks required a column length of ten feet, with a resulting elution time nearly 20 minutes.

Resolution of chromatographic peaks improves with decreasing sample size, and a 0.5 μl injection was normally made. This corresponds to mid-scale on the 1.0 μl capacity syringes used for sample injection and is the optimal sample size for a syringe of this size. It was found that if 0.1 μl of air was drawn into the syringe before injection, then tailing was minimized. The injection procedure involved initial pumping of the plunger with the needle immersed in the sample to aid wetting of the bore with hydrocarbon. A slow takeup of about 1.0 μl was then followed by slow and careful depression of the plunger to the desired sample size marking (0.5 μl). The needle was removed from the sample, excess hydrocarbon was carefully wiped from the needle shaft, and 0.1 μl of air was drawn. Injection was made as rapidly as possible. Considerable attention was given to developing consistency in the injection procedure.

A qualitative identification of reaction products was made by comparison of chromatographic traces of the reaction products with injections of pure, known standard compounds. Availability of standards was limited to 2-hexadecanol and 3-hexadecanone; specifications and sources of these compounds are given in Table 2. Retention times of the standards and reaction compounds were identical. In addition, reduction of fermentation samples with $NaBH_4$, using the syringe technique of Fredricks (16), resulted in loss of the ketone peaks accompanied by the increase of corresponding alcohols. Conversely, oxidation of samples with $KMnO_4$ showed loss of the alcoholic peaks with corresponding increase of ketone areas.

Mechanical integrating devices were not available for the recording unit used, and the method used to evaluate peak areas consisted of multiplying the peak height times the width of the peak at half-height. Peak areas are preferable to peak heights since they are less dependent on operating conditions. This method is a rapid, simple and reliable indication of area when the peaks are symmetrical and of accurately measurable width, as was the case. When drift of the baseline occurred, the best possible line was drawn between the start and the finish of the peak, as shown in Figure 3. Justification for these considerations can be found in texts on basic chromatography such as McNair and Bonelli (45).

The chart speed was checked repeatedly and no deviation from

the value reported previously was detected. The attenuation linearity was periodically checked by causing a full-scale deflection of the baseline with the zero adjustment control and noting the response at all positions of the attenuation switch; signal attenuation was found to be quite linear over the full range of the machine.

An absolute analysis was used to relate the experimental peak areas to weight fraction values required for the quantitative analysis of the experimental data. The technique of internal standardization was carefully considered and subsequently eliminated as a means of determining product concentrations. The use of an internal standard is a preferred alternative to the absolute technique, since the former method does not require accurately measured injection quantities and results are not influenced by changes in detector response. Internal standardization requires a calibration in terms of the weight ratios of the reaction products to some standard. Accurately known amounts of the standard material must be added to the unknown before the mixture is chromatographed. The amount of unknown products is then determined by comparing area ratios to the calibration curve. A non-interfering, well resolved standard material must be used. For analysis of the samples of this study, the standard was required to elute after the peaks of interest. This was necessary for accurate measurement of the standard area because of the heavy tailing of the n-hexadecane peak observed at low attenuations. This

had the disadvantage of lengthening the analysis time of each sample by at least 20% in order to establish a good baseline for the standard. A second objection to the technique was the requirement for addition of accurately known amounts of the standard to a large number of very small (0.1 ml) sample volumes; in addition, significant dilution of the samples could not be tolerated, since the level of alcohols was at the lower limit of detection of the chromatograph. It was felt that these disadvantages offset the advantages of the method and the absolute analysis was chosen.

The absolute method of analysis required the use of accurately specified standard samples to construct a calibration curve. These standards were prepared from n-hexadecane, high purity 2-hexadecanol and 3-hexadecanone which were referred to in Table 2. Approximately 20 ml of n-hexadecane was placed in a tared beaker and weighed on a precision analytical balance. The 2-hexadecanol and 3-hexadocanone were added to give accurately known weight fractions on the order of 10^{-2} for each component. Carefully weighed quantities of this standard were then added to various known weights of n-hexadecane to provide a series of dilutions from 10^{-2} to 10^{-5} weight fraction.

In order to characterize the response of the detector, the series of weight fraction standards was injected and a calibration curve was prepared. Figure 4 shows that the detector response was

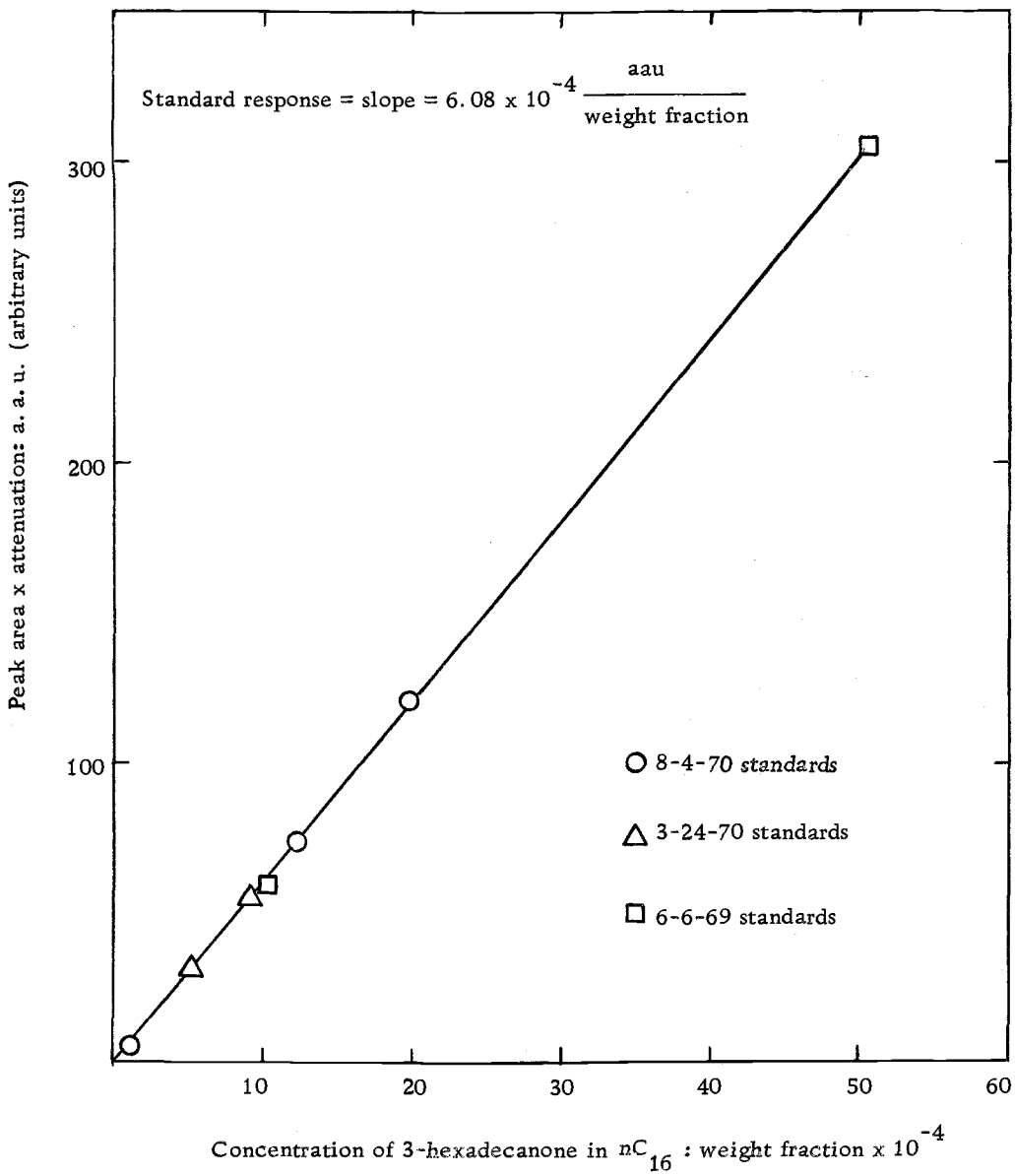

Figure 4. Calibration curve for chromatographic analysis.

quite linear over a very wide range of concentration. In order to minimize any influence of slight changes in the detector response, a series of standards bracketing the range of weight fractions detected in the samples was injected at the beginning and end of each series of sample injections. A standard response was obtained by determining the slope of a straight line through the points of each of these calibration curves, as indicated in Figure 4. The areas of the unknown samples were converted to weight fraction by dividing by the appropriate standard response. The arithmetic average of the standard responses was used in the calibration of all samples injected between two sets of standard injections. Initially the standard response was quite reproducible, but response drift was detected in analysis of some of the later runs; this will be discussed in the section dealing with difficulties encountered with the chromatographic analysis.

Since all isomers of the fermentation products were not available for use as standards, the response of all ketone isomers were assumed to be identical to that of the 3-isomer and the alcohol responses were taken as identical to the 2-hexadecanol response. The validity of this assumption does not influence the conclusions drawn from this study.

The normal procedure for sample injection was injection of samples in the chronological order that samples were taken, which was also the order of increasing concentration of reaction products;

this prevented carryover of products from more concentrated samples between injections.

Analytical Difficulties and Errors

In the present study, there were two primary indications of the magnitude of the error incurred in the chromatographic determination of the weight fractions of reaction products. The standard deviation gives an indication of the precision of the analysis. However, an additional and intermittent source of error not entirely reflected by the standard deviation was discovered. This error, resulting from a non-constant detector response, is considered following a discussion of the standard deviation. A net maximum error for the determined values of the product concentrations is estimated in Appendix II.

Precision

The precision of the chromatographic analysis was determined by repeated injections of a single sample, and was expressed as percent standard deviation relative to the mean value of all injections. Expressed in absolute terms, the standard deviation was of comparable size for all peaks; in terms of percent deviation, the standard deviation was dependent on the size of the peak involved. The absolute magnitude of deviation was larger relative to the small alcohol peaks than it was with respect to the ketone peaks. A standard

deviation of 1.9% was typical for large, well-attenuated (x 16) peaks of the standard samples. The standard deviation for attenuated ketone peaks such as are shown in Figure 3 was 2.0%. Alcohol peaks yielded a maximum standard deviation of 5.5% with an average standard deviation of 3.9%.

The relatively high standard deviation for the alcohol data was the result of the limited capability of the chromatographic unit employed in the analysis. The manufacturer's stated limit of sensitivity for the Varian chromatograph was 10^{-10} gram. A 0.5 microliter injection corresponds to about 10^{-4} gram order of magnitude total material injected; however, the maximum weight fraction of alcohol in the hexadecane injected was 10^{-4}. Therefore, the mass of alcohol was at a maximum level of about 10^{-8} grams. In practice, the lower limit of sensitivity of the machine was 10^{-5} weight fraction; prepared standards could not be qualitatively detected below this level. With the chromatograph functioning at settings of maximum sensitivity, 10^{-4} weight fraction alcohol (or ketone) in n-hexadecane gave an unattenuated peak height which was about 20% of full scale. It was found that when a sample yielding a peak of this size was injected and attenuated, the calculated areas for the attenuated peaks deviated from the area measured at the lowest attenuation. Since attenuation was shown to be linear, this indicated that this peak size was at the lower limit for accurate quantitative determination.

Two possible alternatives to reduce the effect of this difficulty involved either changing the column variables to increase the area response for a given sample size, or increasing the total sample size. Increasing the temperature of the column resulted in a higher response; however, deviation from the optimal column conditions reported previously proved to be unacceptable. For example, when the temperature was increased, the peaks blended together, and resolution was unacceptable at all carrier flow rates. Similarly, a larger sample size effected resolution adversely, and required the use of a ten microliter syringe, which proved difficult to handle at the high column pressure. Consequently, it was necessary to work with the analysis at the lower limit of quantitative accuracy; this was a serious limitation to the data analysis. The problem was unique to the analysis of the alcohol peaks, since ketones accumulated in much higher concentrations and yielded full-scale peaks at higher attenuations.

It was expected that some differences would be detected in the concentrations of duplicate samples. However, variation of multiple samples taken at the same time consistently showed a variation in weight fraction on the same order as the precision of the chromatographic analysis; hence, this source of error was not considered as significant in magnitude.

Detector Drift

A major difficulty encountered in the chromatographic analysis was the drift of the detector response with time. This drift could not be traced to injection technique, sample-column interaction, flow leaks or other detectable flaws in the operation of the chromatograph.

According to Kaiser (30), the flame ionization detector is inherently vulnerable to small amounts of volatile impurities when used at the high sensitivity necessary for high-temperature trace analysis. Such impurities are capable of producing considerable disturbances because of the high basic ionization current produced. In addition, very slight fluctuations in the temperature or the carrier flow rate can significantly disturb the detector response by virtue of their effect on the mass of vaporized liquid phase entering the detector per unit time. The detector itself remains insensitive to temperature or flow changes, but the secondary effect influences the resulting response. It seems likely that these considerations account for the observed drift in the detector response.

Figure 5 gives an indication of the effect of the detector response drift on the display of the results. The figure shows the 2-hexadecanone weight fractions, S_k, of samples taken from a single run, but injected on three separate days. The open circles and squares show the weight fractions for the complete run injected in the

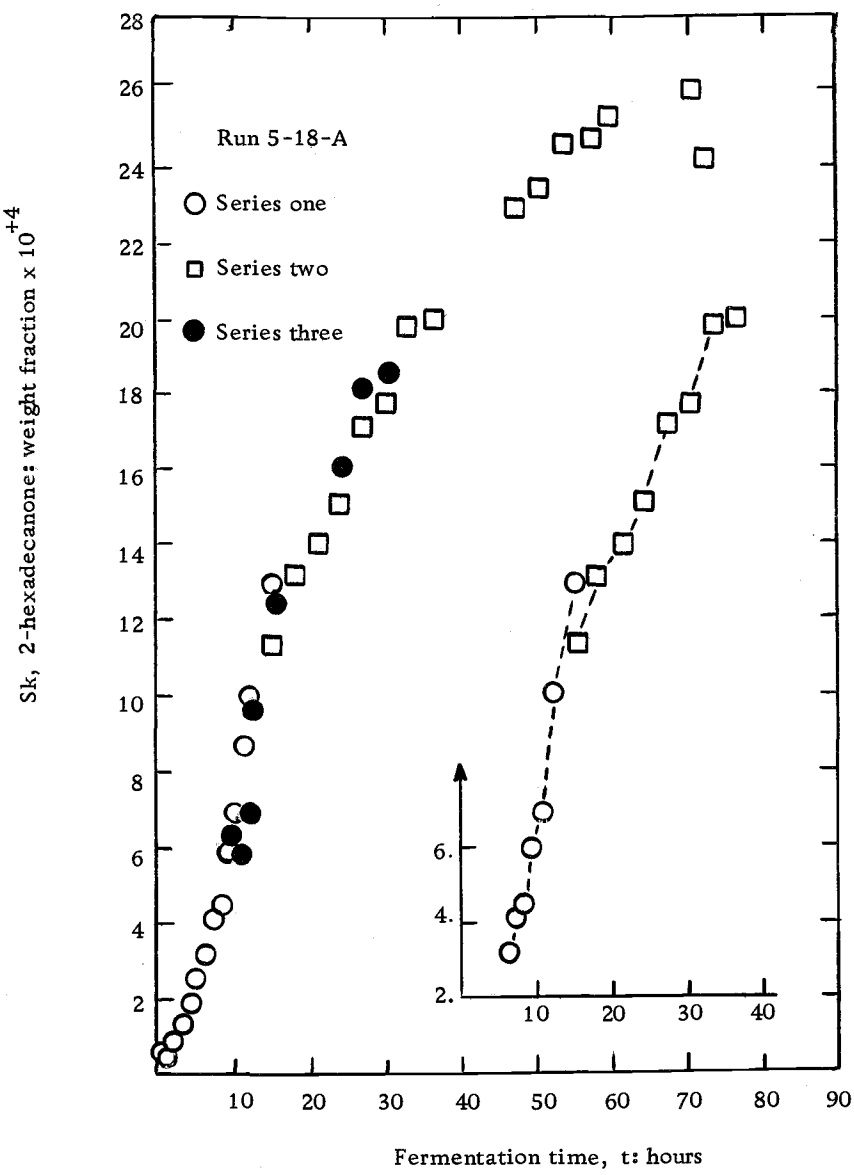

Figure 5. Effect of detector drift on product concentrations.

chronological order of sampling; half of the injections (series one) were made on one day, with the remaining samples (series two) injected on the following day. The final series of injections for the first day and the initial series of injections for the second day are indicated in the inset of Figure 5. The individual points for each series of injections were joined by a dotted line in the inset; each of these sets of injections was preceded and followed by a set of standard injections to determine the area response per unit weight fraction. The average of the two standard response values was then used to convert areas of the bracketed injections to weight fraction values. The effect of the changing response on the calculated weight fraction was particularly obvious at the point of overlap of the two sets of injections. This discrepancy was considerably more than could be accounted for by other sources of error, and was attributed to the varying response of the detector.

The net effect of the changing detector response was to add an additional component of scatter to the data about the average curve through the set of points. This was indicated by the third set of injections of the samples; these values are shown by the darkened circles in Figure 5. Samples for this series were injected in random order, rather than in the chronological order of sampling.

The maximum range of detector response change observed with a single set of injections was 9.6%. The average drift for 37 sets of

injections was 4.2%. This average reflects several observations for which little or no drift occurred. These values also represent the range of error in the computed weight fractions which was the result of the response drift.

DISCUSSION OF EXPERIMENTAL RESULTS

Growth Run

The procedure followed for a growth run was detailed previously; in this case, a nutrient was provided and the cells were actively grown in the presence of n-hexadecane. No growth was observed in the absence of the yeast extract, and the conversion of the hydrocarbon was previously designated as a transformation reaction (33).

The product and cell concentrations for a growth run are presented in Figure 6. The 2-, 3- and 4- isomeric 16-carbon ketones and alcohols were produced, as explained on page 44, but only the 2-hexadecanol weight fraction, S_A, and the 2-hexadecanone weight fraction, S_k, are presented here; no other oxidation products were found with the analysis previously described.

A lag period of about four hours preceded cellular growth and the detectable oxidation of the n-hexadecane. The measured weight fraction of alcohol reached a peak between 10 and 12 hours after initiation of the run. Detectable ketone production generally appeared to lag the production of alcohols, and the alcohol concentration dipped as heavier production of ketones became evident. These results indicated that the formation of ketone from n-hexadecane involved the alcohol as an intermediate. This sequential reaction scheme is compatable with previously postulated pathways for hydrocarbon oxidation. While it was

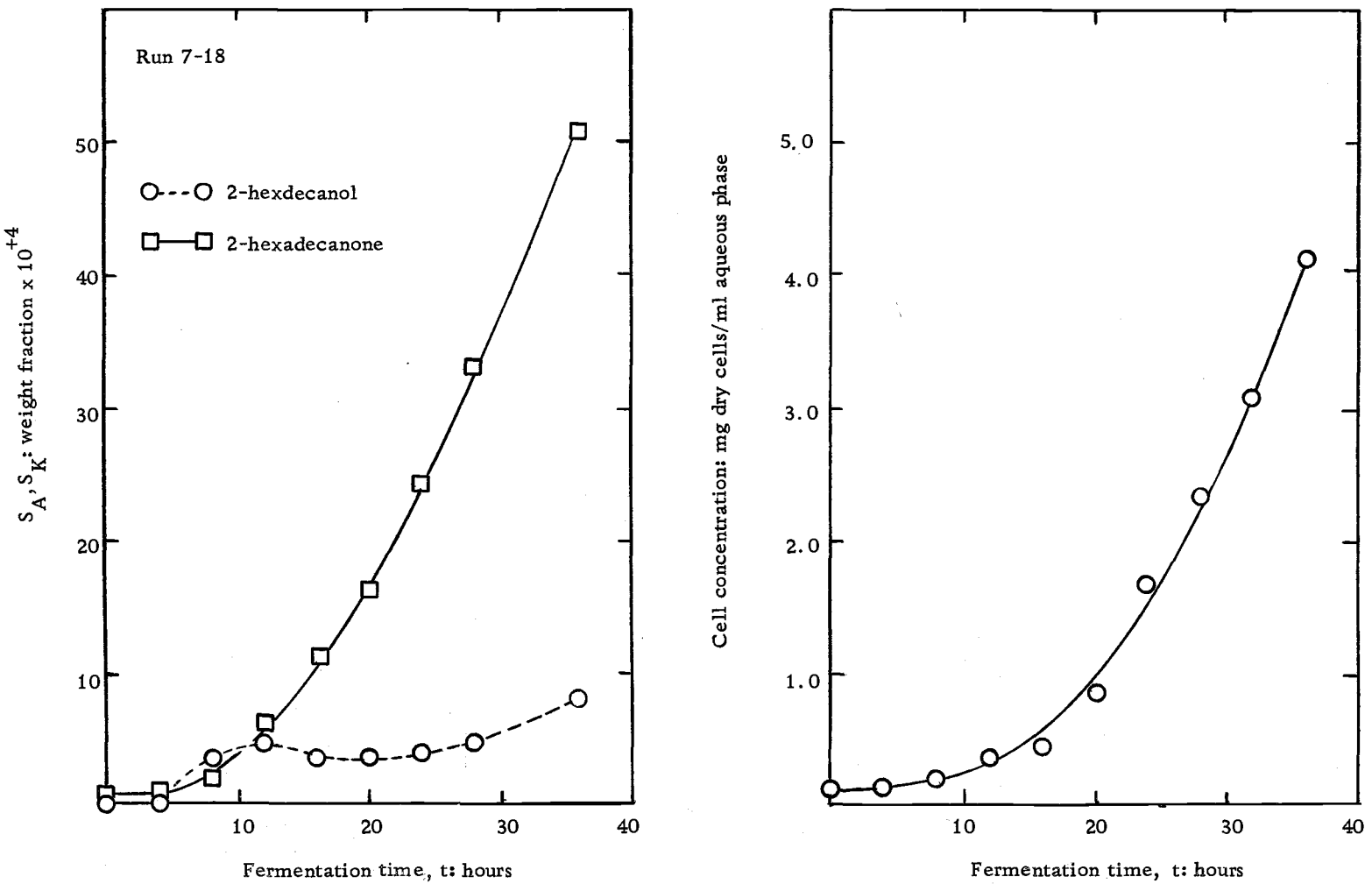

Figure 6. Reaction products and cell concentration for growth run.

difficult to draw conclusions on the basis of this type of experiment alone, it appeared likely that some enzyme induction process was involved in the initial stages of the oxidation process.

It should be noted from Figure 6 that the oxidation products are present in very low concentrations. In the case of the growth run, the hydrocarbon represented less than 6% of the total volume of the system. Products of the oxidation totaled less than 10^{-2} weight fraction relative to the hydrocarbon phase, even after 30 hours of exposure to the cells. The alcohol quickly attained a maximum level of approximately 5.0×10^{-4} weight fraction, while ketone concentrations were an order of magnitude greater than this. This was taken as further evidence for the presence of the alcohol as a relatively transitory intermediate in the sequential oxidation of n-hexadecane to hexadecanone. Further degradation of the hexadecanone was postulated, but this point has not been verified by direct experimental evidence.

It was decided that the growth system was a poor one for the study of the oxidation process. The following points are offered in support of this decision:

1. The growth run necessitated the use of pH control. If the pH was allowed to run its course over the duration of a 70 hour run, an increase of nearly two units over the initial pH of 7.0 was observed. Since the rate of an enzyme reaction is normally a strong function of the pH, study of the kinetics of the system required

conditions of constant pH. It was concluded that the pH control system available was inadequate for the degree of pH control desired in studying the enzymatic reactions involved.

2. The oxygen demand of the system, as measured by the method of Humphrey (4), remained constant for the first 30 hours of the run. After that time, the oxygen consumption increased sharply, showing an approximately linear seven-fold increase with time over the initial demand. The initial level of dissolved oxygen was near saturation; during the later stages of the run, the oxygen demand exceeded the supply capacity so that the dissolved oxygen level fell to 5% of saturation or below. This occurred even at the limits of aeration and agitation of the system, so that the growth system demand exceeded the available oxygen supply capability.

3. Physical properties of the cell mass during growth were adverse to the analyses required. With the onset of cellular growth in the system, extreme emulsification of the hydrocarbon and cells was observed. This hampered conventional methods for following cellular growth. The dry weight of samples was measured with some success, but the complete removal of n-hexadecane from the cell-hydrocarbon emulsion was unsatisfactory for reliable quantitative results. The emulsification of cells and hydrocarbon also impeded recovery of the hydrocarbon for analysis.

4. It was mentioned on page 61 that induction processes were

thought to be involved during the initial period of a run. By definition of the growth process, the total amount of enzyme available to catalyze the hydrocarbon oxidation was changing. Thus, with the growth system, the problem of studying an unknown reaction scheme was complicated by an inaccurately measurable and changing level of catalyst; study of the reaction kinetics required expression of reaction rates on the basis of a unit mass of enzyme, a situation which appeared difficult, at best, with the growth system.

5. A further disadvantage of the growth system was the increased demand for sterility. The nutrient, yeast extract, provided a source of growth for a wide spectrum of microorganisms. The system exhibited a high demand for oxygen, and the problem posed was maintaining a high rate of sterile, sparged air for prolonged periods of time. This strongly increased the possibility of contamination of the vessels before termination of the run, with subsequent uncertainty of the results.

The use of resuspended cells for study of the hydrocarbon oxidation was considered for all of the above reasons. The system adopted for all ensuing runs was described previously and exhibited a number of expected advantages.

Resuspended Cell Run

The specific run conditions for the resuspended cell runs can

be found in Appendix I. A summary of important conditions common to all runs is reviewed here.

In all cases, resuspended cells not previously exposed to hydrocarbon were added to 7.0 liters of nitrogen-free mineral salts solution and 160 ml of n-hexadecane. The final cell concentration was approximately 0.25 mg/ml. The initial pH was 6.70 $\pm$ 0.10 and remained constant, with no control, throughout the run. High aeration (4.0 liters air/minute) and vigorous agitation (400 rpm) were sufficient to maintain the dissolved oxygen level of the medium at saturation.

It was confirmed visually that the cells had immediate exposure to the hydrocarbon. Cells exposed to the hydrocarbon under conditions of the run were very rapidly coated so that the cell density became less than that of the aqueous phase. This process was quite rapid, and for samples drawn within one hour of the initiation of a run, the bulk of the added cells rose with the hydrocarbon to the surface of the aqueous phase. This is demonstrated in Figure 7, which compares the turbidity of a sample taken before hydrocarbon addition to the turbidity of samples taken shortly after the initiation of a regular experimental run.

The level of hydrocarbon relative to the aqueous phase was 23 mg/ml; since the dry weight of cells relative to the aqueous phase was 0.25 mg/ml, the mass of hydrocarbon was considered to be large

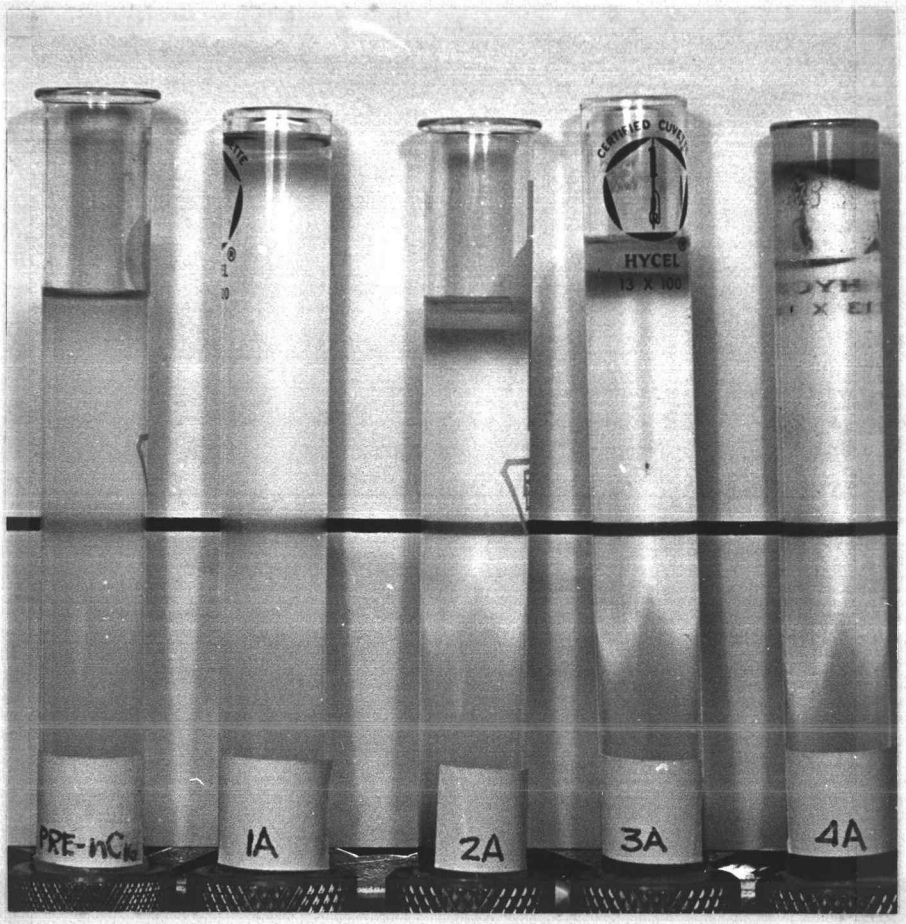

Run Sample	Time from Addition of Hydrocarbon: hours
Pre-nC_{16}	Before hydrocarbon addition
1A	0.00
2A	0.25
3A	1.00
4A	2.00

Figure 7. Rapid coating of cells by hydrocarbon.

with respect to the level of cells. This was also confirmed visually by the layer of free hydrocarbon generally observed above the cell-hydrocarbon layer. The growth of the cells and consumption of hydrocarbon were not detected during any of the resuspended cell runs.

Figure 8 depicts the results of a typical resuspended cell run, run 5-18-A. The weight fractions of 2-hexadecanone and 2-hexadecanol in n-hexadecane are presented as functions of time. The n-hexadecane used in this series of runs contained no externally added (exogenous) reaction products; runs of this type are hereafter referred to as regular runs.

Several typical characteristics of the regular runs are evident in Figure 8 and deserve emphasis.

1. The n-hexadecane used in the regular runs contained very low initial levels of components giving chromatographic peaks identical to 2-hexadecanol and 2-hexadecanone. These low initial levels resulted from the autoclaving of the hydrocarbon, and thus are seen to vary slightly from run to run. It is noted in Figure 8 that the initial ketone level dropped sharply before production of ketone was apparent at time equal to three hours. If this disappearance were the result of reaction, a rather high rate of disappearance of ketone by reaction would be indicated. Later model studies confirmed that the observed initial rate of disappearance was much larger than could be explained by this reaction. In addition, when the initial level of hexadecanone

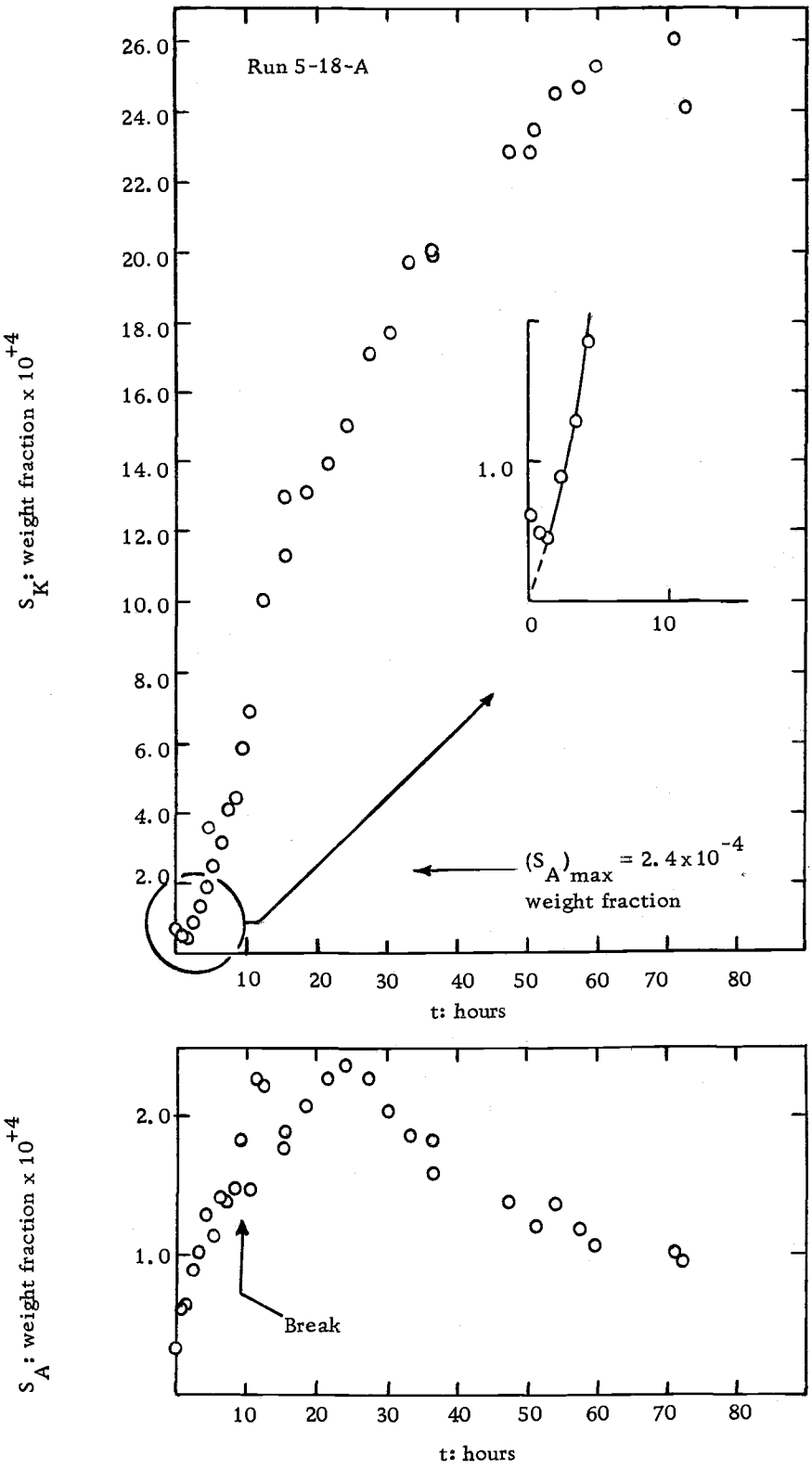

Figure 8. Product concentrations of a resuspended cell run.

was zero, the immediate production of ketone was observed; this suggested the immediate production of alcohol after hexadecane was added to the cells. Consequently, if slight initial levels of ketone were present, immediate production of ketone beyond that level would be expected. Two possible explanations for this discrepancy are proposed:

(a) The peak which eluted at the 2-ketone position was not actually 2-hexadecanone, but rather an interfering peak of similar retention time. Initial quantities were generally too small to prevent positive verification of the identity of the components.

(b) The peak did, in fact, represent the 2-ketone, but disappearance was by a mechanism different than reaction. For example, the exogenous ketone could first have been absorbed to the enzyme surface before conversion of the ketone occurred. It is possible that the relatively small initial quantities of ketone which were present were removed from the hydrocarbon by adsorption to the cell mass, with the reaction occurring at a much slower rate.

Either of these alternatives could provide explanation for the observed dip in the ketone concentration. In either case, however, the S_K versus time, t, curve would actually represent the simultaneous disappearance of the interfering component superimposed on the curve representing the appearance of the ketone from zero initial concentration. This suspicion was reinforced by the observation that

the ketone weight fraction curve could always be extrapolated to the origin as shown in the magnified insert in Figure 8.

2. A relatively high concentration of cells grown on yeast extract was used in the regular runs. In view of the immediate production of both alcohol and ketone, it was assumed that the enzymes responsible for the oxidation of n-hexadecane were pre-induced. That is, the level and activity of the enzymes that existed during the run were attained in the bacterial system before the cells were exposed to n-hexadecane.

3. Close scrutiny of the alcohol data shows that there appears to be a break in the trend of the data in the region of $t = 10.0$ hours. A curve representative of the data before $t = 9$ hours cannot be smoothly extrapolated to include the data immediately following the break point. The "hump" in the data was observed approximately ten hours after the initiation of all regular runs. While all regular runs showed this characteristic, it was considerably more pronounced in some runs, with no apparent explanation. It was generally observed that the alcohol data following the break exhibited more scatter than data taken in the region before the irregularity occurred.

4. A gradual decline in the level of alcohol was generally observed following the appearance of the indicated break in the data. The extent of this decline varied considerably with the individual run, and the observed value of S_A after 50 hours varied from 20% to 80%

of the maximum value of weight fraction attained during the run. The rate of decline was observed to decrease with time. The break and subsequent decline of the alcohol data indicated the possibility of a mechanistic change in the oxidation scheme after the first ten hours of the run. This point will be developed in the section which deals with discussion of the model equations.

5. It should be emphasized that the ketone concentrations attained were large compared to the values of alcohol concentration. The curves of Figure 8 are on the same time scale, but the ordinate of the alcohol scale is expanded four-fold relative to the ketone scale; the maximum weight fraction of alcohol is indicated on the ketone plot to allow comparison on the same scale. The implications of this observation will also be considered in the discussion of the proposed model equations.

The objective of the experimental work was to provide data for the development of a quantitative mathematical description of the oxidation of hexadecane to alcohols and ketones. In order to more clearly define the qualitative nature of the physical phenomena involved, a number of other types of runs were undertaken. The results of these runs helped to establish qualitative boundaries for the validity of the proposed model equations.

Exogenous Alcohol Run

For clarity in the following discussion, the physical situation is pictured in Figure 9. The oxidation system is depicted as a series of distinct enzyme regions on the surface of the cell. This is not meant to imply that the enzyme "system", in fact, resides on the cell surface. It simply symbolizes the observed ready access of the reaction mechanism to the n-hexadecane. The reaction scheme is assumed to consist of adsorption to the given enzyme, reaction at some site on the enzyme, desorption and mass transfer to the region of the next enzyme, with repetition of the process in that region.

The terms "alcohol" and "A" are used interchangeably in the following discussion to refer to 2-hexadecanol. "Ketone" and "K" refer exclusively to 2-hexadecanone. Similarly, S_A and S_K denote the corresponding weight fractions of the 2-isomers. Reference to other alcohol or ketone isomers are by specific name.

The format for the exogenous alcohol run followed that of the regular runs, with the exception that the hydrocarbon added to the test vessel contained an initially high level of alcohol. Before the n-hexadecane was added to the resuspended cells, high-purity 2-hexadecanol was added to give an initial alcohol concentration approximately twice the maximum level attained during a regular run. The results of the test and the control vessels (each using half of the same batch of

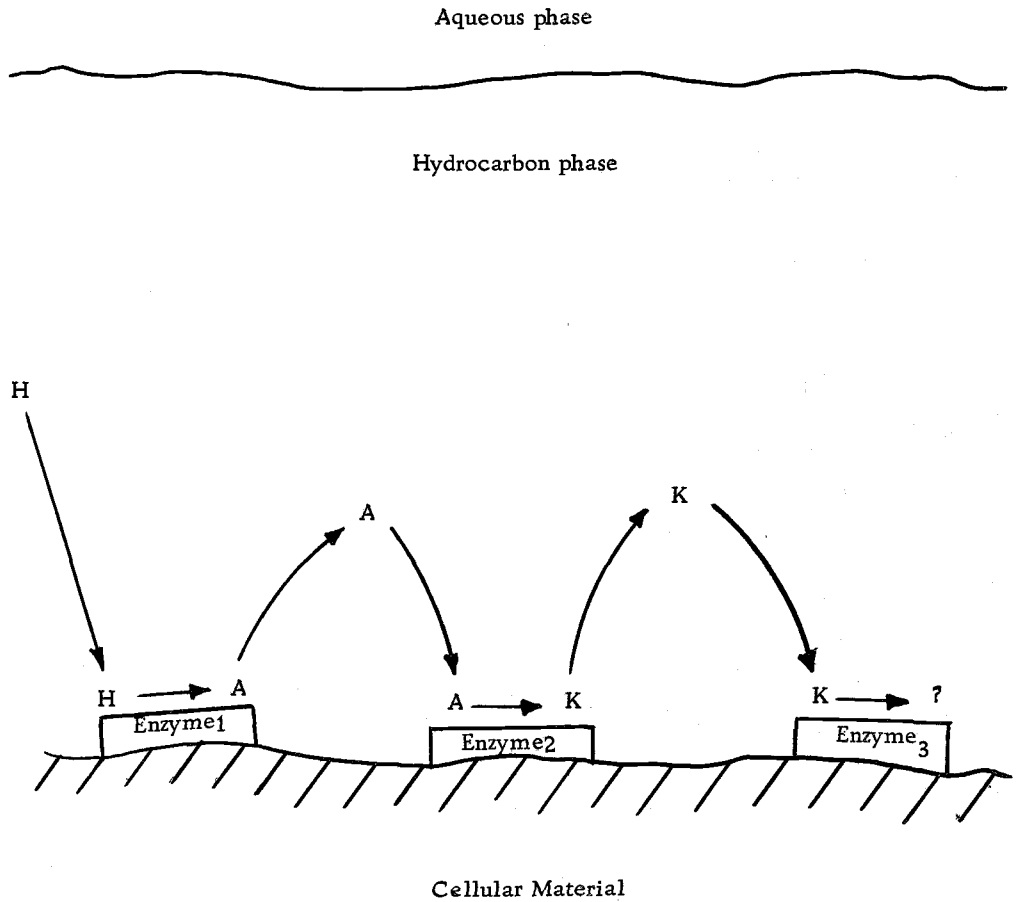

Figure 9. Schematic representation of n-Hexadecane oxidation by cells.

resuspended cells) for this run are displayed in Figure 10. As before, the alcohol data are plotted on an expanded ordinate relative to the scale used for the ketone weight fractions. Several conclusions were drawn from the results shown in Figure 10:

1. It was observed that the S_K versus t curve could be extrapolated back to the origin for both run vessels; this is indicated in the magnified inset. Since an immediate linear decrease in the exogenous alcohol concentration was observed, a simultaneous linear increase in the corresponding ketone concentration would be expected. The fact that the simultaneous, immediate production of K was not apparent from the observed S_K reinforced the possibilities outlined under point (1) on page 66.

2. Although the data of the control run appear to be typical of the regular runs, it is noted that the analysis of the data, to be considered in a later section, revealed atypical characteristics of the control run. The results of this run for the first 20 hours were verified with a second short-term run, but long-term quantitative comparison between vessels for the run shown is subject to some question.

3. The immediate disappearance of exogenous alcohol at a constant rate was observed from the alcohol data presented in Figure 10. In light of the simultaneous linear appearance of ketone with time, this was interpreted to mean that the conversion of A to K was taking place at a constant rate. This zero order rate was maintained until

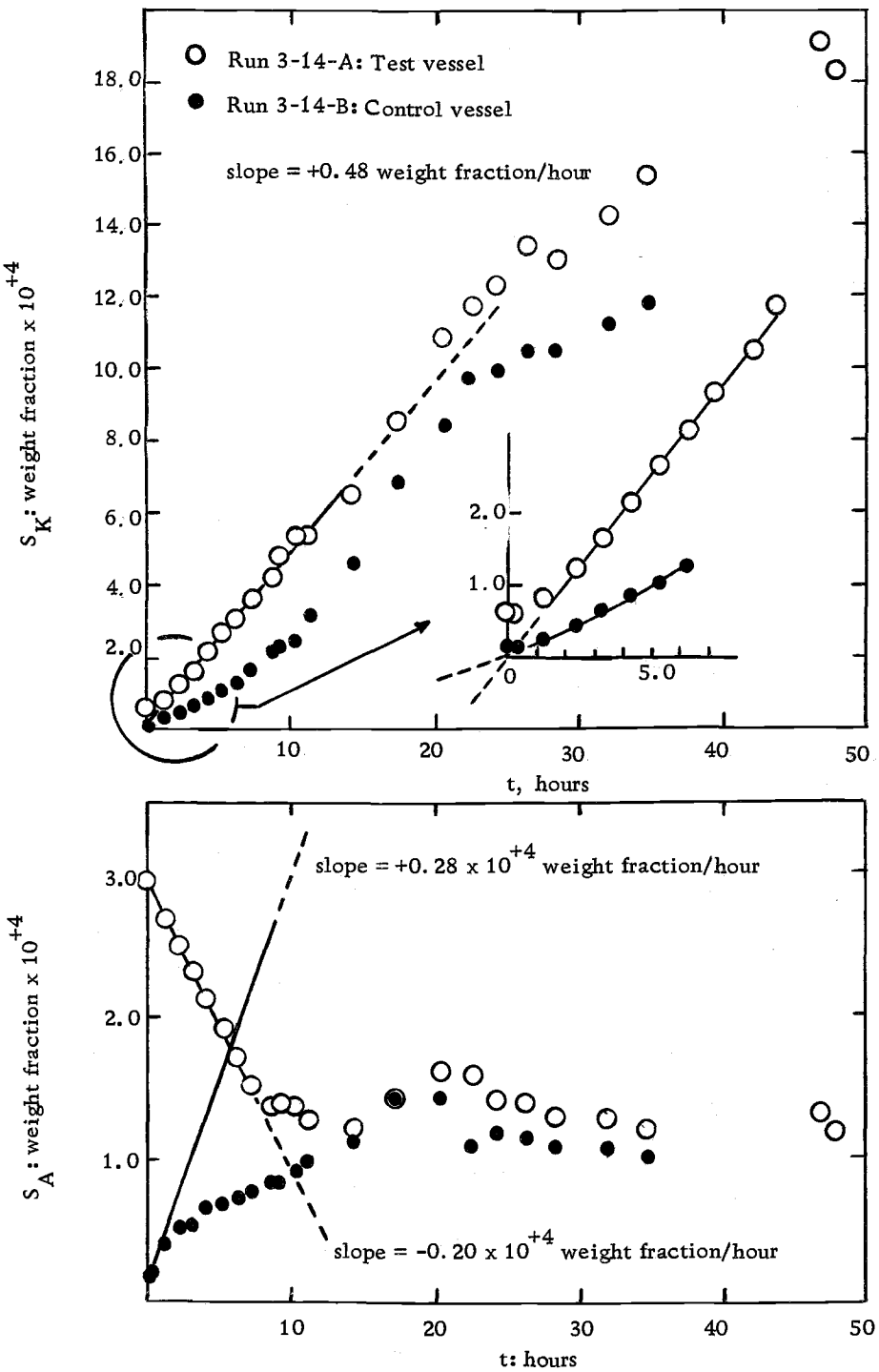

Figure 10. Product concentrations for exogenous alcohol run.

the alcohol weight fraction reached a value of 1.5×10^{-4} weight fraction; at this point, the alcohol concentration appeared to undergo transition to a region of qualitative behavior which paralleled the control run. In consideration of point (2) above, it cannot be concluded with certainty that this transition in the test vessel occurred at an alcohol concentration corresponding to the maximum value of S_A observed in the control vessel, although this appears to be possible from a comparison of the two S_A curves.

The appearance of a zero order rate is generally taken as an indication that the overall process is a made up of series of sequential steps, with some concentration-independent step acting as a bottleneck. A rate of disappearance of alcohol that is independent of S_A suggests that the conversion of alcohol to ketone was limited by a relatively slow surface reaction or by desorption of ketone from the reactive surface. The reasoning for this conclusion is as follows:

It is a basic assumption that the reaction must occur on the surface of an enzyme. Thus, mass transfer to the region of the enzyme, adsorption to the reactive site, desorption from the site and mass transfer of the product to the surrounding fluid are all considered part of the total process of converting alcohol to ketone. Since the observed rate of disappearance of A is independent of the concentration of A, this suggests that the slow step in the chain of events is also independent of the concentration of A. If a

concentration-dependent step such as adsorption of A to the enzyme surface were the slowest step, then factors affecting the speed of that step would influence the speed of the total process. Thus, a decreasing level of alcohol would change the net rate of reaction by exerting a direct influence on the rate of adsorption; since this was not observed, adsorption is eliminated as a possible bottleneck.

The reaction on the enzyme surface would be independent of the reactant concentration if the reaction were the slowest step in the total process; all possible reactive sites would always be in contact with a reactant molecule "waiting" for the relatively slow reaction step to take place. Similarly, desorption of the product from the surface is independent of S_A; this is a process dependent on the relative product concentrations at the enzyme surface and in the surrounding fluid. Consequently, if either desorption of ketone from the enzyme or the surface reaction step were slow relative to the other steps, the zero order disappearance of alcohol would be expected.

4. The production of ketone was observed to be linear over the region of constant alcohol depletion. This suggests that the degradation of ketone to some further unknown product was occurring at a negligibly small rate relative to ketone production for the range of ketone concentrations in the linear region. Thus, for the first eight hours of the run, the situation was effectively that of accumulation of ketone. Under these circumstances, if the limiting step in the

mechanism of conversion of A to K were concentration dependent, linearity of S_K versus t (similarly S_A versus t) would not be expected. This eliminates the possibility of a desorption-limiting step. On the basis of this evidence, it would appear that a surface reaction step was limiting for the regions of the run where concentrations were linear with respect to time.

5. The immediate and constant rate of conversion of A to K indicated that the enzyme system had immediate physical access to the hydrocarbon, as well as immediate chemical access to the alcohol. The constant reaction rate supports the presumption that the enzyme system was fully-induced at the time of addition of the hydrocarbon to the cells.

6. From Figure 10, it is observed that the alcohol disappeared at a rate of 0.20×10^{-4} weight fraction/hour over the linear region of the plot. However, the rate of appearance of 2-hexadecanone was 0.48×10^{-4} weight fraction/hour over the same period of time. Since the net rate of appearance of ketone was nearly two and one-half times greater than the measured net rate of disappearance of alcohol, it is apparent that the reaction was exposed to a source of alcohol other than the exogenous 2-hexadecanol. The simultaneous production of alcohol by reaction from hexadecane offers an explanation for the observed difference in rates. Several implications may be made on the basis of this presumption.

(a) A mass balance on alcohol with respect to the total hydrocarbon phase gives:

$$\begin{bmatrix}\text{Net rate of change}\\ \text{of A (measured)}\end{bmatrix} = \begin{bmatrix}\text{Rate of production of}\\ \text{A by reaction from H}\end{bmatrix} - \begin{bmatrix}\text{Rate of production of K}\\ \text{by reaction from A}\end{bmatrix}$$

where H represents n-hexadecane. Substituting values of rates determined from the plots of S_A and S_K as functions of time over the linear regions yields:

$$\begin{bmatrix}\text{Rate of production of}\\ \text{A by reaction from H}\end{bmatrix} = +0.48 \times 10^{-4} \quad -0.20 \times 10^{-4}$$

$$= 0.28 \times 10^{-4} \text{ weight fraction/hour}$$

Thus, if the difference between the measured rate of disappearance of A and the measured rate of appearance of K is explained by the production of A from n-hexadecane, the rate of production of A by this reaction must be 0.28×10^{-4} weight fraction/hour. (Weight fraction is equivalent to mole fraction for comparisons of alcohols and ketones, since there is negligible difference in the molecular weights.) This calculation makes the assumption that the reaction of H to A proceeds at a constant rate; the validity of this assumption will be discussed in the next section.

(b) Unless the conversion of n-hexadecane to hexadecanol was limited by the desorption of alcohol molecules from the surface of the

enzyme (or some other alcohol concentration-dependent step), it is reasonable to postulate that this reaction occurred at a constant rate. Since the maximum total concentration of oxidation intermediates was on the order of 10^{-3} weight fraction, the enzyme catalyzing the initial oxidation of hydrocarbon was exposed to an effectively constant concentration of n-hexadecane throughout the run. Furthermore, if the rate-limiting step in the conversion of H to A were dependent upon the concentration of A exposed to the enzyme (for example, the desorption-limiting case), the high initial levels of A present in the test vessel would have significantly slowed the production of A from H. If this were the case, the conversion of A to K would draw alcohol primarily from the exogenous pool of A molecules. This should result in a measured rate of depletion of A equal to the rate of production of K; this is inconsistent with the actual observation detailed above, and it is concluded that the production of alcohol occurred at a constant rate.

(c) The significance of the departure of the measured rate of disappearance of alcohol from a zero order process in the test run is now discussed. It was postulated in part (a) that the measured rate of change of A was the difference between the rate of input of A from the reaction of H and the rate of output of A by reaction to K; this process is represented in Figure 11 by plotting each of these rates against the weight fraction of alchol, S_A. For purposes of illustration,

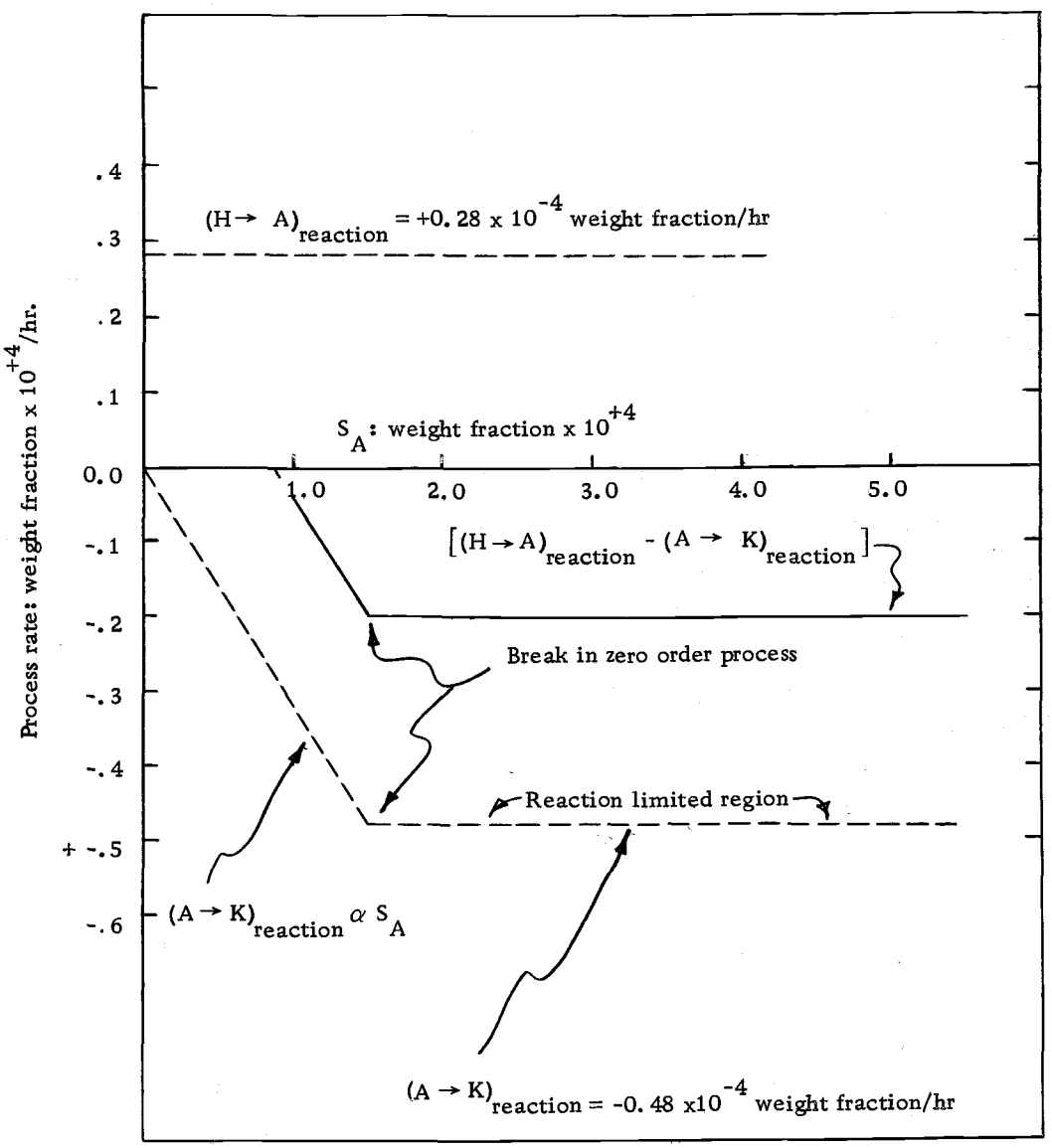

Figure 11. Reaction rates for exogenous alcohol run.

it is assumed that below the value of $S_A = 1.5 \times 10^{-4}$ weight fraction, the reaction of A to K was limited by a concentration dependent step which is considered to be first order with respect to S_A. If the production of A is considered constant over the linear region, the net rate of change is represented by the solid line which is the graphical sum of the reaction rates represented by the dotted lines. For the proposed case, the measured $\frac{dS_A}{dt}$ would begin approaching zero at the point where the concentration-dependent step becomes slower than the maximum surface reaction rate. The net rate of disappearance becomes zero at the point where the rate of production of A equals the rate of conversion to K; K is then produced with no change in concentration of A. According to Figure 11, the "steady state" concentration of A would be slightly below 1.0×10^{-4} weight fraction if the assumed behavior were actually followed. The results of the test run appear to be consistent with the situation discussed above, although it is not necessary that the concentration-dependent step be first order with respect to S_A.

The interpretation of the results of this type of run was complicated by the appearance of the hump in the alcohol data in the region between 10 and 20 hours. The behavior in the transition region of the curve was obscured by the appearance of this irregularity. As mentioned on page 70, this hump was thought to be an indication of some change in the basic mechanism of the process.

(d) If the production of alcohol from hexadecanone proceeded at a rate which was not depressed by the presence of high product concentrations, it is likely that the same rate would have been observed in the control run. Consequently, the rate of production of A by reaction from H in the control was expected to have been close to 0.28×10^{-4} weight fraction/hour, as calculated for the test run in (a) above. Furthermore, if the conversion of A to K was concentration-dependent over the range of S_A values encountered in the control run, then the rate of reaction of A to K initially would have been small, since the concentration of A was initially near zero. Thus, the initial measured rate of appearance of A should have approximately equaled the observed rate of production of A from hexadecane. In order to test this possibility, a line with a slope corresponding to this rate of production was drawn through the initial point of the alcohol data of the control run in Figure 10; this line appears to be a reasonable choice for the initial slope indicated by the data.

7. Figure 12 shows a comparison of the 3-hexadecanol and 3-hexadecanone concentrations in the test and control vessels. A plot of the 3-ketone level in the test vessel against the concentration of the same component in the control vessel is observed to have a slope of 1.0 in Figure 12a. A similar result for a comparison of the 3-alcohol concentration in the two run vessels is indicated in Figure 12b. It is apparent that the presence of relatively high initial levels of

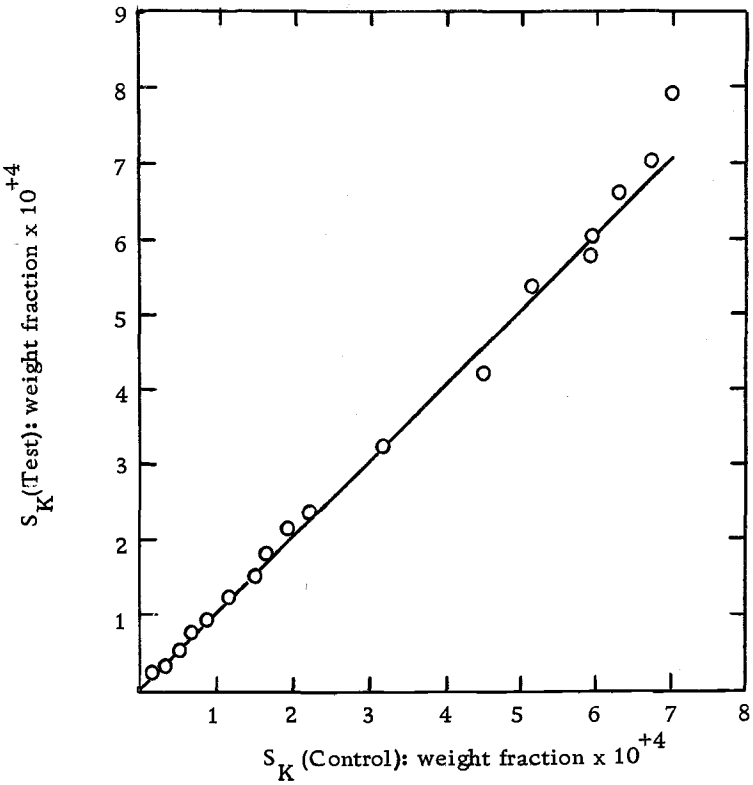

Figure 12a. 3-Hexadecanone weight fraction in test and control vessels.

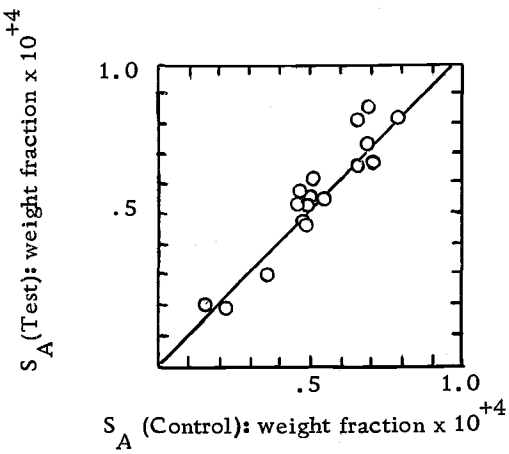

Figure 12b. 3-Alcohol weight fraction in test and control vessels.

2-hexadecanol had no detectable effect on the production of the 3-isomeric alcohols and ketones. Klein (33) made this same conclusion for shaker-flask studies of this oxidation system. This is taken as justification for the quantitative treatment of the 2-isomer reaction sequence independently of the 3-isomer sequence. A quantitative analysis of the 3-isomer oxidation products was not attempted, since 3-hexadecanol was present at levels below the lower limit for adequate quantitative expression of the results.

Exogenous Ketone Run

In order to provide further information about the nature of the hydrocarbon oxidation, a run was made with hydrocarbon which contained a relatively high level of exogenous ketone. It was not possible to perform this experiment using 2-hexadecanone, since that isomer was not available from the suppliers of hydrocarbon standards. Consequently, the run was carried out using high-purity 3-hexadecanone. The hydrocarbon for the test vessel contained an initial level of 3-hexadecanone of 6.3×10^{-4} weight fraction, which was slightly below the maximum level normally attained in a regular run. The control vessel followed the regular run format, and the resuspended cells volume was equally split between the two run vessels. The results of this run are summarized in Figure 13. The following conclusions were drawn from these results:

1. The addition of 3-hexadecanone had no detectable effect on the production of the 2-ketone isomer. This was concluded from the observation that the 2-hexadecanone concentration in the test vessel was equal to the concentration of the same isomer in the control vessel throughout the run. Figure 13a shows that a plot of the 2-ketone concentration in the test vessel versus the control vessel concentration had a slope of 1.0.

2. The addition of the 3-ketone did not influence the production of 2-hexadecanol. This was demonstrated by a similar plot of the 2-alcohol concentration in the test and control vessels, shown in Figure 13b. Even on the expanded scale, the ratio of the concentrations was essentially unity. Observations 1 and 2 further confirmed the presumption that the oxidation sequence of the isomers can be treated independently.

3. Figure 13c is a plot of the 3-hexadecanol concentration of the test vessel against the control vessel 3-alcohol concentration. Considerable scatter is apparent, since the peaks obtained from the chromatographic analysis were too small to be quantified with the degree of accuracy and precision attained for the larger peaks of the other components. A line indicating a slope of 1.0 (equality of concentrations in the test and control vessels) was superimposed on the data and it was concluded that deviation from this line, other than that attributed to random errors of the analysis, was not apparent.

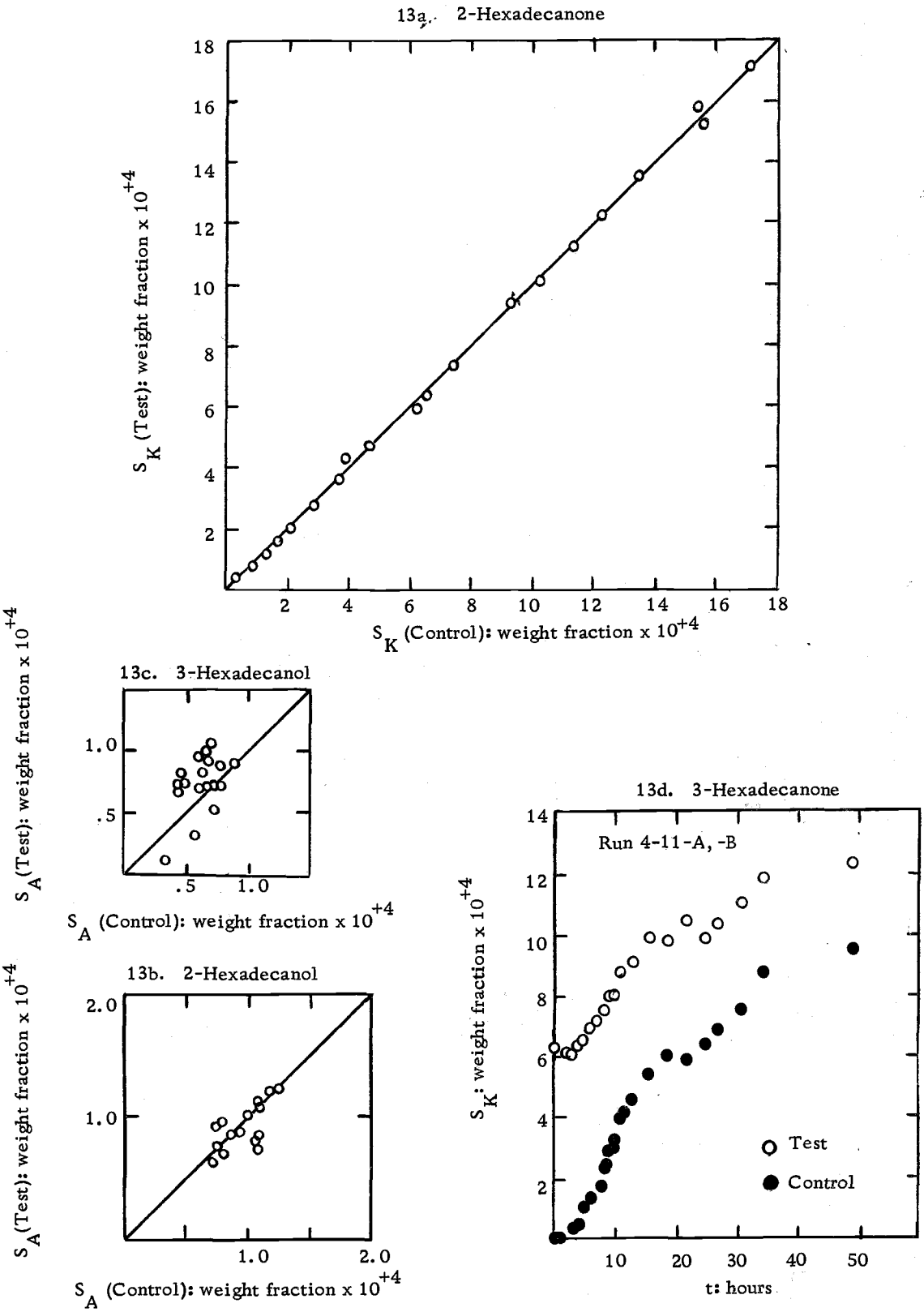

Figure 13. Run results for exogenous ketone run.

This supports previous evidence which indicated that the reversal of the alcohol to ketone conversion did not occur.

4. Figure 13d indicates the measured 3-hexadecanone concentrations in the test and control vessels as functions of time. The peculiar irregularities in the curves in the region of t = 20 hours were attributed to the phenomenon of chromatograph detector drift, as described in detail on page 55. The exogenous level of 3-ketone was below the maximum level attained in the regular runs, and behavior analagous to the zero order disappearance of exogeneous 2-hexadecanol was not observed. If the conversion of 3-hexadecanol to 3-hexadecanone was irreversible as postulated, the expected effect of added 3-ketone (at levels for which there was no change in reaction mechanism) depends on the overall mechanism of the conversion process. Even though the reaction is considered irreversible, the presence of exogenous ketone could still effect the alcohol-ketone conversion. For example, if the desorption of K from the enzyme surface is the limiting step in the production of K, the net process would be slowed by exposing the enzyme to higher concentrations of ketone. A similar effect would be possible if some other ketone-concentration step were limiting in the reaction of A to K.

In addition to this effect, if it existed, an increase in the concentration of K would tend to speed up the conversion of ketone to the next reaction product; again, this influence would be expected only if

the limiting step in the degradation of ketone were dependent on the ketone concentration.

The net effect of adding exogenous ketone is seen to depend on the relative magnitude of the two effects described above. Consequently, positive interpretation of the results is difficult. However, if the experimental evidence discussed in point 3 can be interpreted to mean that exogenous ketone produced no effect on the conversion of alcohol to ketone, then the effect of the added product would be solely the effect on the degradation of K. If this were the case, the lower rates of appearance of ketone shown in Figure 12d for the test vessel (relative to the control vessel) would be the result of a higher rate of disappearance of K to a further product with no change in production of K from A.

DISCUSSION OF MODELING RESULTS

Summary of Conclusions About the Nature of the Oxidation Process

At this point, it is helpful to summarize the previous discussion and indicate the assumptions made in the development of the model for the oxidation process. All references to alcohol and ketone refer to the 2-isomers of hexadecanol and hexadecanone, respectively, unless otherwise indicated.

1. The net reaction was found to follow the scheme:

$$H \longrightarrow A \longrightarrow K \longrightarrow X$$

where

H = n-hexadecane (C_{16})

A = 2-hexadecanol

K = 2-hexadecanone

X = further degradation products

2. All reactions were considered to be enzymatic, and the presence of a different enzyme for each step was assumed.

3. Each reaction step was considered to be irreversible.

4. The reaction sequence was found to apply independently to each of the corresponding positional isomers. For example, the formation of the 2-hexadecanone isomer (with 2-hexadecanol as an intermediate) occurred as follows:

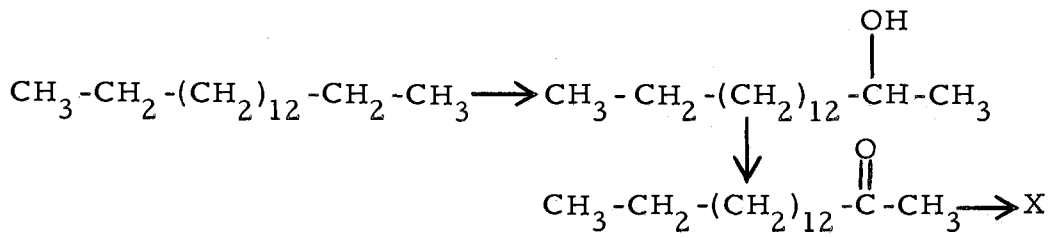

This was assumed to be quantitatively describable independently of the analagous reaction sequence for the formation of other positional isomers.

5. The cells were found to have immediate and continued direct contact with the hydrocarbon phase.

6. The reactions were considered to occur in the hydrocarbon directly in contact with the cell; negligible reaction of dissolved hydrocarbon from the aqueous phase was assumed.

7. Consumption of hydrocarbon during the course of the run was not detected.

8. No growth (cellular division) was detected during the run.

9. The enzymes catalyzing the reaction sequence were considered to be fully-induced during growth of the cells on yeast extract in the absence of hydrocarbon.

10. The net rate of the reaction converting H to A was considered to be constant.

11. Under conditions of a regular run, the conversion of A to K and the conversion of K to some further reaction product were found to be dependent on the concentrations of A and K, respectively.

12. It was assumed that the reaction sequence was not subject to inhibition or control schemes which influenced the level or activity of the enzymes involved.

13. It was assumed that negligible enzyme deactivation occurred during the course of the run.

14. It was assumed that energy or oxygen availability did not limit the progress of the reaction.

Development of the Model Equations

The first step in the development of a mathematical model representative of the oxidation process was to define the rate of reaction. Since the oxidation is a surface-catalyzed reaction, it would be logical to express the rate of reaction on a per unit weight of catalyst basis. However, in the case of cellular kinetics, this is not an exactly-measurable quantity. In addition, the catalyst mass differs for each step in the reaction sequence. Consequently, the simplest basis is the total mass of cellular material. For the runs which used resuspended cells, this is taken simply as the total cell concentration based on a dry weight measurement expressed relative to the aqueous phase. It is emphasized that the relationship of any of the involved enzymes to the dry weight of cells is unknown, but presumed to be constant. The rate of reaction for component i is symbolically defined as follows:

$$\frac{1}{W}\left[\frac{dN_i}{dt}\right]_{rxn} = \frac{\text{moles i formed by reaction}}{\text{(unit concentration cells) (time)}}$$

where

W = dry weight of cells relative to the aqueous phase: mg/ml

N_i = moles component i

t = time: hours

One may now write the rate expression for each step in terms of the measured concentrations of alcohol and ketone. These expressions can then be used to write the equations for the product concentrations as functions of time.

It was concluded from previous discussion that, for a given level of cells, the rate of production of alcohol from n-hexadecane was a constant. This rate is now defined as:

$$R' = \frac{\text{Moles A formed by reaction from H}}{\text{(mg cells/ml aqueous) (hour)}}$$

From the previous discussion of the regular runs, it was concluded that the limiting steps for the conversion of A to K and further degradation of K were concentration dependent. It was found that a first order concentration dependence for each of these reaction steps was adequate for the description of the experimental data. This is not necessarily inconsistent with the Monod expression, which indicates a first order dependence at low concentrations. The use of first

order rate terms was attractive from a modeling viewpoint, since the constants of the resulting model expressions could be evaluated from the data by means of straight-forward graphical techniques. The rate expressions for the second and third reaction steps are defined as follows:

$$-r_A''' = r_K''' = \frac{\text{moles K formed by reaction from A}}{\text{(mg cells/ml aqueous) (hour)}} = k'_A C_A$$

and

$$-r_K''' = \frac{\text{moles K reacted to X}}{\text{(mg cells/ml aqueous) (hour)}} = k'_K C_K$$

where

C_A = concentration of alcohol in hydrocarbon; moles/ml

C_K = concentration of ketone in hydrocarbon; moles/ml

k'_A = rate constant; $\frac{\text{ml hydrocarbon}}{\text{(mg cells/ml aqueous) (hour)}}$

k'_K = rate constant; $\frac{\text{ml hydrocarbon}}{\text{(mg cells/ml aqueous) (hour)}}$

These rate expressions can now be used to define the equations representing the change of product concentrations with time. For the hydrocarbon phase, a mass balance on each of the components gives:

$$\left[\begin{array}{c}\text{Rate of accumulation}\\ \text{of moles of A}\end{array}\right] = \left[\begin{array}{c}\text{moles A formed by}\\ \text{reaction from H}\end{array}\right] - \left[\begin{array}{c}\text{moles A re-}\\ \text{acted to form K}\end{array}\right]$$

and

$$\left[\begin{array}{c}\text{Rate of accumulation}\\ \text{of moles of K}\end{array}\right] = \left[\begin{array}{c}\text{moles of K formed by}\\ \text{reaction from A}\end{array}\right] - \left[\begin{array}{c}\text{moles K re-}\\ \text{acted to form X}\end{array}\right]$$

Substitution of the rate expressions in the corresponding mass balances gives:

$$\frac{1}{W}\frac{dN_A}{dt} = R' - k'_A C_A = \frac{(M_H/\rho_H)}{W}\frac{dC_A}{dt}$$

and

$$\frac{1}{W}\frac{dN_K}{dt} = k'_A C_A - k'_K C_K = \frac{(M_H/\rho_H)}{W}\frac{dC_K}{dt}$$

where

M_H = total mass of hydrocarbon: grams

ρ_H = density of hydrocarbon: grams/ml

The $\frac{dN_i}{dt}$ term in each of the expressions above can be rewritten directly in terms of concentration, since the total volume of the hydrocarbon phase, (M_H/ρ_H), is constant throughout the course of the run. Since products were present in final concentrations on the order of 10^{-4} weight fraction, the volume of hydrocarbon is computed from the properties of pure n-hexadecane.

The chromatographic analysis was expressed in terms of weight fraction of the products in n-hexadecane, and these expressions were rewritten in terms of mass fractions for the data analysis. Substituting weight fraction for concentration leads directly to:

$$\frac{dS_A}{dt} = R - k_A S_A \qquad (1)$$

and

$$\frac{dS_K}{dt} = k_A \left[\frac{MW_K}{MW_A}\right] S_A - k_K S_K \qquad (2)$$

where

S_i = weight fraction of component i in n-hexadecane

(MW_i) = molecular weight of component i: grams/mole

The rate constants in these final expressions are defined by:

$$R = \frac{R' W \rho_H (MW_A)}{M_H (MW_H)} \quad : \text{ weight fraction/hour} \qquad (3)$$

$$k_A = \frac{k_A' W \rho_H}{M_H} \quad : \text{ hour}^{-1} \qquad (4)$$

$$k_K = \frac{k_K' W}{M_H} \quad : \text{ hour}^{-1} \qquad (5)$$

It should be noted that for practical purposes, the ratio of molecular weights (MW_K/MW_A) appearing in Equation (2) can be taken as unity, since the actual value is 0.992.

In applying Equations (1) and (2) to the experimental data, it was immediately obvious that modifications of these expressions were required. Equation (1) was adequate for describing the data in the initial region of the runs, but after a time designated t*, it was necessary to include a term accounting for the decay of enzyme activity.

Furthermore, it was found that different values of k_A resulted when the model constants were evaluated by application of Equations (1) and (2) to the experimental data. This discrepancy was alleviated by the introduction of the constants ϕ_A and ϕ_K into Equations (1) and (2). As a result, the final form of the model equations was as follows:

$$\frac{dS_A}{dt} = \frac{R}{\phi_A} - k_A S_A \qquad \text{for } t < t^* \qquad (6)$$

$$\frac{dS_A}{dt} = \frac{R}{\phi_A} e^{-k_D (t-t^*)} - k_A S_A \qquad \text{for } t > t^* \qquad (6a)$$

and

$$\frac{dS_k}{dt} = \left[\frac{MW_K}{MW_A}\right] (k_A \frac{\phi_A}{\phi_K}) S_A - k_K S_K \qquad \text{for } t > 0 \qquad (7)$$

Equations (3), (4) and (5) were unchanged. These modifications will be discussed following the outline of the calculational procedure used to evaluate the model constants from the experimental data. The experimental data used in illustrating the calculational techniques are for the regular run 5-18-A, and are shown in Figure 8. These data are representative of the results obtained for other regular runs. The final forms of the model equations are used, with the value of MW_K/MW_A taken as unity.

Evaluation of the Model Constants from the Data

A variety of techniques can be used to evaluate the constants contained in the model equations. The methods presented in this section were chosen as the most effective methods of those considered, and were used to obtain the values of constants used in the presentation of model results. The arguments for choosing the particular techniques used are presented in Appendix III.

Evaluation of k_A and S_A^*

Equation (6) can be integrated to give:

$$S_A = S_{AO} + (S_A^* - S_{AO})(1 - e^{-k_A t}) \qquad (8)$$

where S_{AO} is defined as the initial weight fraction of 2-hexadecanol. The quantity S_A^* is defined as the value of S_A attained at large times, and it is related to the other parameters by setting $dS_A/dt = 0$ in Equation (6), as follows:

$$S_A^* = \frac{(R/\phi_A)}{k_A}$$

The method used to evaluate k_A was based on equation (8). Application of the technique required previous knowledge of the value of S_A^*. In order to provide a consistent estimate of S_A^*, a smoothed plot of $\ln S_A$ as a function of t was constructed as illustrated in Figure

14. The basis of the plot is the defining equation for $\bar{S}$:

$$\bar{S} = \frac{S_A}{S_K}$$

which leads to:

$$\ln S_A = (\ln S_K) + \ln(\bar{S})$$

The value of $\bar{S}$ was computed directly from the ratio of alcohol and ketone peaks which resulted from the chromatographic analysis of each sample. The data, in the form of $\ln S_K$ versus t and $\ln \bar{S}$ versus t plots, were smoothed by eye. The smoothed curves were then graphically added to provide a smoothed plot of $\ln S_A$ versus t. The quantity S_A^* is easily read from this plot as the value of S_A for which $dS_A/dt = 0$; in this case, $S_A^* = 1.95 \times 10^{-4}$ weight fraction.

Using equation (8), lines of constant S_A were computed for several convenient values of $(k_A t)$ and superimposed on the $\ln S_A$ versus t plot, as shown in Figure 15. A choice of k_A then fixed the intersection of the model curve with each of these lines of constant $(k_A t)$. The k_A value was determined by trial, with the acceptability of fit being judged by eye. For example, it appears that a reasonable model line might intersect the $(k_A t) = 1.0$ line at ten hours. This corresponds to $k_A = \frac{1.0}{(10)}$ hr^{-1}, or $k_A = 0.1$ hr^{-1}. Accordingly, the model intersection with the $(k_A t)$ lines having values of 0.25,

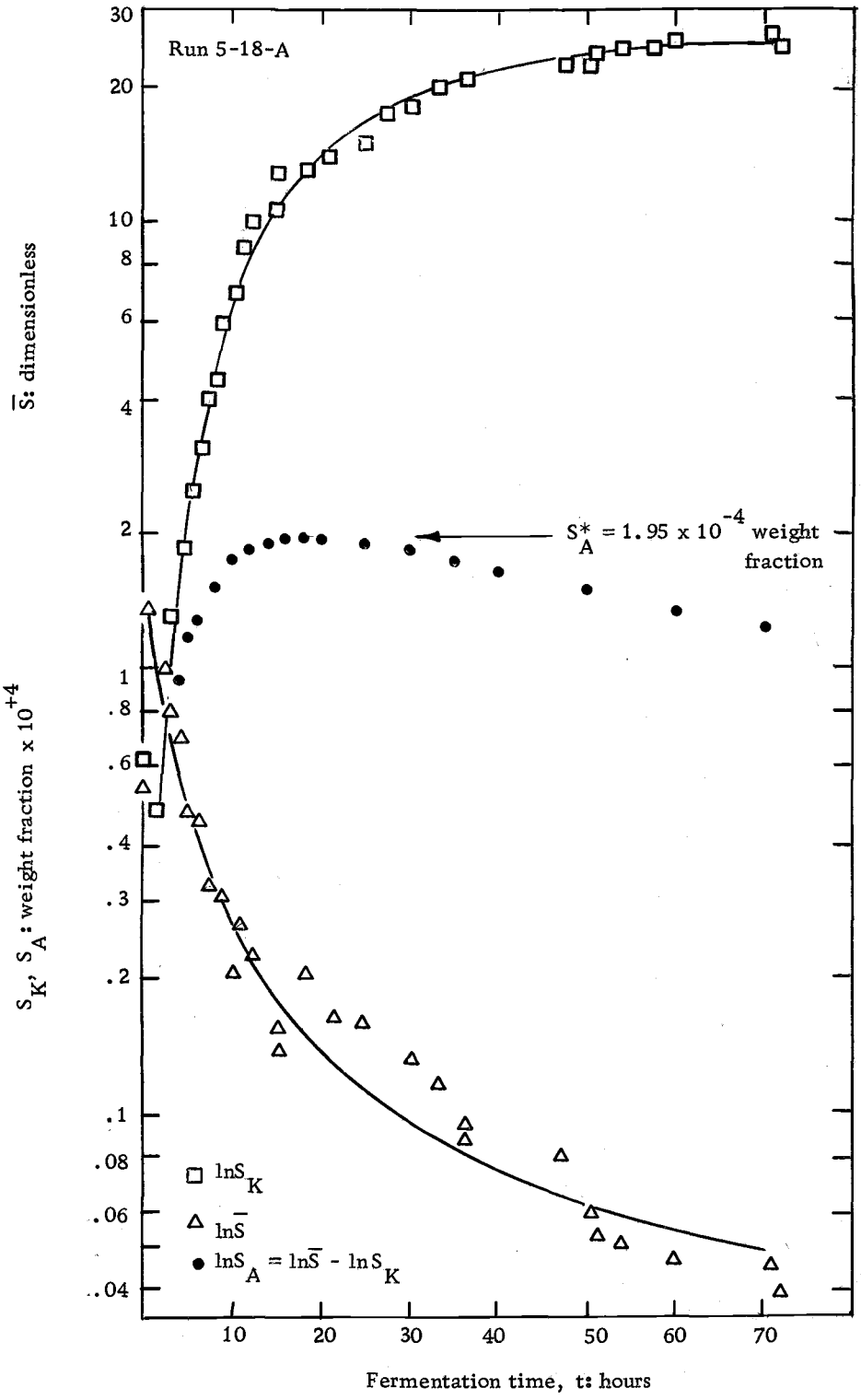

Figure 14. Graphical determination of S_A^* from smoothed S_A data.

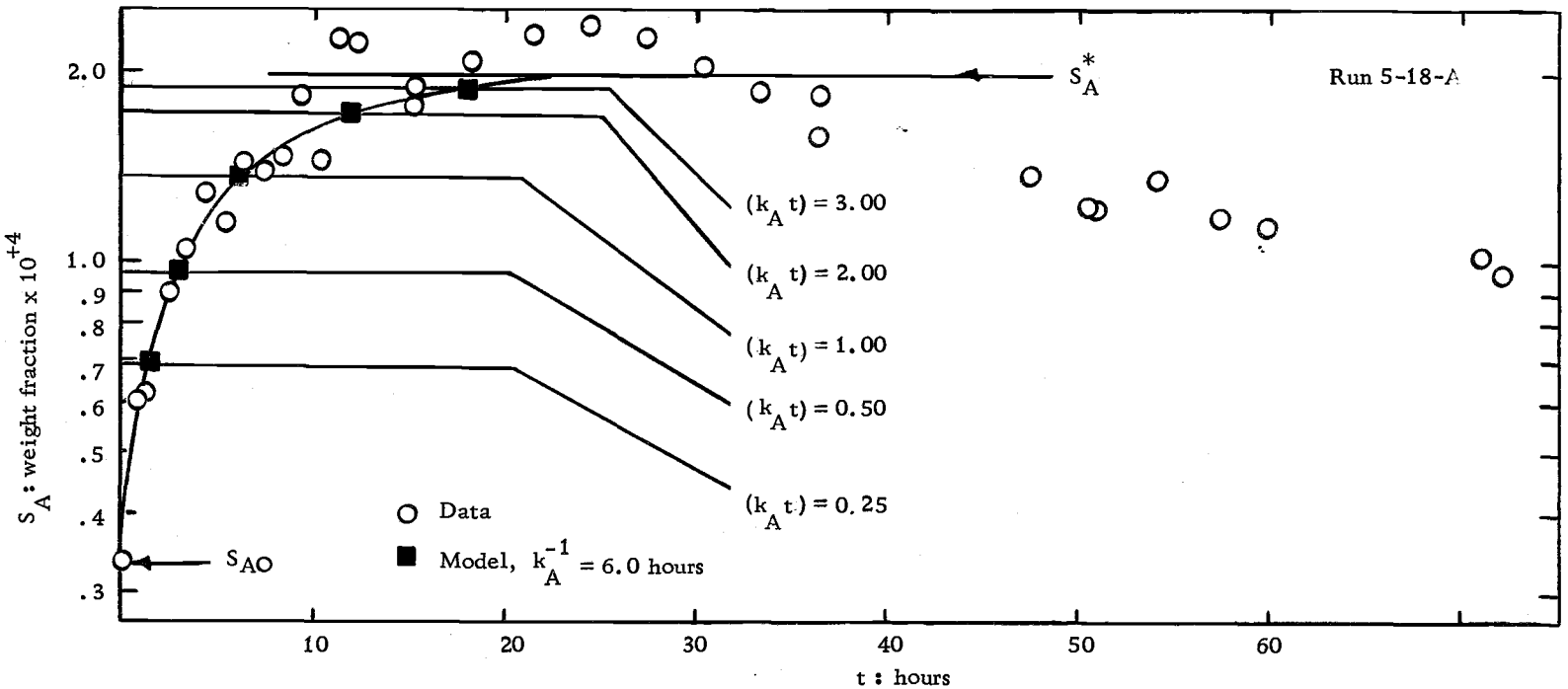

$S_A^* = 1.95 \times 10^{-4}$ weight fraction

$S_{AO} = .33 \times 10^{-4}$ weight fraction

$(S_A^* - S_{AO}) = 1.62 \times 10^{-4}$ weight fraction

CALCULATION OF LINES OF CONSTANT $(k_A t)$

$(k_A t)$	$(1-e^{-k_A t})$	$(1-e^{-k_A t})(S_A^* - S_{AO}) + S_{AO} = S_A$
Dimensionless		Weight fraction x 10^{+4}
0.25	0.22	0.69
0.50	0.39	0.97
1.00	0.63	1.36
2.00	0.865	1.71
3.00	0.950	1.88

Figure 15. Graphical determination of k_A from Equation (8).

0.5, 2.0 and 3.0 are fixed at t values of 2.5 hours, 5.0 hours, 20 hours and 30 hours, respectively; this would give a model curve passing unacceptably to the right of the data points over a large region of the run. The value of $k_A = 0.167$ hour^{-1} was chosen as the value resulting in the best model curve.

Evaluation of k_D and t*

For times larger than t*, equation (6a) must be applied to the data. This equation can be rearranged to give:

$$\ln\left[S_A + \frac{1}{k_A}\frac{dS_A}{dt}\right] = \ln S_A^* - k_D(t-t^*) \qquad (8a)$$

If the ordinate $\ln(S_A - 1/k_A\, dS_A/dt)$ is plotted against t, a straight line of slope $(-k_D)$ should result. Furthermore, this line should intersect a line of constant S_A^* at the value of t*. Since dS_A/dt changes slowly over the entire range of decay, and since $1/k_A\, dS_A/dt$ is small relative to S_A, a constant average value of dS_A/dt was assumed over the region of decay. For the data shown in Figure 15, a value of $dS_A/dt = 0.028 \times 10^{-4}$ weight fraction/hour was assumed. The resulting plot to determine k_D and t* is given in Figure 16.

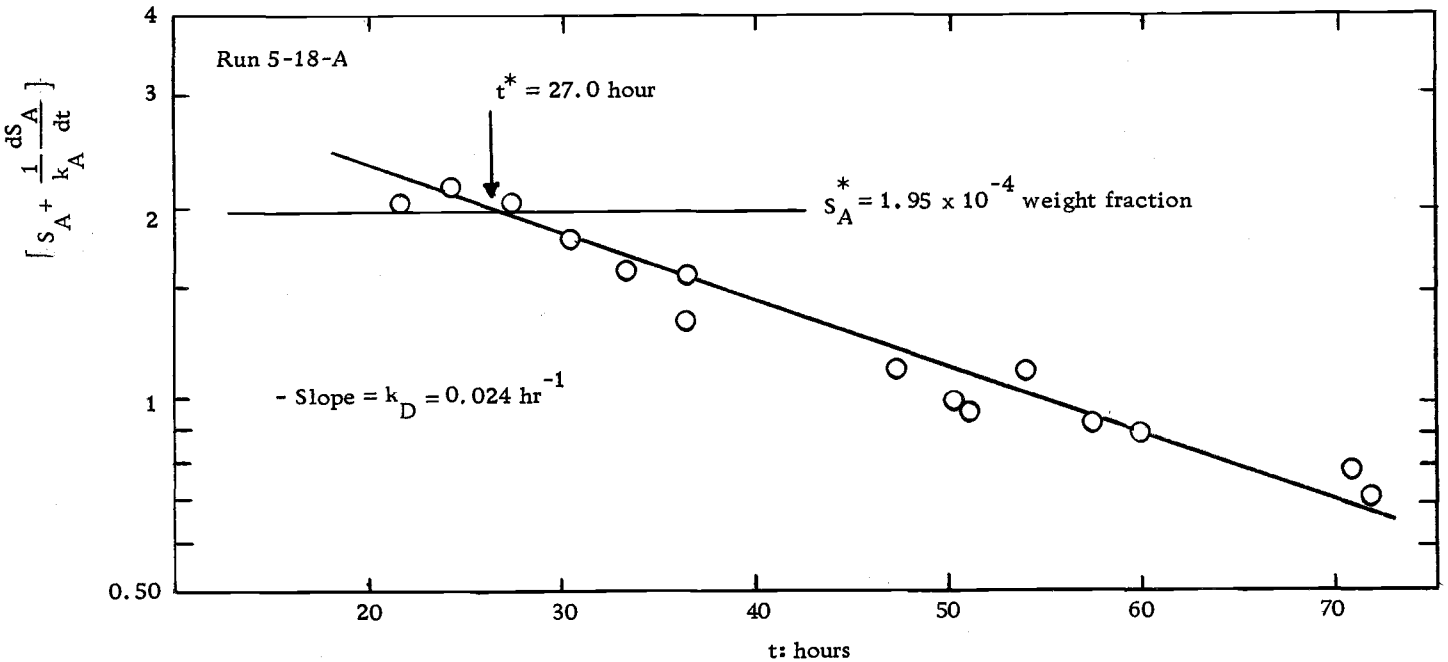

Figure 16. Graphical determination of k_D and t^* from Equation (8a).

Evaluation of $(k_A \frac{\phi_A}{\phi_K})$ and k_K

The values for $(k_A \frac{\phi_A}{\phi_K})$ and k_K were determined by utilizing equation (7).

Dividing by S_K yields:

$$\frac{d\ln S_K}{dt} = (k_A \frac{\phi_A}{\phi_K}) \bar{S} - k_K \qquad (9)$$

Thus, a plot of $(d\ln S_K/dt)$ versus $\bar{S}$ should be linear, with a slope equal to $(k_A \frac{\phi_A}{\phi_K})$ and an intercept equal to $-k_K$. In constructing this graph, the data were first plotted in the form of $\ln S_K$ versus t. A companion plot of $\bar{S}$ versus t was made directly from the peak ratios of each sample injection (corrected for the differing response of alcohols and ketones). Tangents were drawn at convenient points on the $\ln S_K$ versus t plot, slopes computed, and the $\bar{S}$ value at the corresponding time read from the second plot. The plot of $\bar{S}$ versus t is given in Figure 17; the $\ln S_K$ plot was shown in Figure 14. The resulting evaluation of $(k_A \frac{\phi_A}{\phi_K})$ and k_K is shown in Figure 18.

Discussion of ϕ

If Equations (1) and (2) are taken as the basis for the data reduction, which is equivalent to letting the ϕ values equal unity in

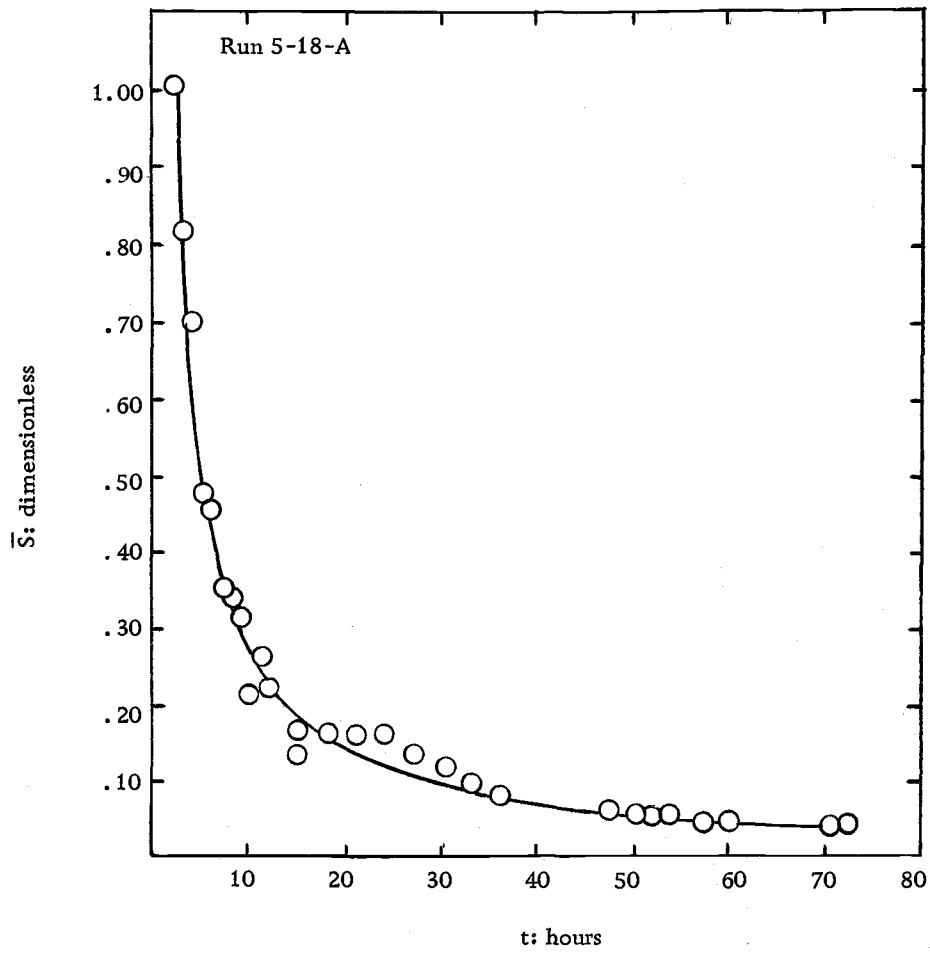

Figure 17. Plot of $\bar{S}$ versus t.

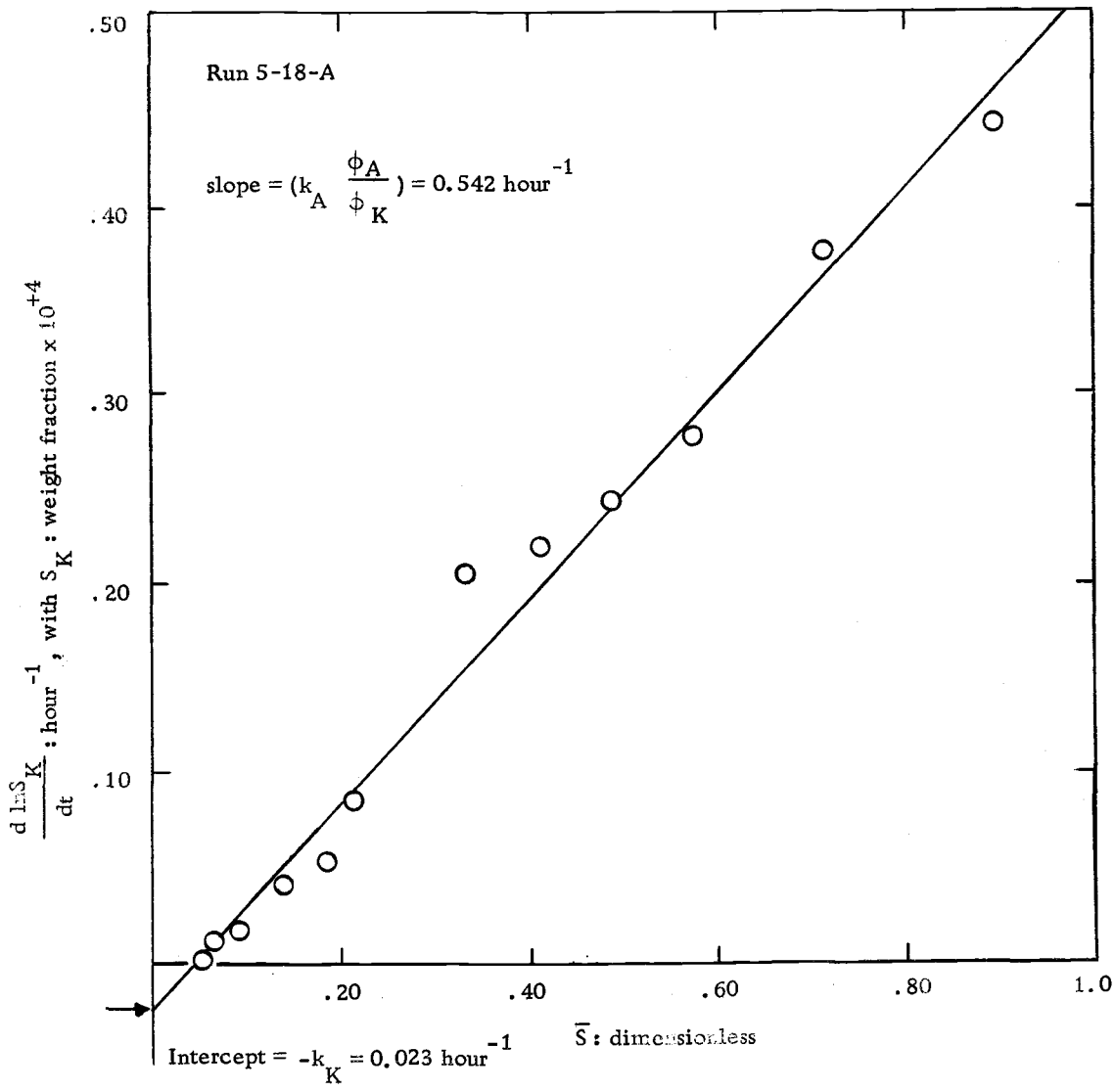

Figure 18. Graphical determination of $(k_A \frac{\phi_A}{\phi_A})$ and k_K

Equations (6) and (7), a disparity is apparent. The k_A value predicted in Figure 15 is still 0.167 hour^{-1}. However, the slope of the plot shown in Figure 18, which should also give the value of k_A, is equal to 0.542 hour^{-1}. Clearly, the original two model equations do not appear to be consistent with each other. It should be emphasized that despite this discrepancy, the analysis of the data showed that the form of each of these model equations was consistent with the data. For example, the excellent linearity of the $d\ln S_K/dt$ versus $\bar{S}$ plot indicated that Equation (2) was acceptable as a possible descriptive equation. Alternative model forms which possessed constants that retained physical significance were not found, and an explanation for the conflicting k_A values was sought.

For the physical situation considered in the derivation of Equations (1) and (2), a stoichiometric relationship between A and K would be expected. It was observed in the discussion of the regular run results on page 70 that the measured values of S_K appeared to be abnormally large with respect to the measured S_A values. A plausible explanation for this is the possibility that the measured concentrations of oxidation products are not equal to the concentrations "seen" by the reacting system. The observed physical result could be qualitatively explained by the existence of any factor which tends to cause A to react to form K near the cell surface more readily than A is released to the bulk of the hydrocarbon relatively far from the

region of reaction. A number of situations can be envisioned where this is the case.

1. The existance of a cellular membrane or effective film surrounding the cell which tends to concentrate the products of oxidation at the surface while the run is in progress would account for the observed result. The term "surface" must be used advisedly, since the actual physical location of the enzymes with respect to the cell is unknown. This is equivalent to a high mass transfer resistance between the enzymes and the hydrocarbon bulk.

2. The relative position of the enzymes with respect to each other and the bulk of the hydrocarbon droplet could affect the relative distribution of A and K. For example, if the path of A molecules to the hydrocarbon bulk surrounding the cell is blocked by the enzyme surface where A is converted to K, then more A molecules would react to form K than would be indicated by the measurement of A in the hydrocarbon.

Either of the cases 1 or 2 might be considered somewhat analagous to the situation which exists when reactants must diffuse into a porous catalyst in order for the reaction to occur. For a sequential reaction $A \longrightarrow B \longrightarrow C$ where all reaction must occur in the interior of the catalyst pellet, it might be expected that the measured concentration of C would be higher with respect to the measured concentration of B than would be the case if the reaction occurred in the homogenous

fluid. If the rate of conversion of B to C is high with respect to the mass transfer rate of B from the pores to the bulk, then more molecules of B will react than will find their way to the surface. In the extreme case, no B will diffuse to the bulk, and only C will be measured.

It is postulated that a region of local concentration existed during the actual run and that this accounted for the anomalous observed ratio of alcohol and ketone concentrations. In order to explain this phenomenon quantitatively, the following simple relationship between local and measured concentrations was assumed:

$$s_i = \phi_i S_i \tag{10}$$

where

s_i = the local concentration of component i

S_i = the measured concentration of component i

ϕ_i = a constant factor relating the local and measured concentrations.

If Equations (1) and (2) are written in terms of the local concentrations:

$$\frac{ds_A}{dt} = R - k_A s_A$$

and

$$\frac{ds_K}{dt} = k_A \left[\frac{MW_K}{MW_A}\right] s_A - k_K s_K$$

If Equation (10) is substituted into these expressions, the appropriate manipulations lead to Equations (6) and (7).

It is emphasized that the "true" value of k_A is predicted by Equation (8) regardless of whether or not a local region of concentration is assumed to exist. However, if such a region does exist, the value of the slope obtained from Equation (9) would represent the "true" k_A value multiplied by the ratio (ϕ_A/ϕ_K). This explains why two different "k_A" values were obtained from the original model equations, which did not account for the presence of a local region of concentration.

Discussion of Decay

If the values of k_A and S_A^* obtained from Equation (8) are used in Equation (6) to generate S_A as a function of time, the generated curve indicates that S_A approaches a maximum value of S_A^*. The exponential approach of S_A to this maximum value provides a reasonable description of the alcohol data in the initial region of the curve, but the model equation dictates that this maximum value should be maintained for the remainder of the run. Since the data exhibited a gradual decline in the alcohol concentration after the maximum value of

S_A^* was attained (cf. Figure 8), a modification of Equation (6) was required in order to describe the data over the entire time course of the run. On page 70 it was suggested that the break in the trend of the data at about t = 9 hours indicated the possibility that some change in mechanism took place. It is now proposed that this break marked the transition to a region of decaying enzyme activity. This would modify assumption (13) on page 91. Enzyme deactivation was initially considered to be negligible throughout the course of the run. Several considerations seem to justify the inclusion of a term to account for enzyme decay in the model scheme.

Although the factors determining enzyme stability are complex and poorly understood, some general quantitative characteristics of enzyme deactivation have been suggested. Humphrey (60) has pointed out that when loss of enzyme activity occurs, it is generally an exponential process. For a pure enzyme, the exponential loss of activity begins immediately, but for crude, non-purified enzyme preparations this decay can be preceded by a period of induction and a period of relatively constant enzyme activity. The possibility of an induction period for the oxidation system under study seemed unlikely in view of the zero-order rates observed when exogenous 2-hexadecanol was added; this suggested that the enzymes were induced at the time of hydrocarbon addition. However, since the cells were resuspended in a nitrogen-free medium with no carbon source other than the

n-hexadecane, it seems reasonable that the enzymes were subject to eventual loss of their activity.

It was decided that only a single decay term would be considered, that being for decay of the activity of the enzyme catalyzing the initial oxidation of hexadecane to hexadecanol. In agreement with Equation (3), R is considered to be directly proportional to the total mass of catalyst, as measured by the dry cell weight concentration, W.

The decay term multiplied by W can be thought of as the mass of active catalyst. Mathematically, the R term in Equation (1) is replaced by:

$$R \cdot f(t)$$

where

$$f(t) = 1 \qquad \text{for } t < t^*$$

and

$$f(t) = e^{-k_D(t-t^*)} \qquad \text{for } t \geq t^*$$

The value of t* is defined as the time, in hours, at which decay of the first-step enzyme begins. The decay constant, k_D, has units of reciprocal hours and is an indication of the speed of the decay process. This form of decay function was used in a simulation study of penicillin amidase deactivation made by Humphrey and Ho (25).

Modification of Equations (1) and (2) by the inclusion of the decay term and the ϕ factors results in the final form of the model for the description of n-hexadecane transformation, which is summarized

in Equations (6), (6a), and (7).

Comparison of the Model with Experimental Data

Figures 19 through 33 display the results of several experimental runs, along with the corresponding curves predicted by the model equations. The lower plot on each figure indicates the values of S_A, and is on an expanded scale relative to the plot of the S_K values. The explanation of the plots is summarized in the following table:

Table 4. Explanation of Figures 19 through 33.

Plot	Representation in Figure	Model Equation	Significance
Lower	Open circles	-	2-Hexadecanol data, S_A
Lower	Upper solid curve	(6)	S_A model with no decay
Lower	Lower solid curve	(6) $t < t^*$ (6a) $t > t^*$	S_A model with decay after t^*
Upper	Open circles	-	2-Hexadecanone data, S_K
Upper	Upper solid curve	(7)	S_K model with no decay
Upper	Lower solid curve	(7)	S_K model with decay after t^*

All model curves were generated on an analog computer using the values of the model parameters determined by the calculational techniques outlined previously. The accuracy of the analog method of

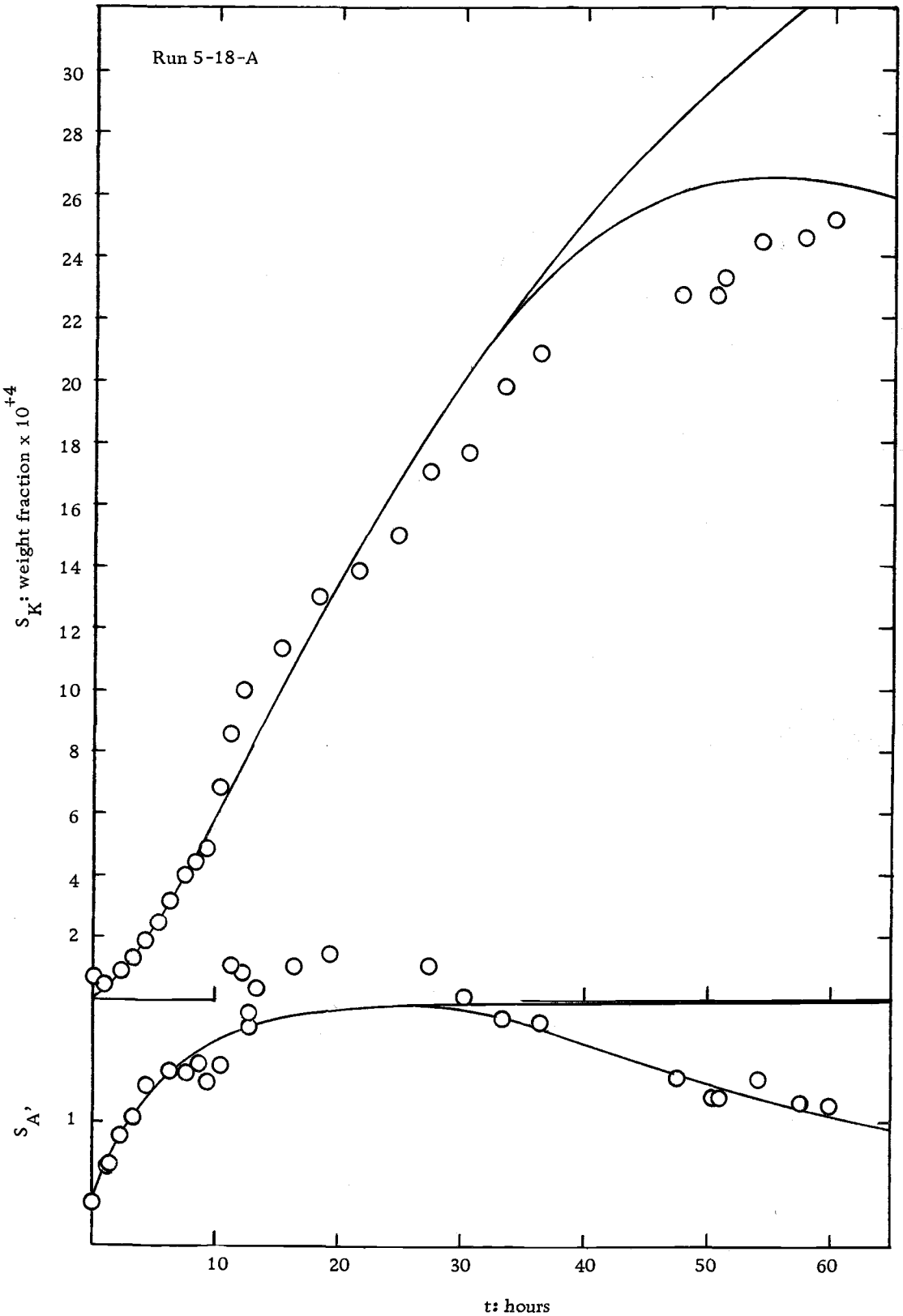

Figure 19. Model-data comparison.

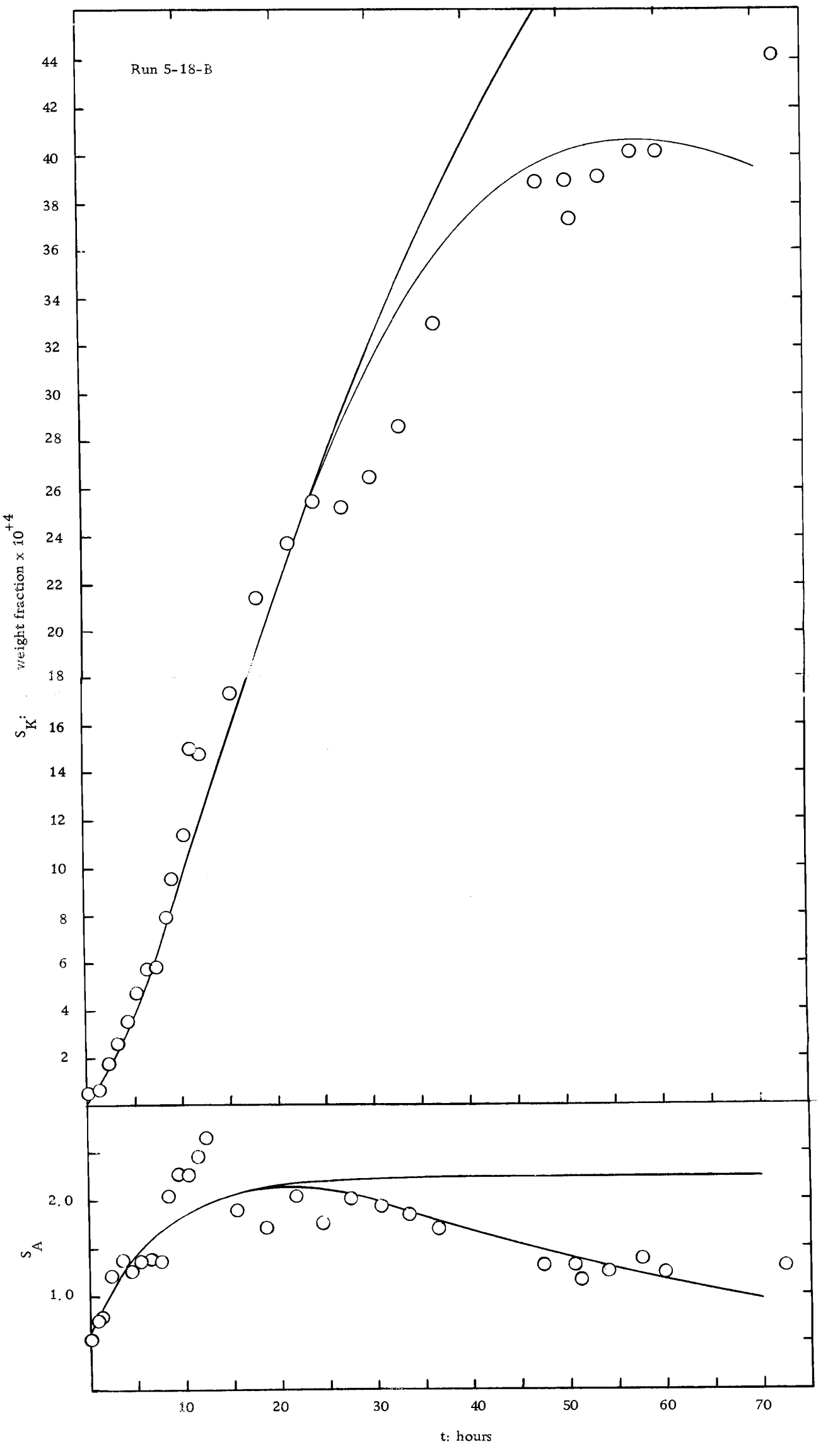

Figure 20. Model-data comparison.

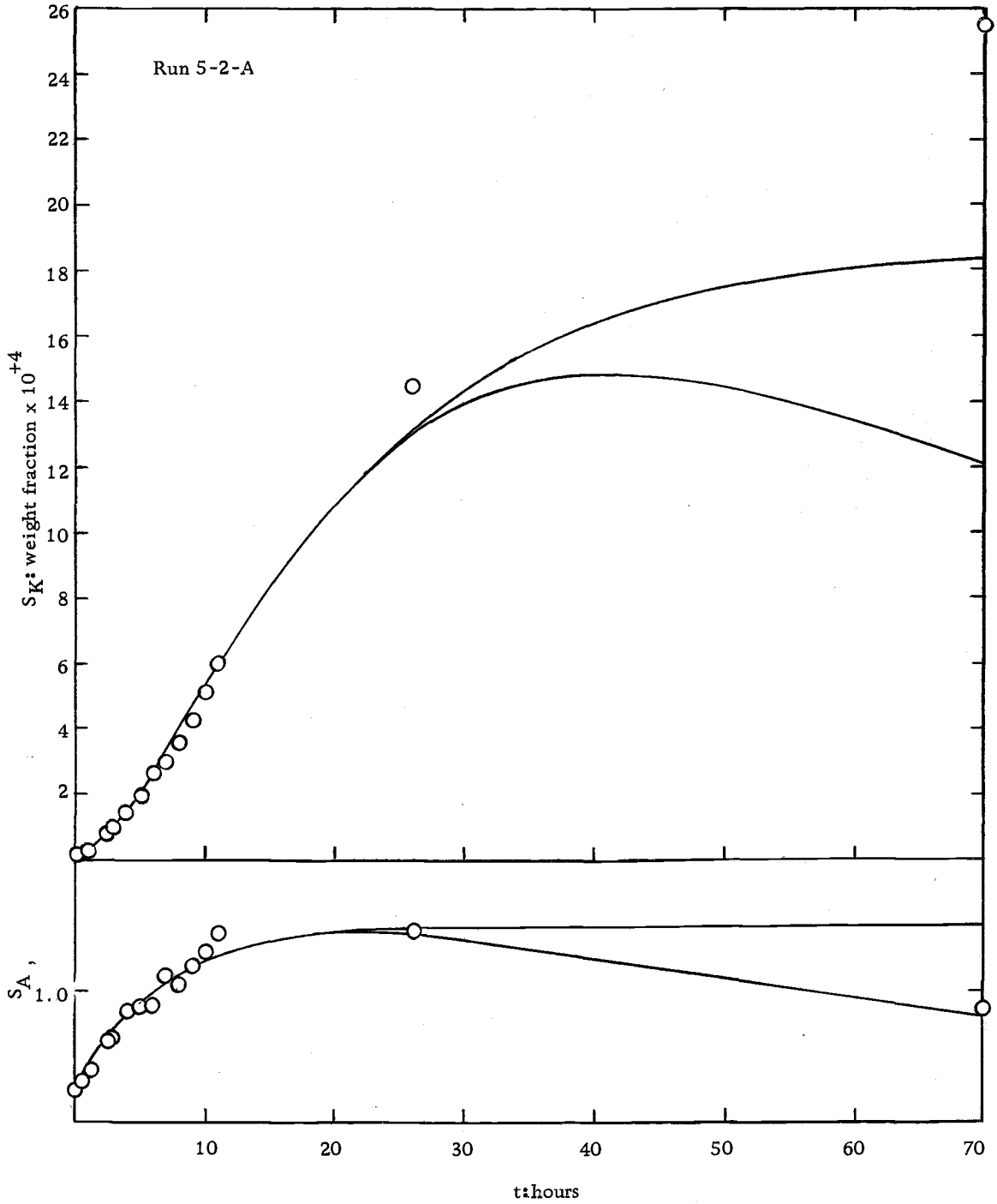

Figure 21. Model-data comparison.

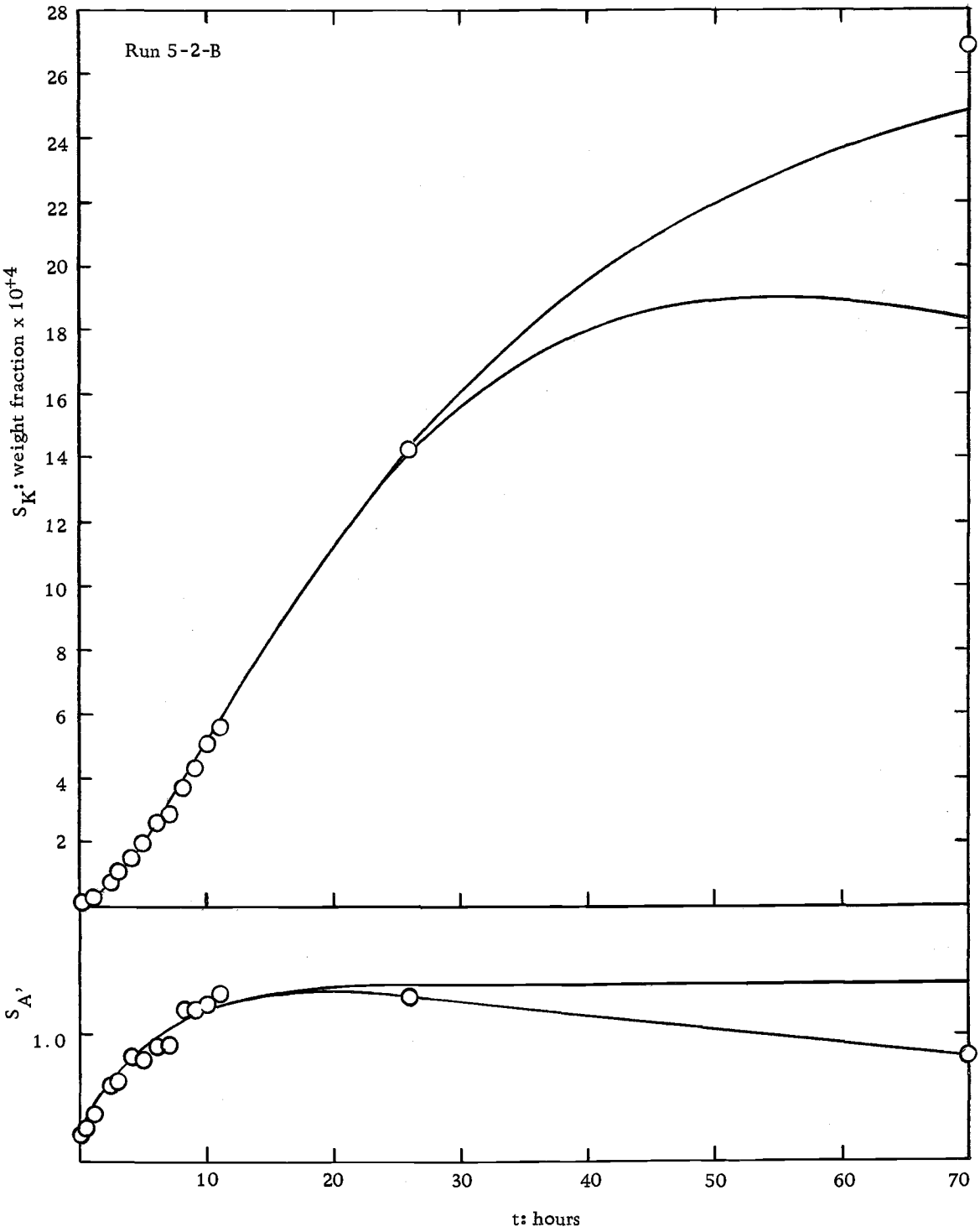

Figure 22. Model-data comparison.

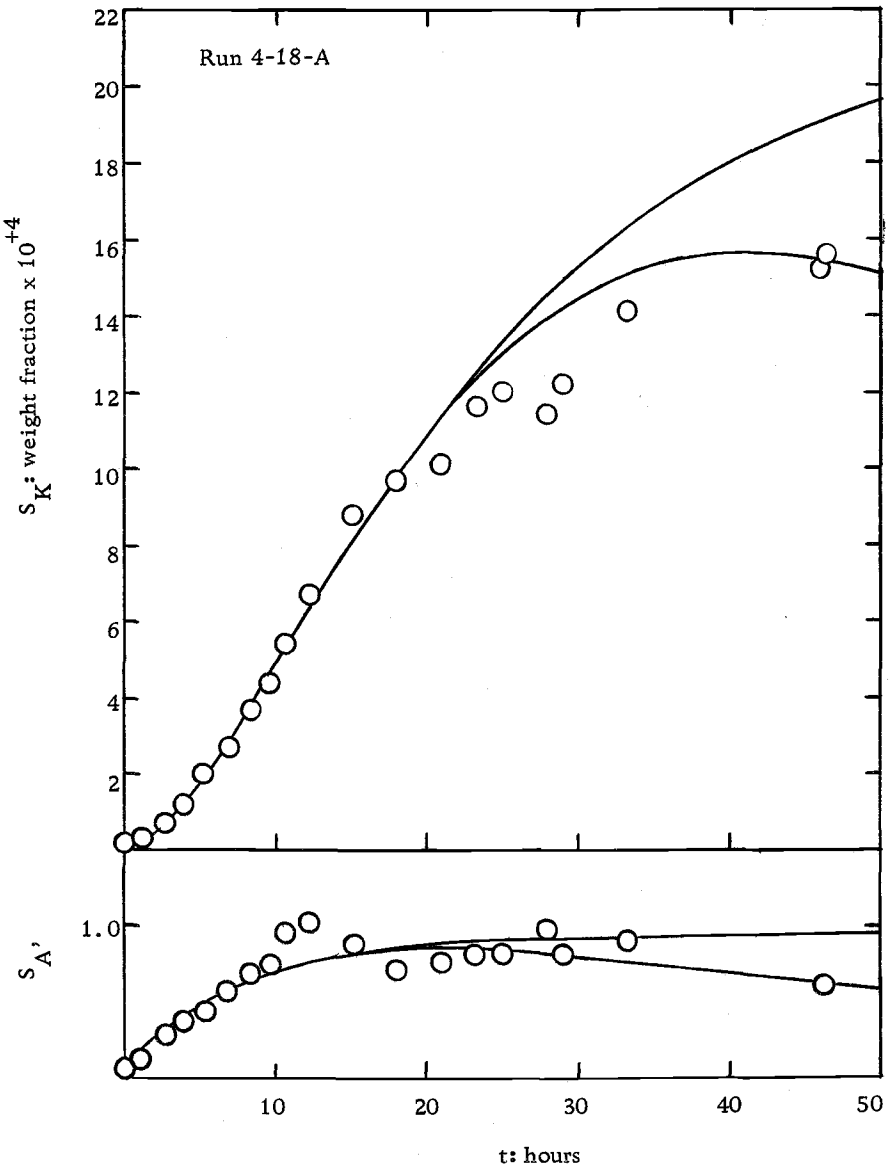

Figure 23. Model-data comparison

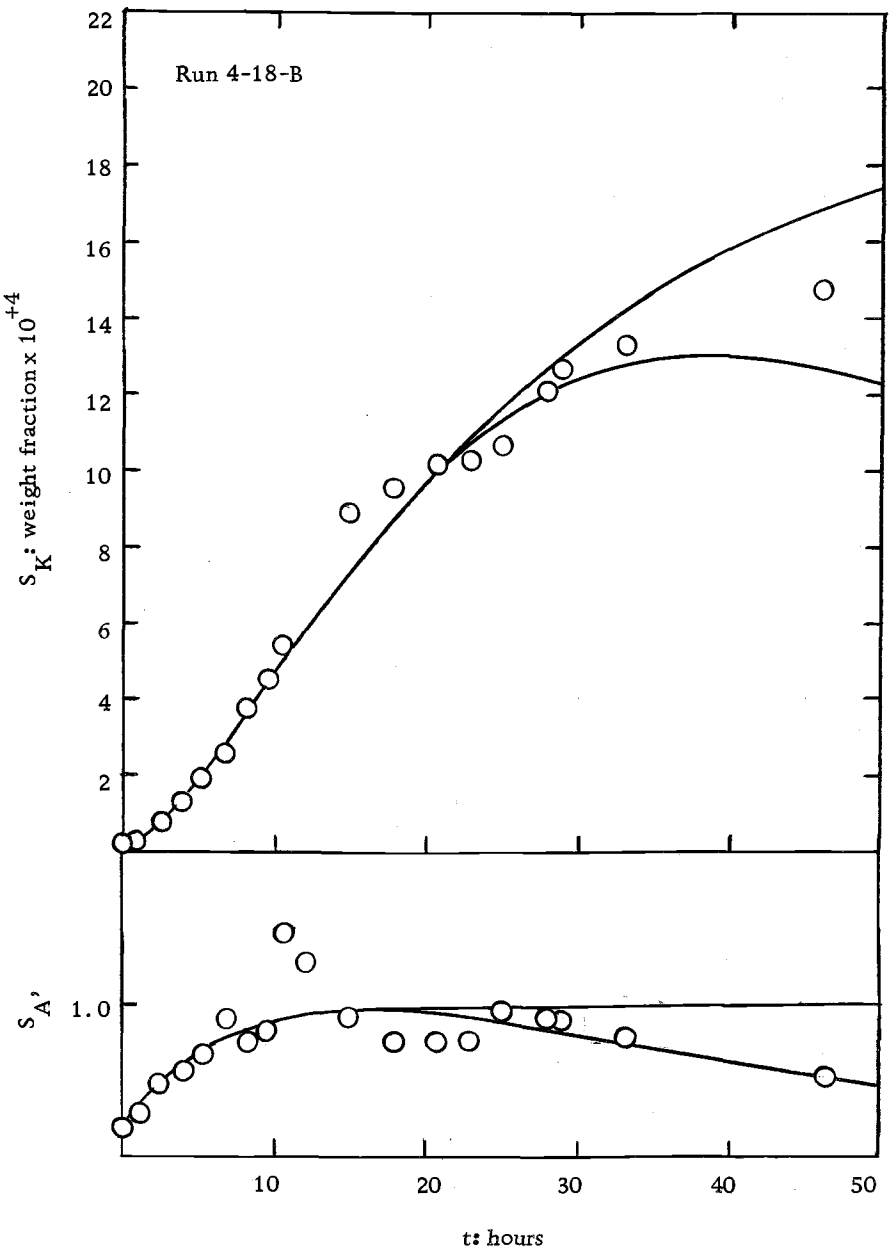

Figure 24. Model-data comparison.

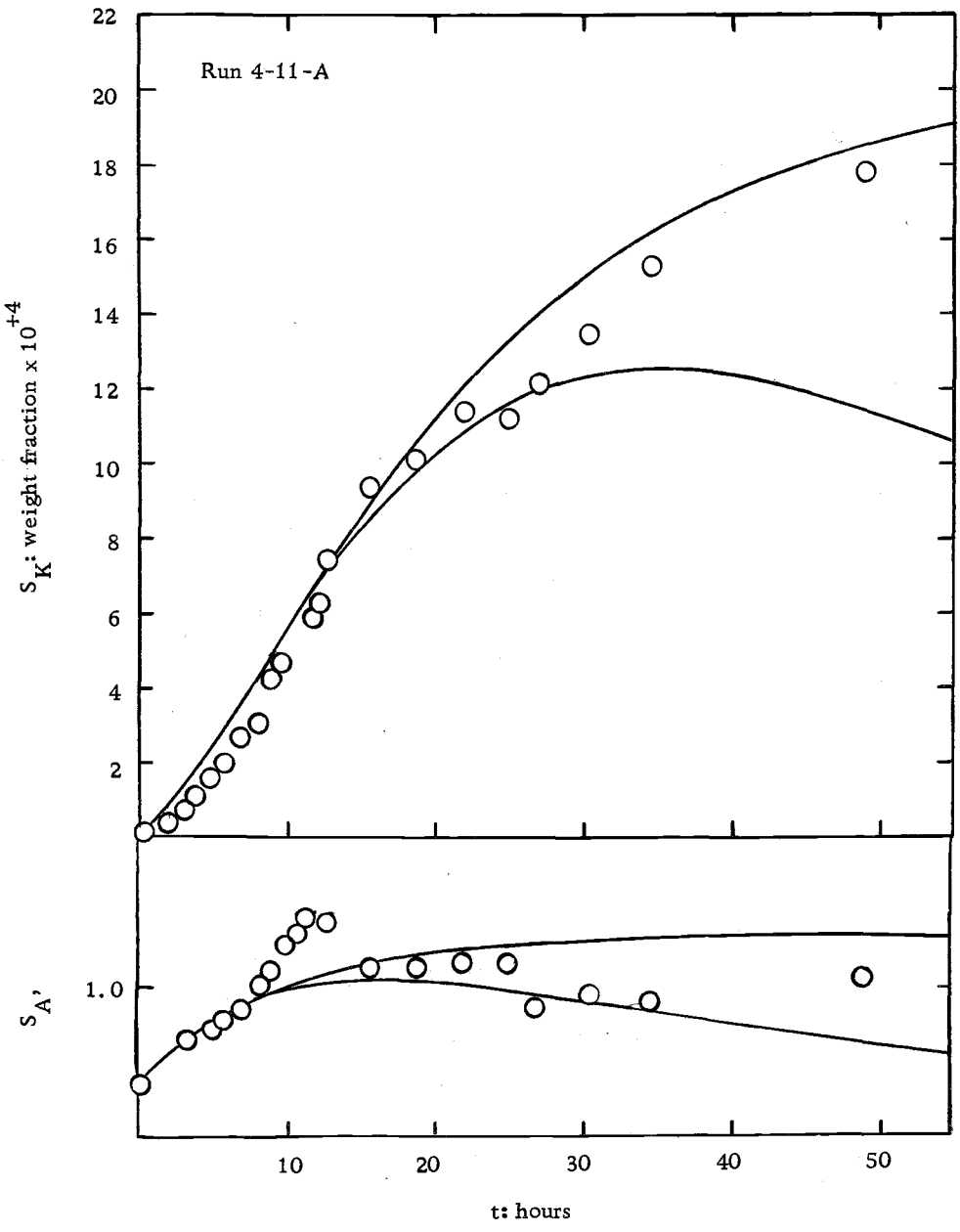

Figure 25. Model-data comparison.

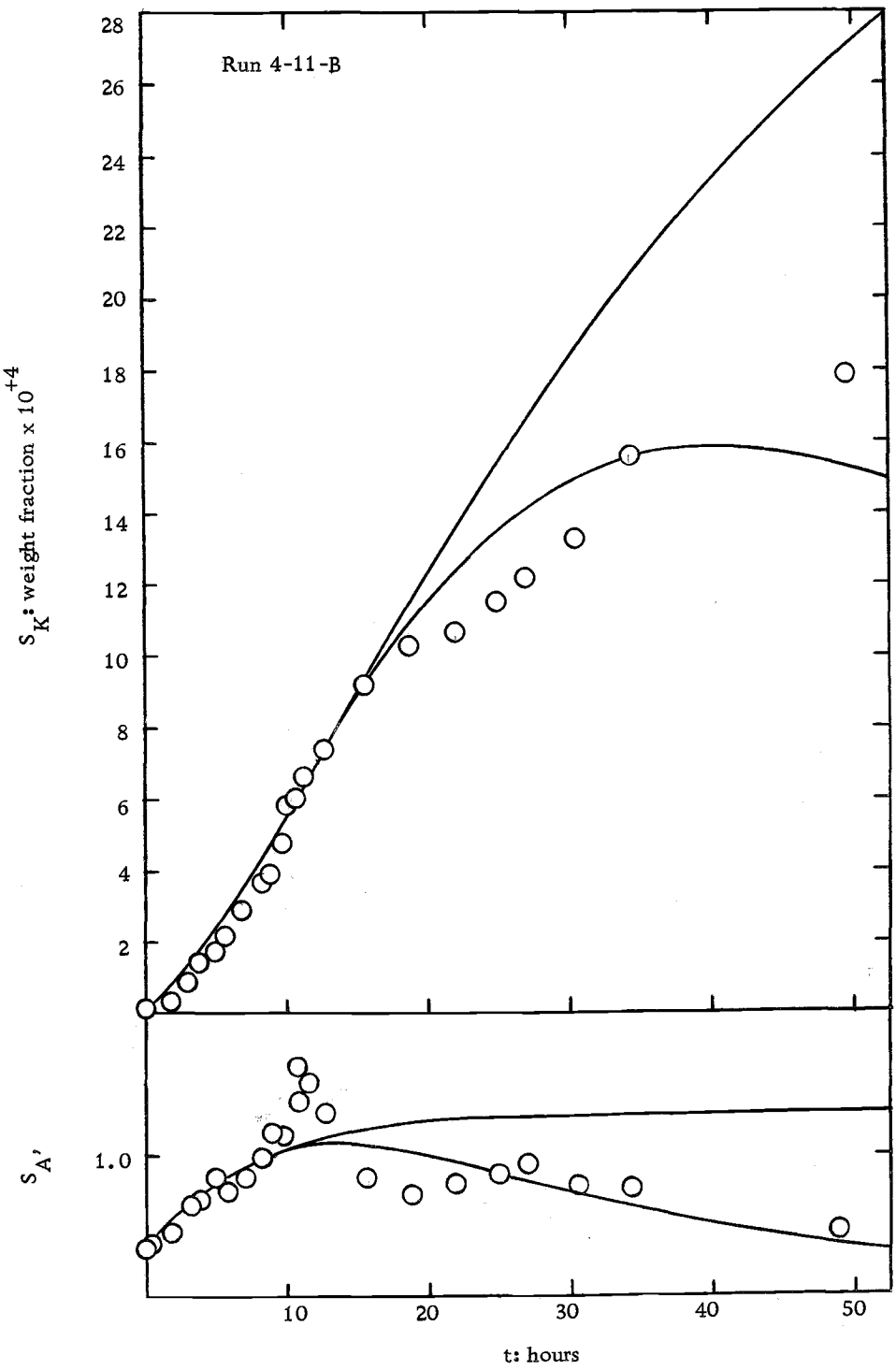

Figure 26. Model-data comparison.

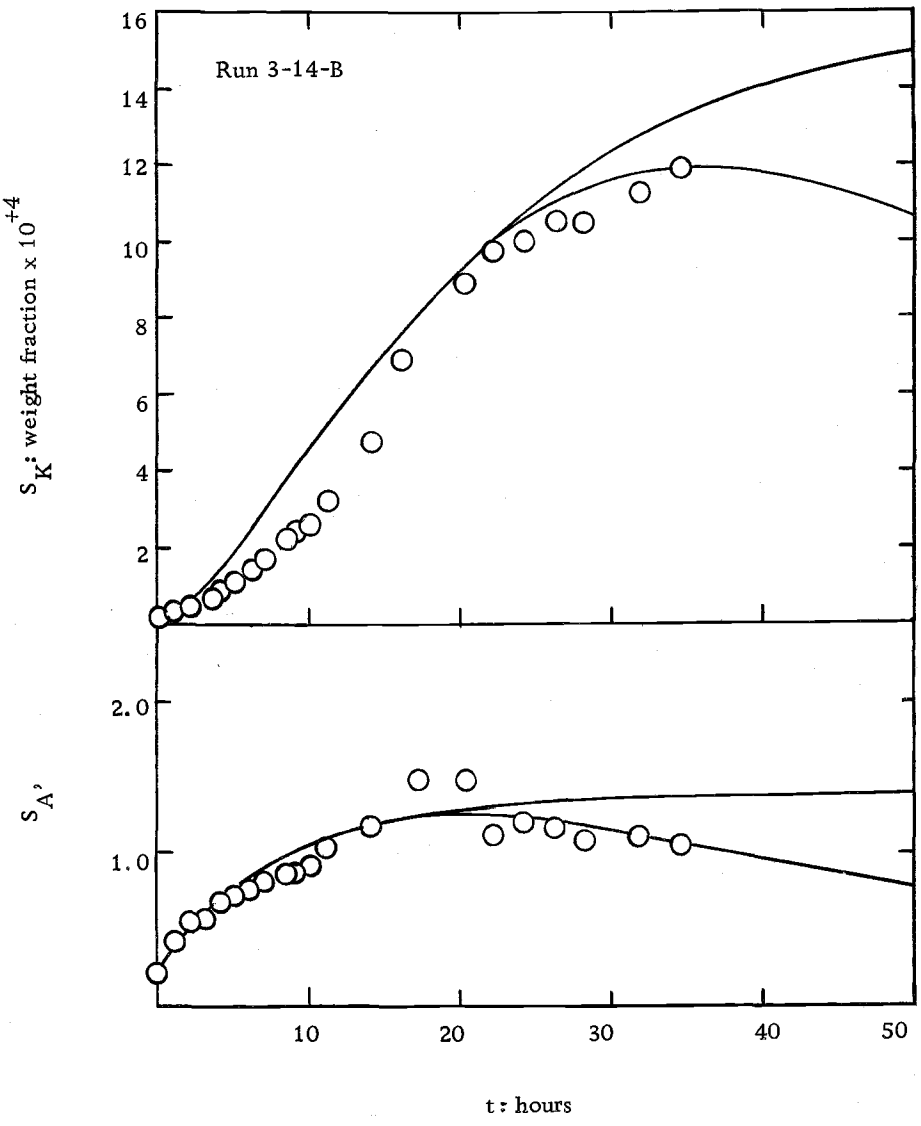

Figure 27. Model-data comparison.

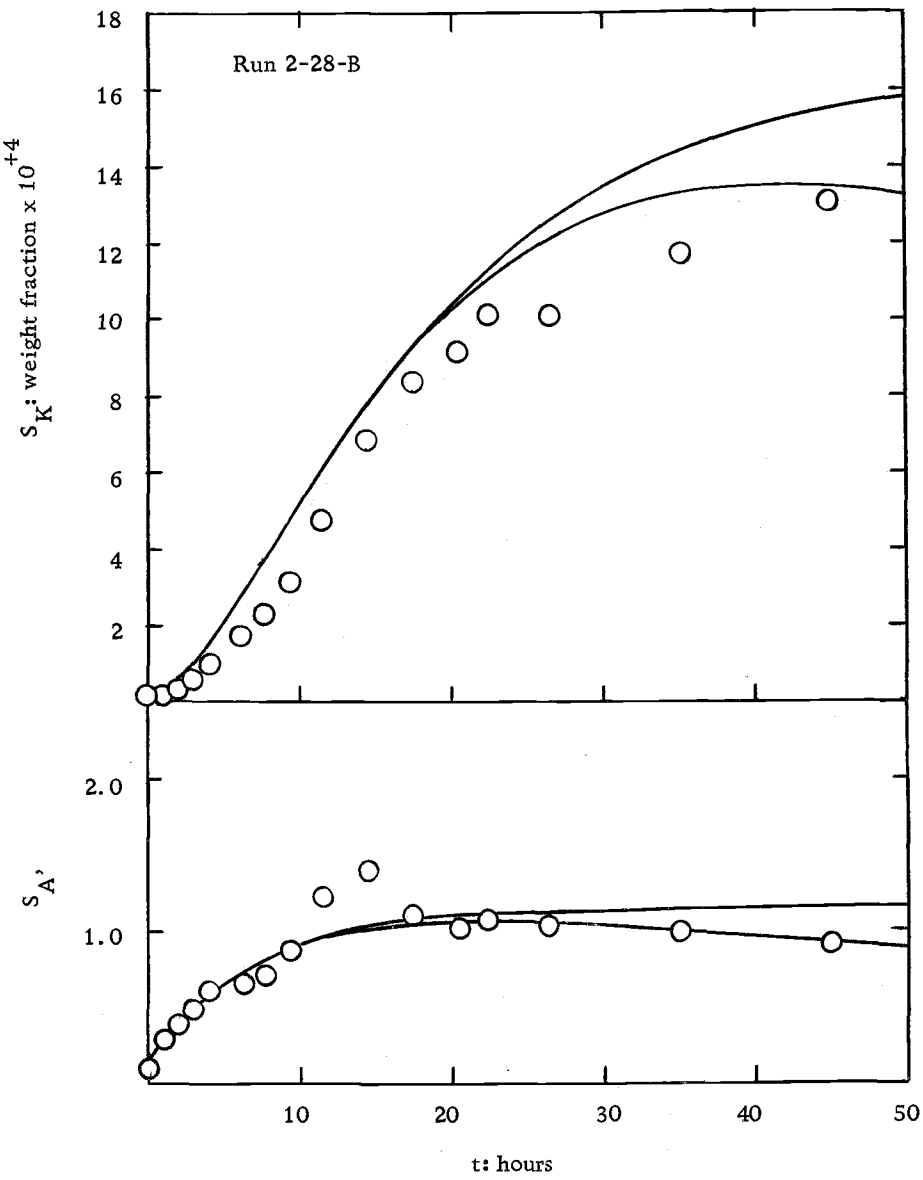

Figure 28. Model-data comparison.

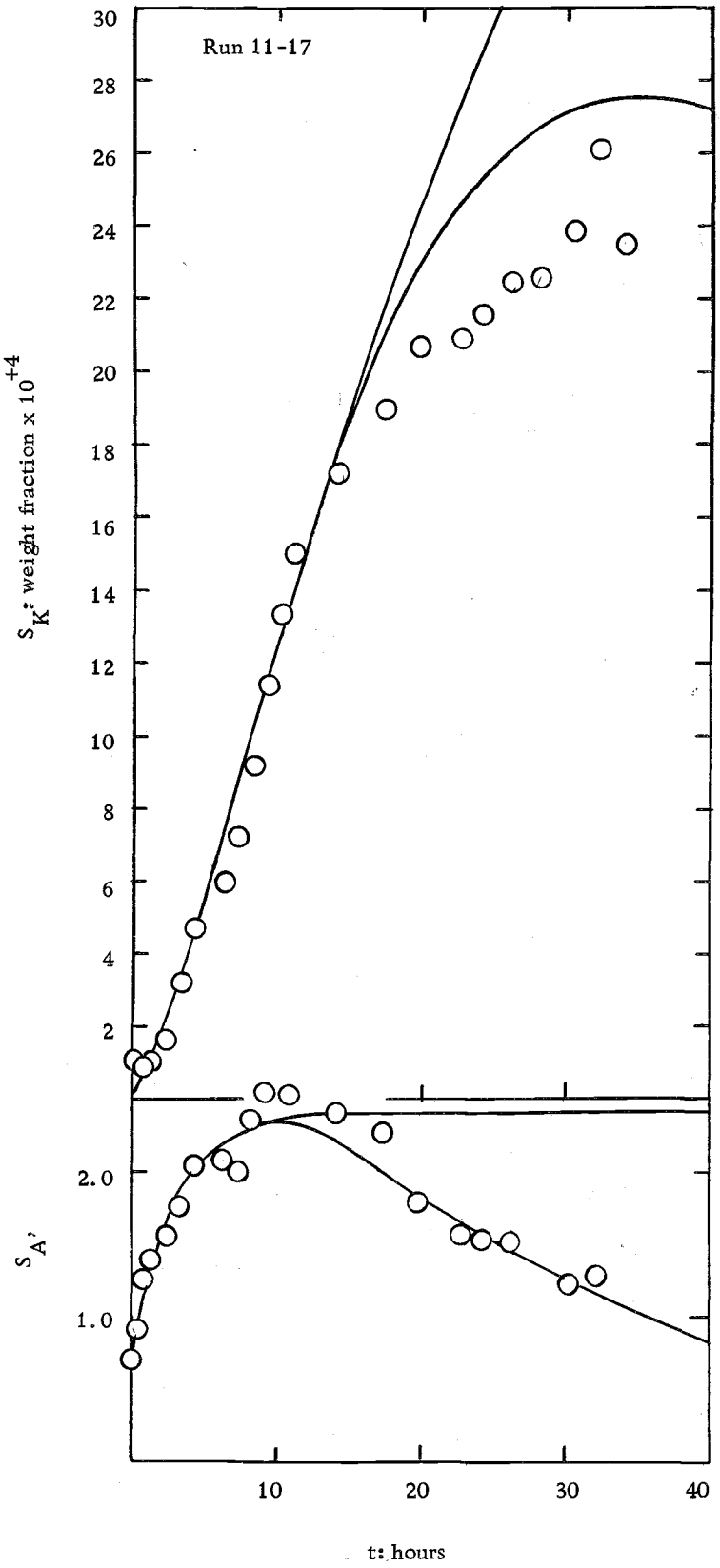

Figure 29. Model-data comparison.

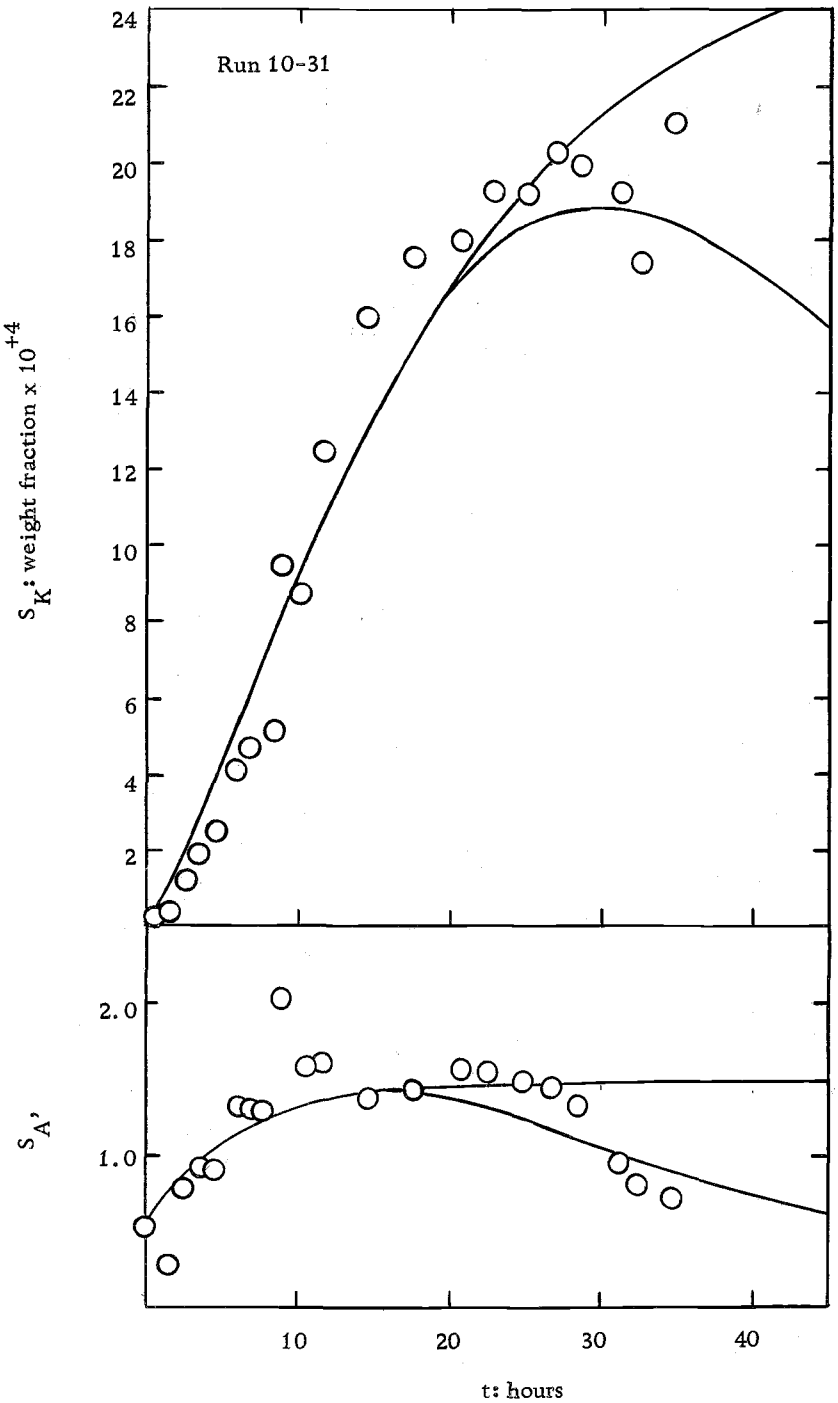

Figure 30. Model-data comparison.

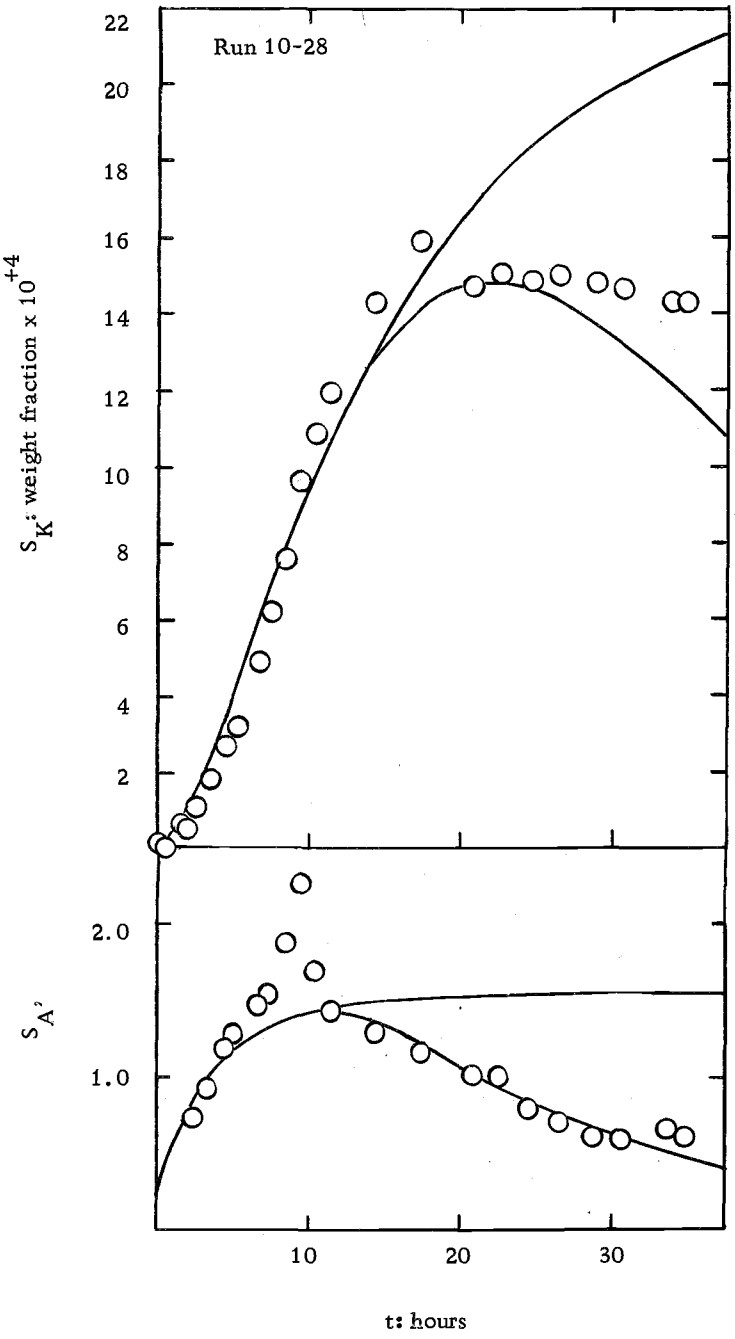

Figure 31. Model-data comparison.

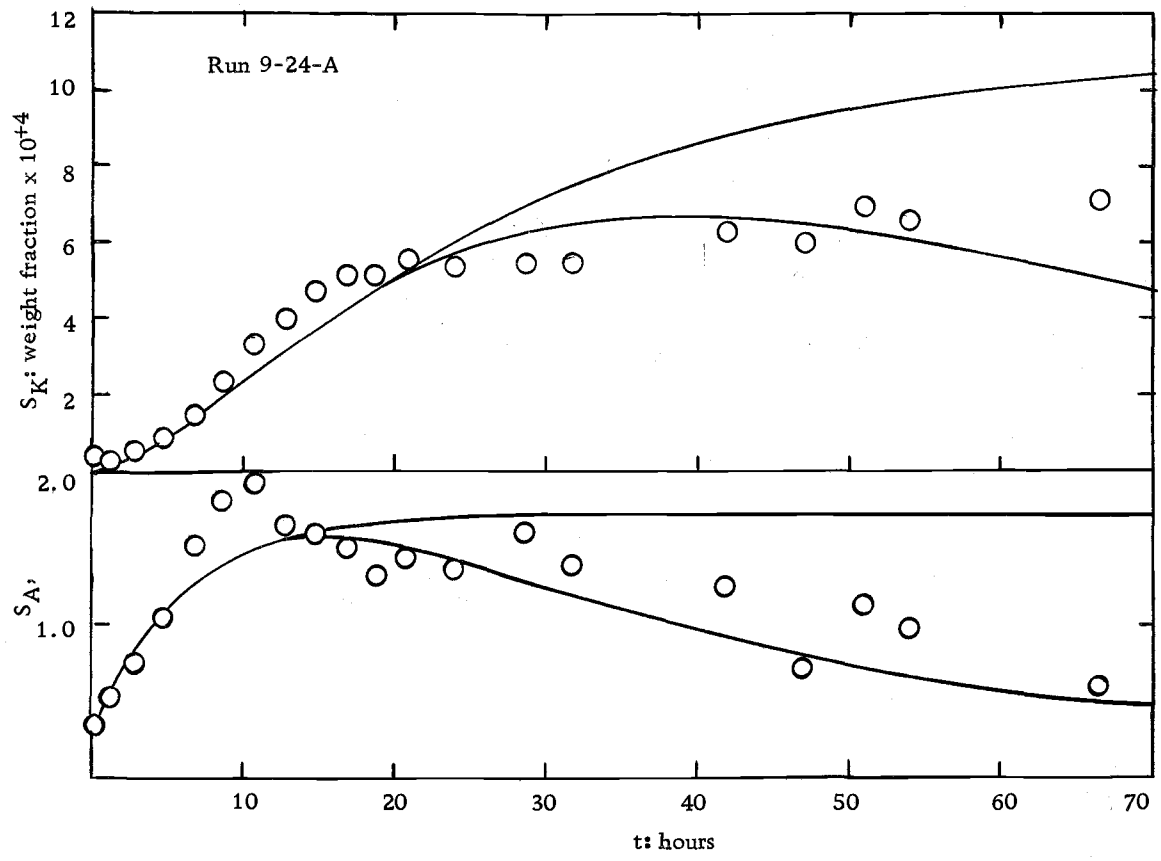

Figure 32. Model-data comparison.

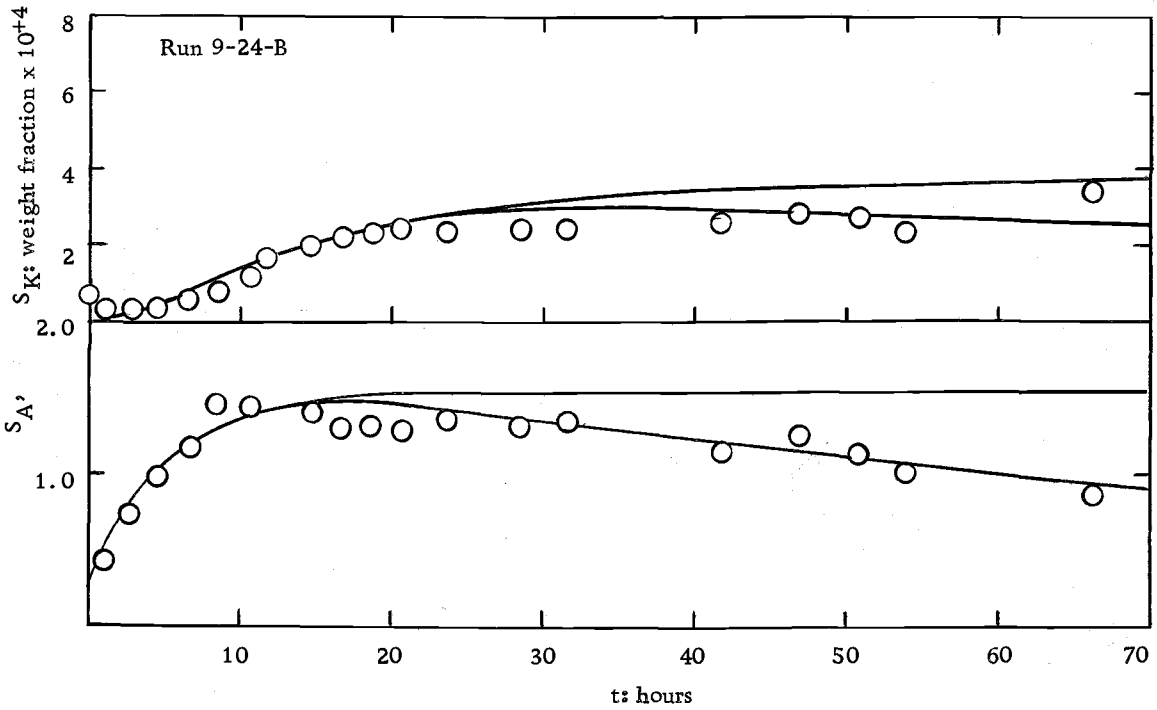

Figure 33. Model-data comparison.

solution was verified by comparison to the solution of both the differential and integrated forms of the model equations on a digital computer. The model parameters for each of the runs depicted are given in Appendix I. The values of (R/ϕ_A) and (ϕ_A/ϕ_K) computed from the model parameters are also included in the summary. It was not possible to compute separate values of ϕ_A and ϕ_K from the experimental data.

Parameter Errors

The estimated maximum errors for the calculated values of the model parameters are summarized in Appendix II. The largest error reported was for the value of k_K. The maximum error for this parameter was calculated to be $\pm$ 50%. This reflects the sensitivity of the intercept of the $(d\ln S_K/dt)$ versus $\bar{S}$ plot to slight changes in the position of the curve through the data points. Although many of the error values appear to be rather large, it is emphasized that these are maximum values of the error incurred in evaluating the parameters. Extreme situations were used in computing these values, and the possibility of compensating errors was not considered. Therefore, it seems rather unlikely that the actual errors of all of the parameters for a given run would approach the magnitude of the maximum error values. This is demonstrated by the excellent fit of the model curve to the S_A data over all regions of the run. The net

experimental error for the measured S_A values was estimated to be $\pm$ 12% (cf. Appendix II), and the model curve represents the experimental data well within these limits of experimental error. Similarly, the net experimental error in the measured S_K values was found to be $\pm$ 6.2%, and the model is generally within these limits in the initial regions of the run. Deviation of the S_K model from the data is more pronounced for large times, and the possible reasons for this are discussed in the final section.

Figures 34, 35 and 36 give an indication of the relative influence of each of the parameters on the model equations. The curves on each plot were prepared by generating the limiting model curves for a $\pm$ 10% variation in the designated model parameter. All other parameters retained the values used to generate the model curves for Run 5-2-A, illustrated in Figure 21.

Run-to-Run Comparisons

It is expected that the computed values of (R/ϕ_A) and (ϕ_A/ϕ_K) would be comparable for the test and control vessels of a given run. For example, the conditions for runs 5-2-A and 5-2-B were identical, and the computed (R/ϕ_A) and (ϕ_A/ϕ_K) values (cf. Appendix II) are certainly within experimental error. An exception is Run 4-18. The (ϕ_A/ϕ_K) values for the A and B vessels of this run are in considerable disagreement. From a calculational standpoint, the difference in

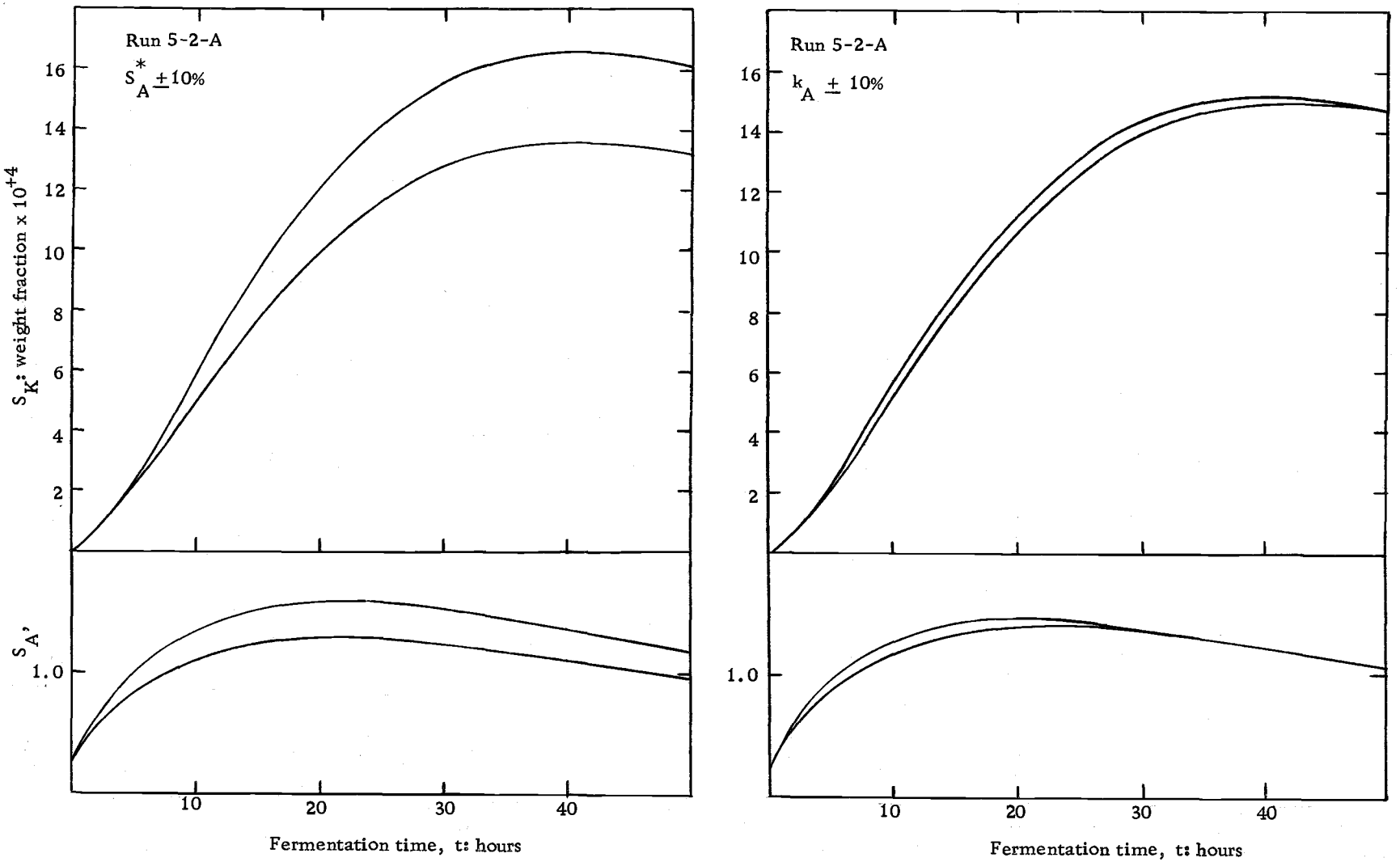

Figure 34. Effect of S_A^* and k_A on model curves.

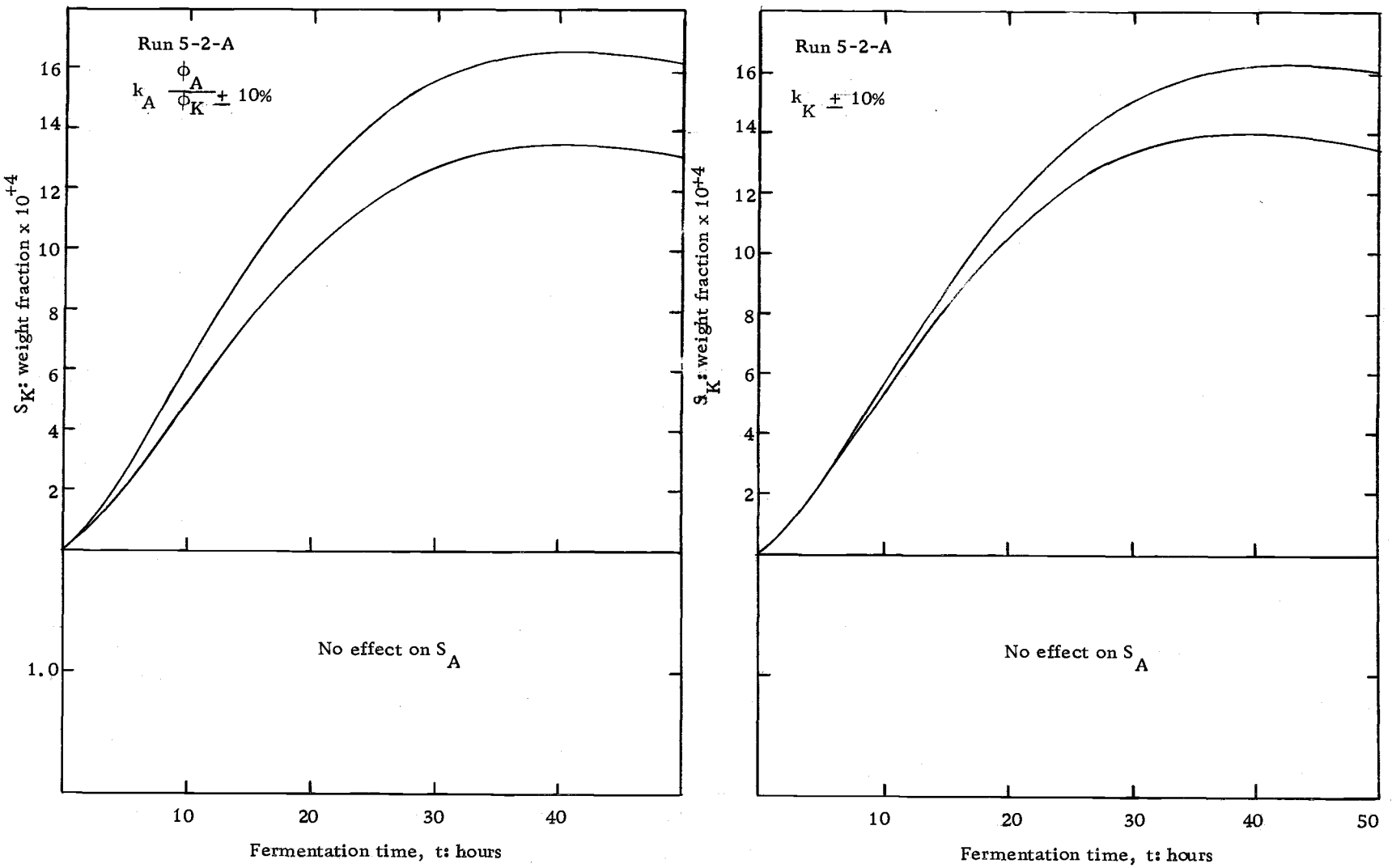

Figure 35. Effect of $k_A \frac{\phi_A}{\phi_K}$ and k_K on model curves.

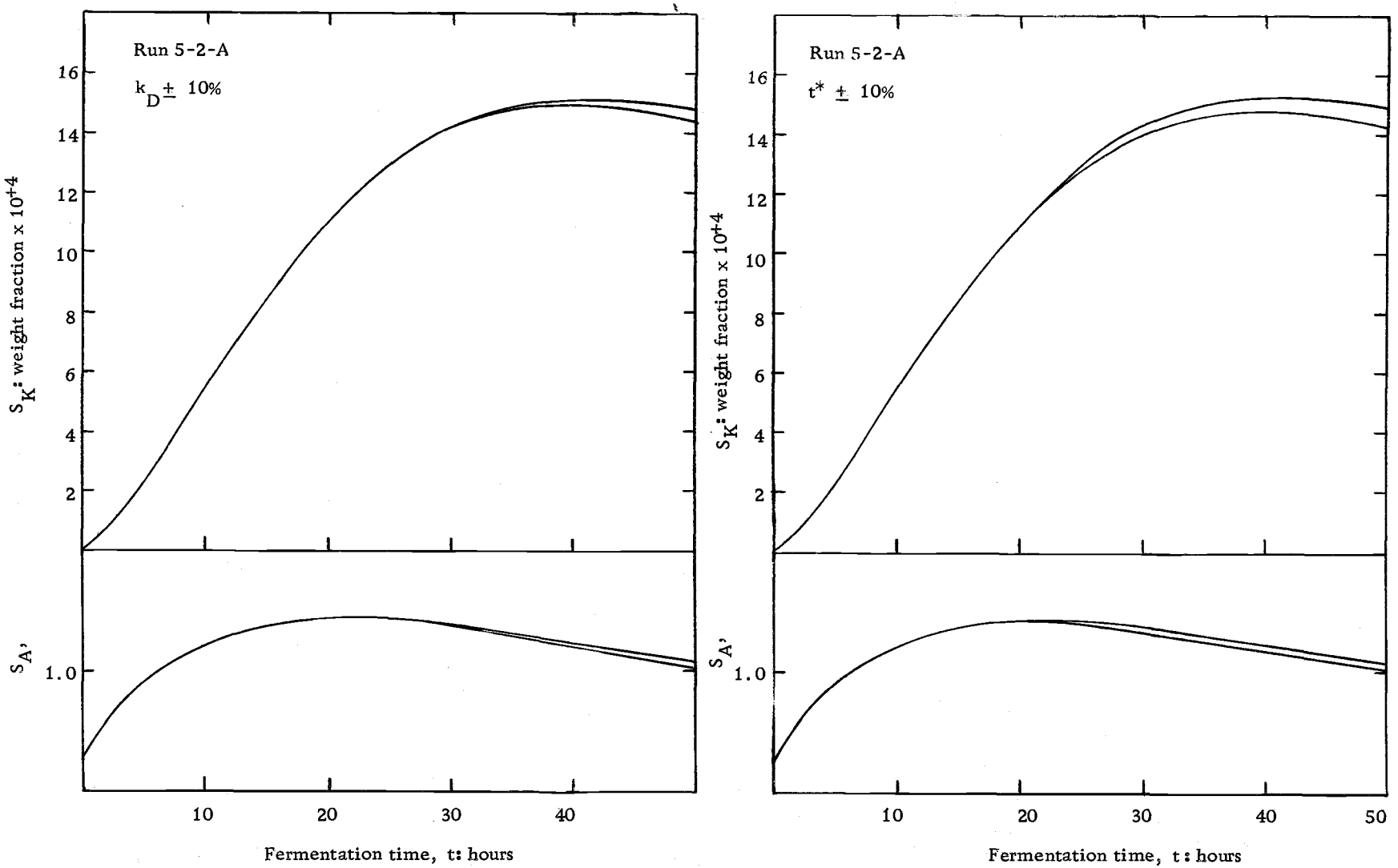

Figure 36. Effect of k_D and t^* on model curves.

these values is almost entirely due to slightly lower values of S_A in the A vessel during the first ten hours of the run. This points out the sensitivity of the computed parameter (ϕ_A/ϕ_K) to small differences, in the data.

The model equations predict that the value of S_A^* is independent of the cell level. However, in addition to differences attributed to experimental error, there appear to be very real differences in the values of S_A^* attained in the different runs. For example, the values obtained in the 5-18 runs were more than twice the values obtained for the 4-18 runs. In general, this variation was not correlated with the cell level or other experimental conditions. Apparently, this difference was primarily the result of the inherent biological variability of the factors which determined S_A^*.

Parameter Dependence on (W/M_H)

It was decided that there were insufficient data to verify the predicted dependence of the model parameters on (W/M_H), the ratio of the cell concentration to the mass of hydrocarbon (cf. Equations (3) through (5)). This dependence was obscured by the variability observed from run to run. In an attempt to clarify the effect of varying (W/M_H), the total hydrocarbon level was varied in the two vessels of a single run (Run 5-18), while other factors were held constant. The value of M_H in the A vessel was twice the value in the B vessel. Using

Equations (3), (4) and (5), the model parameters for the B vessel can be predicted from the parameters of the A vessel. The B vessel parameters were computed from the experimental data as usual, and a comparison of the model curves generated from the two sets of values is given in Figure 37. It was concluded that the model curve predicted from the A vessel model was in agreement with the model curve computed from the B vessel data, within the limits of experimental error.

Model Restrictions

It was concluded from Figures 19 through 33 that the model Equations (6), (6a) and (7) are capable of describing the oxidation of n-hexadecane over the entire course of a 70-hour run. Runs of longer duration were not made. The qualitative agreement of the model with the data is excellent. Quantitative deviations of the model equations from the data were observed primarily for times greater than 20 hours after initiation of the fermentation. While it was concluded that these deviations were within the limits of the experimental errors involved, certain restrictions concerning the validity of the model should be pointed out.

Decay

The model accounts for decay by assuming that the first step

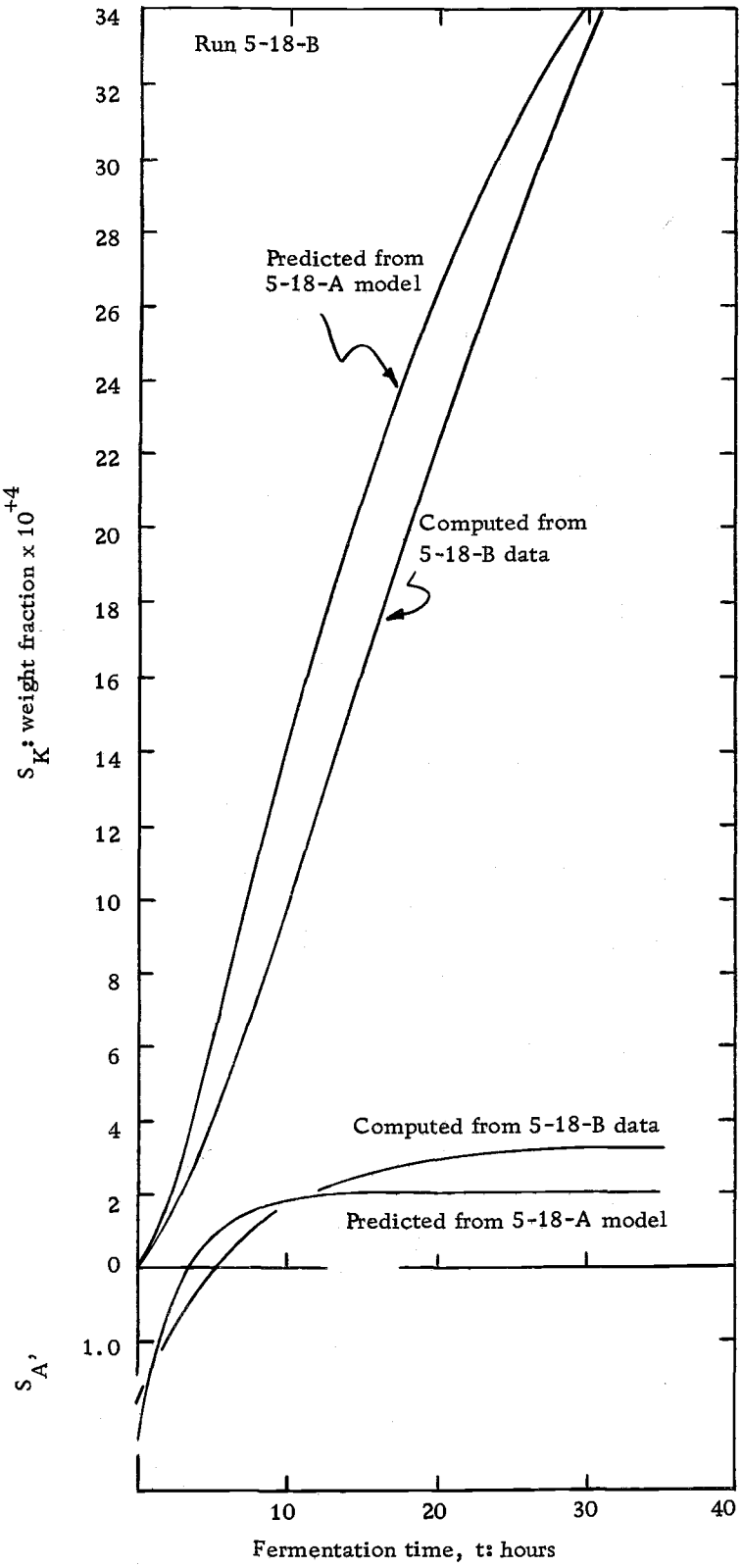

Figure 37. Predicted and observed effect of (W/M_H).

enzyme only is subject to loss of activity. Realistically, it should be assumed that all of the enzymes are subject to decay. However, from a modeling viewpoint, it is quite difficult to quantitatively account for such a situation while retaining the direct physical significance of the model parameters. For this reason the more general situation was not considered. In view of the fact that the simple decay term appeared to be consistent with the qualitative and quantitative description of the experimental data, an alternate physical interpretation might be suggested. For example, a mixed-function oxidase is normally considered to be required for the formation of alcohols from alkanes. Such enzymes normally exhibit a requirement for a cofactor. It seems reasonable that a decline in the ability of the microorganism to supply or regenerate the cofactor for the first conversion step would have the same net effect as a decay of the first step enzyme itself.

Choice of S_A^*

The value of S_A^* is chosen so as to allow a continuous representation of the alcohol data over two apparently different regions. This is discussed in more detail in Appendix III. Strictly speaking, S_A^* should be chosen with respect to the initial portion of the curve, and the inability to do this was considered to be a limitation of the resulting model.

Constancy of ϕ

The values of ϕ were assumed to be constant throughout the course of the run. Since this factor represents the heterogeneous nature of the region between the reaction surface and the surroundings, it seems likely that it is subject to variation as the cell ages.

During an experimental run, the fluid loss from sampling and evaporation consisted of from 6-10% of the total initial fermentation volume. It seems possible that this loss may have indirectly influenced the chemical transformation by virtue of its effect on the physical nature of the relationship between the cells, the hydrocarbon and the aqueous phase.

SUMMARY

The results of this investigation show that the oxidation of n-hexadecane to 2-hexadecanol and 2-hexadecanone by non-growing microbial cells can be described by a mathematical model. The constants of the model have direct physical significance, and they are easily evaluated from the measured product concentrations by the application of simple graphical procedures. The qualitative and quantitative characteristics of the hydrocarbon transformation were described by the following expressions:

$$\frac{dS_A}{dt} = \frac{R}{\phi_A} - k_A S_A \qquad \text{for } t < t^*$$

$$\frac{dS_A}{dt} = \frac{R}{\phi_A} e^{-k_D(t - t^*)} - k_A S_A \qquad \text{for } t \geq t^*$$

$$\frac{dS_K}{dt} = \left(k_A \frac{\phi_A}{\phi_K}\right) S_A - k_K S_K \qquad \text{for } t > 0$$

where the physical significance of the model parameters is as follows:

Constant	Physical Significance
R: (weight fraction) hour^{-1}	Constant rate of reaction: H$\rightarrow$A
k_A: hour^{-1}	Reaction rate constant: A$\rightarrow$K
k_K: hour^{-1}	Reaction rate constant: K$\rightarrow$?
k_D: hour^{-1}	Decay constant denoting the speed of enzyme deactivation for the reaction: H$\rightarrow$A
t*: hour	Time at which enzyme decay is initiated.
$\frac{\phi_A}{\phi_K}$: dimensionless	Measure of the extent of the reaction product localization in the region of the transformation enzymes.

BIBLIOGRAPHY

1. Aiba, Shuichi, Shiro Nagai, Yoshinori Nishizawa and Masayuki Onodera. Energetic and nucleic analyses of a chemostatic culture of Azotobacter vinelandii. Journal of General and Applied Microbiology 13: 73-83. 1967.

2. Allen, J. E. and A. J. Markovetz. Oxidation of n-tetradecane and 1-tetradecene by fungi. Journal of Bacteriology 103: 426-434. 1970.

3. Andrews, John F. A mathematical model for the continuous culture of microorganisms utilizing inhibitory substrates. Biotechnology and Bioengineering 10: 707-723. 1968.

4. Bandyopadhyay, B. and A. E. Humphrey. Dynamic measurement of the volumetric oxygen transfer coefficient in fermentation systems. Biotechnology and Bioengineering 9: 533-544. 1967.

5. Baptist, J. N., R. Gholson and M. Coon. Hydrocarbon oxidation by a bacterial enzyme system. I. Products of octane oxidation. Biochimica et Biophysica Acta 69: 40-47. 1963.

6. Dunn, Irving J. An interfacial kinetics model for hydrocarbon oxidation. Biotechnology and Bioengineering 10: 891-894. 1968.

7. Edwards, Victor H. and Charles R. Wilke. Mathematical representation of batch culture data. Biotechnology and Bioengineering 10: 205-232. 1968.

8. Erickson, L. E., A. E. Humphrey and A. Prokop. Growth models of cultures with two liquid phases. I. Substrate dissolved in dispersed phase. Biotechnology and Bioengineering 11: 449-466. 1969.

9. Erickson, L. E. and A. E. Humphrey. Growth models of cultures with two liquid phases. II. Pure substrate in dispersed phase. Biotechnology and Bioengineering 11: 467-489. 1969.

10. Forney, F. W. and A. J. Markovetz. Oxidative degradation of methyl ketones. II. Chemical pathway for degradation of 2-tridecanone by Pseudomonas multivorans and Pseudomonas aeruginosa. Journal of Bacteriology 96: 1055-1064. 1968.

11. Forney, F. W. and A. J. Markovetz. Subterminal oxidation of aliphatic hydrocarbons. Journal of Bacteriology 102:281-282. 1970.

12. Forney, F. W., A. J. Markovetz and R. E. Kallio. Bacterial oxidation of 2-tridecanone to 1-undecanol. Journal of Bacteriology 93: 649-655. 1967.

13. Foster, J. W. Bacterial oxidation of hydrocarbons. In: Oxygenases, ed. by Osamu Hayaishi, New York, Academic Press, 1962. p. 241-271.

14. Foster, J. W. Chemical activities of fungi. New York, Academic Press, 1949. 648p.

15. Foster, J. W. Hydrocarbons as substrates for microorganisms. Antonie van Leeuwenhoek, Journal of Microbiology and Serology 28:242-274. 1962.

16. Fredricks, Kerstin M. Products of the oxidation of n-decane by Pseudomonas aeruginosa and Mycrobacterium rhodochrous. Antonie van Leeuwenhoek, Journal of Microbiology and Serology 33: 41-48. 1967.

17. Fuhs, G. W. The destruction of hydrocarbons by microbes. Magazine for Microbiology 39: 374-422. 1961.

18. Gholson, R. K. and M. J. Coon. Conversion of octane to octanol by a Pseudomonas enzyme system. (Abstract) Abstracts of Papers of the American Chemical Society 138:29C. 1960.

19. Goepfert, G. J. Studies in the mechanism of dehydrogenation by Fusarium lini Bolley. XIV. Dehydrogenation of higher primary and secondary alcohols. Journal of Biological Chemistry 140: 525-534. 1941.

20. Hansen, R. W. and R. E. Kallio. Inability of nitrate to serve as a terminal oxidant for hydrocarbons. Science 125: 1198-1199. 1957.

21. Harris, John O. Respiration studies of a Micrococcus capable of oxidizing hydrocarbons. Archives of Biochemistry and Biophysics 70: 457-463. 1957.

22. Herbert, D., R. Elsworth and R. C. Telling. The continuous culture of bacteria: a theoretical and experimental study. Journal of General Microbiology 14: 601-622. 1956.

23. Heringa, J. W., R. Huybregtse and A. C. van der Linden. n-Alkane oxidation of a Pseudomonas: formation and beta oxidation of intermediate fatty acids. Antonie van Leeuwenhoek; Journal of Microbiology and Serology 27: 51-58. 1961.

24. Heydeman, M. T. Studies on a paraffin utilizing pseudomonad. Biochimica et Biophysica Acta 42: 557-558. 1960.

25. Ho, L. and A. Humphrey. Optimal control of an enzyme reaction subject to enzyme deactivation. I. Batch process. Biotechnology and Bioengineering 12: 291-311. 1970.

26. Hopkins, J. S. and A. C. Chibnall. Growth of Aspergillus versicolor on higher paraffins. Biochemical Journal 26: 131-142. 1932.

27. Humphrey, A. E., S. Aiba and N. F. Millis. Biochemical engineering. New York, Academic Press, 1965. 333p.

28. Iida, M. Microbial studies on petroleum and natural gas. IX. Candidal oxidation of decane. Journal of General and Applied Microbiology 12: 119-126. 1966.

29. Kahn, M. Y. Ali, A. N. Hall and D. S. Robinson. Microbial transformation of n-octane into dicarboxylic acids. Nature 198: 289. 1963.

30. Kaiser, Rudolf. Gas phase chromatography. London, Butterworths, 1963. Volume I.

31. Kester, A. S. and J. W. Foster. Determinal oxidation of long-chain alkanes by bacteria. Journal of Bacteriology 85: 859-869. 1963.

32. Klein, D. A., Judith A. Davis and L. E. Casida, Jr. Oxidation of n-alkanes to ketones by an Arthrobacter species. Antonie van Leeuwenhoek; Journal of Microbiology and Serology 34: 495-503. 1968.

33. Klein, D. A. and F. A. Henning. Role of alcoholic intermediates in formation of isomeric ketones from n-hexadecane by a soil Arthrobacter. Applied Microbiology 17: 676-681. 1969.

34. Knowles, G., A. L. Downing and M. J. Barrett. Determination of kinetic constants for nitrifying bacteria in mixed culture with the aid of an electronic computer. Journal of General Microbiology 38:263-278. 1965.

35. Koga, S., C. R. Burg and A. E. Humphrey. Computer simulation of fermentation systems. Applied Microbiology 15:683-689. 1967.

36. Kono, Takehiko. Kinetics of microbial cell growth. Biotechnology and Bioengineering 10:105-131. 1968.

37. Kono, T. and T. Asai. Kinetics of fermentation processes. Biotechnology and Bioengineering 11:293-321. 1969.

38. Ladd, J. N. The oxidation of hydrocarbons by soil bacteria. I. Morphological and biochemical properties of a soil diptheroid utilizing hydrocarbons. Australian Journal of Biological Sciences 9:92-104. 1956.

39. Leadbetter, E. R. and J. W. Foster. Incorporation of molecular oxygen in bacterial cells utilizing hydrocarbons for growth. Nature 184:1428-1429. 1959.

40. Leadbetter, E. R. and J. W. Foster. Bacterial oxidation of gaseous alkanes. Archiv fur Mikrobiologie 35:92-104. 1960.

41. Luedeking, R. Fermentation process kinetics. In: Biochemical and biological engineering science, ed. by N. Blakebrough. Vol. I. London, Academic Press, 1967. p. 181-240.

42. Luedeking, Robert and Edgar L. Piret. A kinetic study of the lactic acid fermentation. Batch process at controlled pH. Biotechnology and Bioengineering 1:393-412. 1959.

43. Lukins, H. B. and J. W. Foster. Methyl ketone metabolism in hydrocarbon-utilizing mycobacteria. Journal of Bacteriology 85: 1074-1087. 1963.

44. McKenna, E. J. and R. E. Kallio. The biology of hydrocarbons. Annual Review of Microbiology 19:183-208. 1965.

45. McNair, H. M. and E. J. Bonelli. Basic gas chromatography. Oakland, California, Consolidated Printers, 1967. 248p.

46. Monod, J. Recherces sur la croissance des cultures bacteriennes, Paris, Hermann et Cie, 1942. (Cited in: Hinshelwood, C. N. The chemical kinetics of the bacterial cell. Oxford, Clarendon Press, 1952, p. 68)

47. Moser, H. The dynamics of bacterial populations maintained in the chemostat. Washington, Carnegie Institute of Washington, 1958. (Cited in: Andrews, John F. A mathematical model for the continuous culture of microorganisms utilizing inhibitory substrates. Biotechnology and Bioengineering 10: 707-723. 1968).

48. Neilands, J. B. and P. K. Stumpf. Outlines of enzyme chemistry. 2d ed. New York, John Wiley and Sons, 1958. 411p.

49. Powell, E. O. Continuous culture methods and their application: Discussion. In: Recent progress in microbiology: Symposia held at the Seventh International Congress for Microbiology, Stockholm, 1958. Springfield, Illinois, Thomas, 1959. p. 422-423.

50. Proctor, M. H. A paraffin oxidizing pseudomonad. Biochemica et Biophysica Acta 42: 559. 1960.

51. Raymond, R. L., V. W. Jamison and J. O. Hudson. Microbial hydrocarbon co-oxidation. I. Oxidation of mono- and dicyclic hydrocarbons by soil isolates of the genus Nocardia. Applied Microbiology 15: 357-365. 1967.

52. Shu, Ping. Mathematical models for the product accumulation in microbiological processes. Biotechnology and Bioengineering 3: 95-109. 1961.

53. Stanier, R. Y. Simultaneous adaption; a new technique for the study of metabolic pathways. Journal of Bacteriology 54: 339-348. 1947.

54. Stewart, J. E., W. R. Finnerty, R. E. Kallio and D. P. Stevenson. Esters from bacterial oxidation of olefins. Science 132: 1254. 1960.

55. Stewart, J. E., R. E. Kallio, D. P. Stevenson, A. C. Jones and D. O. Schissler. Bacterial hydrocarbon oxidation. I. Oxidation of n-hexadecane by a gram-negative coccus. Journal of Bacteriology 78: 441-448. 1959.

56. Teissier, G. (title unknown) Ann. Physiol. Physiochim. Biol. 12: 527. 1936. (Cited in: Andrews, John F. A mathematical model for the continuous culture of microorganisms utilizing inhibitory substrates. Biotechnology and Bioengineering 10: 707-723. 1968.)

57. Thijsse, G. J. E. and A. C. van der Linden. Iso-alkane oxidation by a Pseudomonas. Part I. Metabolism of 2 methylhexane. Antonie van Leeuwenhoek; Journal of Microbiology and Serology 27: 171-179. 1961.

58. Thijsse, G. J. E. and J. T. Zwilling-De Vries. The oxidation of straight and branched alkanes by Pseudomonas strains. Antonie van Leeuwenhoek; Journal of Microbiology and Serology 25: 332. 1959.

59. Walter, C. Steady state applications in enzyme kinetics. New York, Ronald, 1965. 263p.

60. Wang, Daniel I. C. and Arthur E. Humphrey. Enzyme detergents, already a multimillion-dollar industry, are but one concrete result from biochemical engineering. Chemical Engineering 76: 108-120. December 15, 1969.

61. Webley, D. M., R. B. Duff and V. C. Famer. Evidence for beta-oxidation in metabolism of saturated hydrocarbons by the soil species Nocardia. Nature 178: 1467-1468. 1956.

62. White, Abraham, Philip Handler and Emil L. Smith. Principles of biochemistry. 3d ed. New York, McGraw-Hill, 1964. 1106p.

63. Zajic, James E. Biochemical reactions in hydrocarbon metabolism. Developments in Industrial Microbiology 6: 16-27. 1964.

APPENDICES

APPENDIX I. RUN SUMMARY

Table 5. Summary of deviation from experimental procedure.

Run	Inoculum vessel	Growth vessel		Blend vessel	Run vessel			Comments
	Incubation time: hours	Incubation time: hours	Aqueous volume: liters	Hold time: minutes	Aqueous volume: liters	Cell conc., W: mg/ml	Mass n C_{16}, M_H: ml	
7-18	48	--	--	--	5.00	--	150	Growth run
9-24-A	25	24	10.0	180	8.10	0.23	217	Two cell levels
9-24-B	25	24	10.0	180	7.30	0.07	196	
10-28	25	38	10.0	50	7.50	0.24	160	
10-31	23	32	10.0	43	7.50	0.48	160	
11-17	25	47	12.0	65	7.50	--	160	
2-28-B	24	49	12.0	20	8.00	0.26	160	
3-14-B	48	48	12.0	7	7.00	0.28	160	
4-11-A	46	48	12.0	5	7.00	0.32	160	Test: Exogenous 3-ketone
4-11-B	46	48	12.0	10	7.00	0.31	160	Control
4-18-A	38	48	12.0	10	7.00	0.36	160	Test: Exogenous 3-ketone
4-18-B	38	48	12.0	20	7.00	0.35	160	Control
5-2-A	48	48	12.0	20	7.00	0.37	160	5-2-A and 5-2-B, identical conditions
5-2-B	48	48	12.0	30	7.00	0.38	160	
5-18-A	47	45	12.0	10	7.00	$(W)_A = (W_B)$	160	Control
5-18-B	47	45	12.0	15	7.00		80	$(M_H)_B = 0.5\ (M_H)_A$

Table 6. Summary of model parameters.

Run	S_{AO}	S_A^*	k_A	$(k_A \frac{\phi_A}{\phi_K})$	k_K	S_{KO}	k_D	t^*	$(R/\phi_A)=\frac{S_A^*}{k_A}$	$\phi_A/\phi_K=\frac{(k_A \frac{\phi_A}{\phi_K})}{k_A}$
	weight fraction $\times 10^4$		$hour^{-1}$	$hour^{-1}$	$hour^{-1}$	weight fraction $\times 10^4$	$hour^{-1}$	hour	weight fraction $\times 10^{+4}$/hour	dimensionless
9-24-A	.30	1.73	.167	.273	.042	0.0	.026	11.5	.29	1.6
9-24-B	.20	1.55	.200	.192	.081	0.0	.010	11.5	.31	1.0
10-28	.23	1.52	.250	1.160	.078	0.0	.058	10.5	.38	4.7
10-31	.54	1.48	.167	1.153	.065	0.0	.039	15.5	.25	6.9
11-17	.69	2.38	.330	.713	.026	0.0	.040	10.0	.78	2.2
2-28-B	.09	1.15	.143	1.100	.078	0.0	.008	10.0	.16	7.7
3-14-B	.21	1.37	.125	.812	.070	0.0	.024	16.0	.17	6.5
4-11-A	.35	1.34	.111	.936	.062	0.0	.023	5.5	.15	8.4
4-11-B	.35	1.32	.125	.773	.025	0.0	.042	8.5	.17	6.2
4-18-A	.07	.93	.125	1.310	.056	0.0	.019	15.5	.12	10.5
4-18-B	.21	1.02	.182	.841	.042	0.0	.026	15.5	.19	4.6
5-2-A	.25	1.52	.143	.786	.064	0.0	.014	17.5	.22	5.5
5-2-B	.21	1.38	.167	.708	.035	0.0	.011	15.0	.23	4.2
5-18-A	.33	1.96	.167	.542	.023	0.0	.024	27.0	.33	3.2
5-18-B	.55	2.24	.143	.748	.022	0.0	.019	18.0	.32	5.2

APPENDIX II

ESTIMATION OF ERRORS

Net Error in Measured Product Concentrations

The factors which contributed to the errors in the measured values of S_A and S_K were discussed on page 52. The contributions of the standard deviation and the drift error to the total error are not completely independent. However, in order to provide a measure of the maximum net experimental error, these two contributions were treated as independent errors. Making this assumption, and using the maximum value of the drift error, the net maximum error was estimated to be $\pm$ 6.2% for the measured values of ketone concentration and $\pm$ 12% for values of the alcohol concentration.

Maximum Errors of the Model Constants

The maximum errors of the model parameters are summarized in Table 7. The basis for the estimation of these maximum error values is briefly outlined following this table.

Table 7. Estimated errors in the model parameters.

Parameter	Maximum Error
k_A	$\pm$ 20%
S_A^*	$\pm$ 8.2%
$(k_A \frac{\phi_A}{\phi_K})$	$\pm$ 14%
k_K	$\pm$ 50%
k_D	$\pm$ 49%
t^*	$\pm$ 39%

The chosen method for evaluation of $(k_A \frac{\phi_A}{\phi_K})$ and k_K required graphical differentiation of the $\ln S_K$ versus t curve. The S_K data showed relatively little scatter, and no difficulty was encountered in placing a smooth curve through the $\ln S_K$ versus t data. The values for $(d\ln S_K/dt)$ were determined by drawing tangents to the curve at desired values of time. The maximum error in the values of $(d\ln S_K/dt)$ was estimated to be $\pm$ 10%. This estimate was obtained by determining the maximum and minimum values of the slopes on the $\ln S_K$ versus t curve in the most sensitive region.

This error was estimated graphically, rather than in terms of the uncertainty in the experimental S_K values. Although the maximum uncertainty in S_K was found to be $\pm$ 6.2%, the actual scatter was not of large enough magnitude to allow significant variation in the

shape of the curve through this data. As a consequence, the error in determining the slope from this curve was attributed primarily to judgement errors in placing the tangent on the curve.

The value of $\bar{S}$ was not subject to the high degree of scatter observed in the S_A versus t data, since $\bar{S}$ was computed directly from the ratio of alcohol and ketone peaks which resulted from a single chromatographic injection. This minimized the effect of chromatographic variations because both peaks responded in the same manner to such changes.

For a large number of injections on several different days, the standard deviation of the ratio of alcohol and ketone peaks from the standard samples was found to be 3.6%. For run samples in a single series of injections the standard deviation of $\bar{S}$ was 2.0%.

Using the error values indicated above, the maximum errors involved in the evaluation of $(k_A \frac{\phi_A}{\phi_K})$ and (k_K) were calculated. The maximum error of $(k_A \frac{\phi_A}{\phi_K})$ was estimated to be $\pm$ 14%. The maximum error of (k_K) was found to be $\pm$ 50%. These estimates were made by using two sets of $\bar{S}$ and $d\ln S_K/dt$ points from a typical run. One set of points from each end of the $\bar{S}$ versus $d\ln S_K/dt$ plot was selected. Using the estimated errors in $\bar{S}$ and $d\ln S_K/dt$ reported above, the deviations from the selected points were chosen so as to maximize and minimize the resulting values of the slope and intercept on this plot. These maximum and minimum values were used to

compute the maximum errors in the parameters. The value of S_A^* was determined by graphically adding values of S_K and $\bar{S}$ on a semi-log plot. Consequently, the error in this parameter is the sum of the errors in S_K and $\bar{S}$, or 8.2%.

An estimate of the maximum error in k_A was obtained by determining the range of possible k_A values which could result from the graphical evaluation technique, while still providing an acceptable model curve. The maximum error for this parameter was found to be $= \pm 20\%$.

APPENDIX III

ALTERNATIVE METHODS OF ANALYSIS

Evaluation of k_A

The method used to evaluate k_A and S_A^* from the experimental values of S_A selected the k_A value which placed the best model curve through the data, as judged by eye. While more rigorous techniques were available, they were unsuitable for application to the alcohol data. Two such methods are briefly explained.

From Equation (6), a plot of (dS_A/dt) versus S_A was expected to be linear, with a slope equal to k_A. However, the scatter of the experimental S_A values required considerable judgement in the placement of a smoothed curve through the data. It was then necessary to graphically differentiate the curve in order to provide the required (dS_A/dt) values. The chosen method was more direct, and not subject to the errors involved in the differentiation procedure.

A second alternative method for the evaluation of k_A is based on the integrated expression for S_A as a function of time. Equation (6) can be integrated and rearranged to give:

$$\ln \left[\frac{S_A^* - S_A}{S_A^* - S_{AO}} \right] = -k_A t \qquad (11)$$

Equation (11) predicts that a plot of $\ln(S_A^* - S_A)$ against t will be linear, with a slope equal to $-k_A$. This method requires knowledge of the value of S_A^* in order to carry out the evaluation technique for k_A. Because of its directness, the plot of Equation (11) was preferred to the method finally chosen to evaluate k_A; in practice, however, the use of this technique was not suitable for use with most of the run data, because the plot of $\ln (S_A^* - S_A)$ versus t was especially sensitive to scatter in the data as S_A approached S_A^*. However, a few runs exhibited a degree of scatter low enough to allow the determination of S_A^* by means of this method. The excellent linearity of the resulting plots of Equation (11) indicated that the form of Equation (6) fit the data quite well in the region preceding the hump. These results provided motivation for the retention of Equation (6) as a model form.

Evaluation of S_A^*

The smoothed data curve was used to provide a consistent, unambiguous choice of S_A^* from the data. Three factors made this choice difficult from the S_A data directly. First, scatter caused uncertainty in the placement of a curve through the data. Secondly, consistently observed irregularities in the alcohol data caused uncertainty in fixing S_A^*. It was apparent from Figure 8 that the smooth increase of S_A with time was interrupted at t = 9.0 hours. This "hump" in the

data appeared regularly in the runs and its appearance was interpreted as an indication that transition to a region of enzyme decay was taking place. Regardless of the interpretation of its physical significance, however, the hump was a clear indication that the trend of the data changed about ten hours after initiation of the run. Thirdly, if decay started before S_A^* was reached, the maximum value of S_A was less than S_A^*.

It is apparent that placement of an average curve through the initial and hump regions of the alcohol data is likely to provide an estimate of S_A^* which is higher than would be predicted from the trend of the initial data. This can be clearly seen from Figure 28, where the two regions are more clearly defined than they were for the typical case. However, for most of the experimental runs, the overlap of these regions was such that S_A^* could not be reliably and consistently predicted from the initial portion of the curve. For these reasons, the chosen method of evaluating S_A^* utilized the previously discussed smoothing technique; it should be recognized that the resulting S_A^* value is probably somewhat larger than indicated by the region of the data to which the model equation most closely applies. Similarly, the resulting S_A model curve represents an average curve for the data covering the two regions. This factor does not represent a significant effect on the resulting model for the alcohol data. However, it is apparent from Figure 34 that the resultant effect on the

ketone model solution is magnified.

Evaluation of $(k_A \frac{\phi_A}{\phi_K})$ and k_K

The alternative procedure for evaluation of $(k_A \frac{\phi_A}{\phi_K})$ and k_K from the experimental data involved integration and rearrangement of Equation (7) to the form:

$$\left[\ln \left(\frac{S_K}{S_{Ki}}\right) - \left(k_A \frac{\phi_A}{\phi_K}\right) \int_{t_i}^{t} \bar{S} dt \right] = -(k_K)(t - t_i)$$

In order to apply this equation, a convenient lower limit of integration, t_i, was chosen and the integral was then evaluated graphically. A plot of the quantity in brackets against $(t - t_i)$ was expected to be linear and pass through the origin with a slope of $-(k_K)$. Because the $\bar{S}$ versus t curve had a very large slope over the time period from two to four hours, t_i was best taken as five hours or some time greater. It was hoped that the slope of the curve (and thus the determined value of (k_K)) would be less subject to the slight uncertainty in placing the line through the data than was the value of the intercept in the chosen method. However, the method possessed two disadvantages. First, a value of $(k_A \frac{\phi_A}{\phi_K})$ was required. Unless used in conjunction with the chosen method, this integral method required the use of trial

values of ($k_A \frac{\phi_A}{\phi_K}$); this was unsatisfactory because linearity of the plot was insensitive to the value of $k_{A\frac{\phi_A}{\phi_K}}$ used. Thus, the method could, at best, only confirm the (k_K) value predicted by the previous method. Secondly, the method proved to be particularly sensitive to the choice of t_i, due to the initially steep slopes of the $\bar{S}$ curve; this caused deviation from linearity over the initial regions of the plot, as well as offsetting of the entire curve from the origin. Consequently, this method was unsuitable for the evaluation of the parameters.